Investigating the physicochemical property changes of plastic packaging material exposed to UV radiation

by

WILLEM JOHANNES CONRADIE

Thesis presented in partial fulfilment
of the requirements for the Degree

of

MASTER OF ENGINEERING
(EXTRACTIVE METALLURGICAL ENGINEERING)

in the Faculty of Engineering
at Stellenbosch University

Supervisor
Prof. G. Akdogan

Co-Supervisor/s
Prof. C. Dorfling
Prof. A.F.A. Chimphango

December 2020

Declaration

By submitting this thesis electronically, I declare that the entirety of the work contained therein is my own, original work, that I am the sole author thereof (save to the extent explicitly otherwise stated), that reproduction and publication thereof by Stellenbosch University will not infringe any third party rights and that I have not previously in its entirety or in part submitted it for obtaining any qualification.

Date: December 2020

Abstract

Global plastic production is increasing, and as a consequence more waste is generated and released into the environment. Oceanic weathering factors such as ultraviolet (UV) radiation, temperature, and salinity result in the degradation of these plastics and subsequent formation of microplastics (MPs). These MPs in-turn pose a specific threat to ecosystems and their respective inhabitants.

This study aimed to evaluate UV induced degradation of conventional packaging material made of polypropylene (PP) homopolymer and amorphous poly(ethylene terephthalate). Plastic sheets were prepared into four different shapes: small circles (6 mm dia.), large circles (12 mm dia.), small rectangles (8x4 mm), and large rectangles (40x10 mm). Sequential degradation was considered with samples initially degraded solely by UV radiation in air. The experiments were conducted in a UV chamber that offered two levels of irradiance exposure: 65 W/m^2 and 130 W/m^2. After the initial degradation in air, samples were further exposed to either constant temperatures (25°C or 60°C) or cyclic UV conditions (65 W/m^2 or 130 W/m^2) while immersed in different aqueous solutions (demineralised water or seawater). Each experimental run commenced for six weeks, and samples were drawn and analysed fortnightly. The physicochemical properties monitored over time were mass, crystallinity, microhardness, and chemical functional groups (carbonyl and hydroxyl). These properties were measured via standard analytical techniques such as precision balance, differential scanning calorimetry (DSC), Vickers microhardness tester, and attenuated total reflectance-Fourier transform infrared (ATR-FTIR) spectroscopy.

Results from the initial experiments indicated that UV irradiance proportionally instigated changes in plastic properties. Increased mass loss accompanied by considerable increases in carbonyl index was observed for the PPs. Shape did not significantly affect mass loss or functional group developments. Clear polypropylene (CPP) reflected the most severe degradation, resulting in the most considerable mass loss, increase in crystallinity, and highest carbonyl content. Overall PPs degraded more than PET; differences were mainly attributed to alternative compositions, with PP having high frequencies of tertiary carbon atoms whilst PET contained stabilising aromatic rings increasing its stability towards photo-oxidative degradation. The peak wavelength sensitivity of PP also almost exactly corresponded to the peak wavelength intensity of the UV lamps used in this investigation. Furthermore, it was suspected that black polypropylene (BPP) contained a UV absorbing additive (carbon black) responsible for shielding its interior from radiation by terminating free radical reactions and converting energy to heat.

Results from experiments performed with plastic samples immersed in aqueous solutions were more irregular. It was concluded that degradation occurred substantially faster in air than in seawater. The most significant property changes in crystallinity, microhardness, and chemical functionalities were observed for material without any previous degradation history. Samples with previous histories showed more resistance to crystallinity changes. This was attributed to prior exposure weakening the material, presenting crosslinking and structural defects which inhibited polymer chains from realigning into crystalline structures. Carbonyl groups reduced for material with previous degradation histories. This was due to the following occurrences: (i) changes in surface energy with polymer chains rearranging leaving carbonyl products concealed below the observed surface and (ii) the degraded surface layer eroding, or hydrophilic products dissolving into the surrounding solution medium leaving a fresh unexposed layer of plastic being analysed. Solution medium did not have a significant effect on the property changes of untreated material.

Opsomming

Globale plastiekproduksie is besig om te verhoog, en as ’n gevolg word meer afval vervaardig en vrygelaat in die omgewing. Oseaniese verweringsfaktore soos ultraviolet (UV)-bestraling, temperatuur, en soutgehalte het die degradering van hierdie plastiek en formasie van mikroplastiek (MP) tot gevolg. Hierdie MPs bied op sy beurt ’n spesifieke bedreiging vir ekosisteme en hul onderskeidelike inwoners.

Hierdie studie het beoog om degradasie van konvensionele verpakkingsmateriaal gemaak uit polipropileen (PP) homopolimeer en amorf poli(etileentereftalaat), wat deur UV veroorsaak word, te evalueer. Plastiek plate is voorberei in vier verskillende vorms: klein sirkels (6 mm dia.), groot sirkels (12 mm dia.), klein reghoeke (8x4 mm), en groot reghoeke (40x10 mm). Sekwensiële degradasie is beskou met steekproewe aanvanklik gedegradeer alleenlik deur UV-bestraling in lug. Die eksperimente is uitgevoer in ’n UV-kamer wat twee vlakke van straling blootstelling gebied het: 65 W/m^2 en 130 W/m^2. Na die aanvanklike degradasie in lug, is steekproewe verder blootgestel aan of konstante temperature (25 °C of 60 °C) of sikliese UV toestande (65 W/m^2 of 130 W/m^2) terwyl dit onderdompel word in verskillende waterige oplossings (gedemineraliseerde water of seewater). Elke eksperimentele lopie is vir ses weke uitgevoer, en steekproewe is tweeweekliks uitgetrek en geanaliseer. Die fisikochemiese eienskappe wat oor tyd gemonitor is, was massa, kristalliniteit, mikrohardheid, en chemiese funksionele groepe (karboniel en hidroksiel). Hierdie eienskappe is gemeet via standaard analitiese tegnieke soos presisieweegskaal, differensiale skandering kalorimetrie (DSC), Vickers mikrohardheidstoetser, en verswakte totale reflektansie-Fourier transformasie infrarooi (ATR-FTIR) spektroskopie.

Resultate van die aanvanklike eksperimente het aangedui dat UV-straling proporsioneel veranderinge in plastiekeienskappe veroorsaak het. Verhoogde massaverlies gepaardgaande met aansienlike verhogings in karbonielindeks is waargeneem vir die PPs. Vorm het nie massaverlies of funksionele groep ontwikkeling beduidend beïnvloed nie. Helder polipropileen (CPP) het die strafste degradasie getoon, wat die mees aansienlike massaverlies, verhoging in kristalliniteit, en hoogste karbonielinhoud tot gevolg gehad het. Oor die algemeen het PPs meer gedegradeer as PET; verskille is hoofsaaklik toegeskryf aan alternatiewe samestellings, met PP wat hoër frekwensies van tersiêre koolstofatome het terwyl PET stabiliserende aromatiese ringe bevat het wat sy stabiliteit teenoor foto-oksidatiewe degradasie verhoog het. Die piek golflengte sensitiwiteit van PP het ook amper presies ooreengestem met die piek golflengte intensiteit van die UV-lampe gebruik in hierdie ondersoek. Verder is dit vermoed dat swart polipropileen (BPP)

’n UV-absorberingsbymiddel (koolstof swart) bevat wat verantwoordelik is vir die beskerming van sy binnekant teen bestraling deur vry radikale reaksies te beëindig en om energie na hitte om te skakel.

Resultate van eksperimente uitgevoer met plastieksteekproewe onderdompel in waterige oplossings was meer onreëlmatig. Dit is beslis dat degradasie aansienlik vinniger in lug as in seewater plaasvind. Die mees beduidende eienskap veranderinge in kristalliniteit, mikrohardheid, en chemiese funksionaliteite is waargeneem vir materiaal sonder enige vorige geskiedenis van degradasie. Steekproewe met vorige geskiedenis het meer weerstand tot veranderinge in kristalliniteit getoon. Hierdie is toegeken aan vroeër blootstelling wat die materiaal verswak het, wat kruisverbinding en strukturele afwykings toon wat polimeerkettings geïnhibeer het om in kristalvormige strukture te hergroepeer. Karbonielgroepe het verminder vir materiaal met vorige geskiedenis van degradasie. Dis as gevolg van die volgende gebeure: (i) verandering in oppervlakenergie met polimeerkettings wat geherrangskik word en karbonielprodukte onder die oppervlak toe hou, of (ii) die degradasie-oppervlaklaag wat verweer (of hidrofiliese produkte wat oplos) in die omliggende oplossingmedium wat ’n vars laag laat van plastiek wat nie blootgestel is nie, wat geanaliseer word. Oplossingmedium het nie ’n beduidende effek op die eienskap verandering van onbehandelde materiaal gehad nie.

Acknowledgements

I would like to express my sincere gratitude and appreciation to the following people:

- My parents, †Retief and Rinette Conradie, for their love, continuous support, and encouragement. Attending Stellenbosch University has been a privilege, and without them, none of this would have been possible.
- My supervisor, Prof. Guven Akdogan, for his patience, understanding, technical advice and guidance.
- My co-supervisors, Prof. Christie Dorfling and Prof. Annie Chimphango, for their valuable insights, advice, and accessibility.
- The technical and administrative staff at the Department of Process Engineering at Stellenbosch University for their assistance. A special thank you is extended to Mr. Alvin Petersen for his support in the laboratories.
- Staff from the Departments of Polymer Science and Chemistry at Stellenbosch University for allowing me to make use of their analytical facilities.
- My family and friends, with a specific mention to Annerie Rossouw, for always listening, understanding, and supporting me over this duration.

This work is based on research supported in part by the National Research Foundation of South Africa (Grant number 118760).

Table of Contents

Nomenclature

Symbols		
E_a	Activation Energy	kJ/mole
W_f	Final mass	g
W_i	Initial mass	g
T_g	Glass transition temperature	°C
ΔH_m	Melting enthalpy per unit mass	J/g
ΔH_m^{ref}	Melting enthalpy per unit mass for 100% crystalline polymer	J/g
HV	Microhardness	kg-f/mm^2

Abbreviations	
AFM	Atomic force microscopy
ANOVA	Analysis of variance
BPA	Bisphenol A
DSC	Differential scanning calorimetry
DMA	Dynamic mechanical analysis
FTIR	Fourier transform infrared
HALS	Hindered amine light stabilisers
HDPE	High-density polyethylene
i-PP	Isotactic polypropylene
LLDPE	Linear low-density polyethylene
MP	Microplastic
PCB	Polychlorinated biphenyl
PE	Polyethylene
PET	Poly(ethylene terephthalate)
PID	Proportional integral derivative
POP	Persistent organic pollutants
PP	Polypropylene
PSU	Practical salinity unit
PS	Polystyrene
PU	Polyurethane
PVC	Polyvinyl chloride
SEM	Scanning electron microscopy
TPA	Terephthalic acid
UV	Ultraviolet
VMHT	Vickers microhardness tester
XPS	X-ray photoelectron spectroscopy
XRD	X-ray diffraction

1. Introduction

1.1 Background

Around the globe, plastic production is increasing and has already reached 359 million tonnes in 2018 (PlasticsEurope, 2019). It is suggested that the per-capita consumption of plastic is also on the increase, as shown by Andrady (2017). This growth in production results in higher amounts of plastic entering the environment, which is specifically detrimental to marine and coastal ecosystems. The World Economic Forum (2016) predicted the total number of plastics to outweigh the total number of fish in the oceans by 2050 unless effective and preventative measures are taken. Carpenter and Smith (1972) were the first to describe floating plastic debris on the ocean surface and foresaw concentrations to increase due to increased production and improper waste disposal practices.

Plastics currently constitute between 60-80% of all floating debris in the oceans and amounts are increasing annually (Gewert et al., 2015; Moore, 2008). These plastic polymers are exposed to a wide range of environmental conditions such as physical stress, ultraviolet (UV) radiation, temperature variations, salinity, oxidising conditions, and microorganism colonisation (Jahnke et al., 2017).

Prolonged exposure to these conditions makes them weather and degrade. The weathering process, in turn, generates microplastic (MP) fragments, releases chemical additives, and possibly produces nanoplastics and chemical fragments cleaved from the polymer backbone. MPs are often ingested by marine species that cannot distinguish plastics from their everyday diets. This causes digestive disruptions, entanglement, and ultimately starvation. Low concentration persistent organic pollutants (POP) in seawater also adsorb to hydrophobic MPs that may act as a transport vehicle to vulnerable ecosystems (Auta et al., 2017).

This study aimed to investigate and monitor plastic degradation, specifically due to UV radiation, by considering a series of sequential degradation stages. Initially, plastic material was degraded solely by UV radiation in air; thereafter, material was further exposed to constant temperatures and cyclic UV conditions in different aqueous environments. Conclusions made could assist in understanding, detecting, and evaluating potential environmental hazards associated with plastic degradation and more specifically, microplastic formation in coastal marine ecosystems.

1.2 Motivation

As described in Section 1.1, the sheer amount of plastics entering and influencing the world's oceans is of particular concern. Plastic packaging is the most widely used and quickly disposed of. Currently, numerous studies in this field have a strong focus on plastic alternatives, innovative collection techniques, quantification, and type determination. A review of some of these focus areas is provided by Rocha-Santos & Duarte (2015) and Wang & Wang (2018). Although these studies provide insights into (location specific) concentration levels, they do not address the actual processes that result in the deterioration and ultimately, the fragmentation of these plastic pieces. Andrady (2011) noted that widely used surface collection techniques severely underestimate the amount of plastic material in our oceans. Fewer studies have considered the actual factors contributing to the formation of ubiquitous MPs and challenges regarding their bulk removal remain tremendous. Brandon et al. (2016) pointed out that due to their small size, chemical inertness, wide spatial distribution, and similarities to plankton and fish eggs, bulk removal is currently impossible.

An enhanced understanding of the degradation processes and the specific factors contributing to MP formation is therefore required. In order to appreciate the ways in which plastics degrade, their properties have to be examined in detail. Plastic properties are known to markedly determine degradation rates as well as influence the nature of their degradation (Allen et al., 1991). By achieving the objectives in Section 1.3, results generated from this investigation could be used to improve knowledge-based policy development and assist in manufacturing decision making to ensure long term marine sustainability.

1.3 Objectives

To successfully investigate the physicochemical property changes of plastic packaging material exposed to UV radiation, the following objectives had to be achieved:

- Conduct a thorough literature review to identify some of the main factors that facilitate plastic degradation and explain their effects.
- Experimentally evaluate and compare degradation behaviour of packaging material made of PP and PET by monitoring property changes including mass (precision balance), crystallinity (DSC), microhardness (Vickers microhardness indentation), and chemical functional groups (ATR-FTIR).

- Describe the effect of key variables on the degradation behaviour of plastic samples. These variables initially included UV irradiance, plastic-type, and shape. Subsequent variables such as temperature, solution medium, and previous degradation history were later introduced.
- Produce property datasets that could supplement the development of future degradation models.

1.4 Approach and scope

To achieve the objectives in Section 1.3, a comprehensive literature study was performed. Aspects covered included previous findings, factors influencing polymer degradation, polymer chemistry and properties, degradation pathways and mechanisms, analytical techniques, and suitable experimental methodologies. Thereafter experimental work was conducted. Plastic sheets were cut into different shapes and sizes and initially exposed to two different levels of UV irradiation; results from these experiments were obtained and analysed over time. The same degraded (as well as untreated) samples were then immersed in glass beakers containing different aqueous solutions (seawater or demineralised water). The beakers were exposed to two levels of UV irradiation and two levels of constant temperature respectively. A simplified overview of the experimental approach is shown below in Figure 1.1.

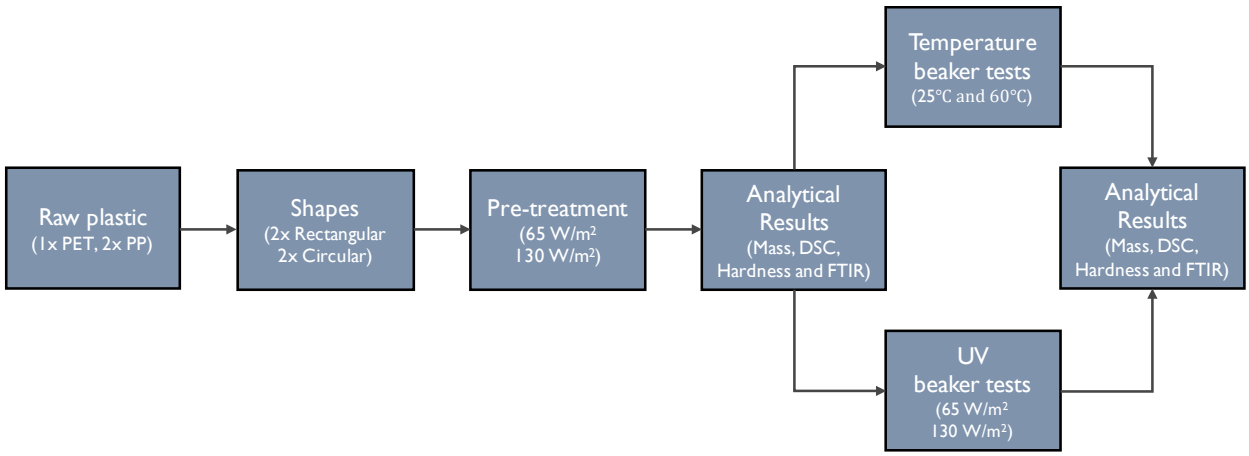

Figure 1.1. Schematic overview of the experimental approach.

Data recorded from the experimental runs could be used to develop regression models that describe physicochemical property changes as a function of degradation conditions. These models may assist in future risk assessment, decision making, and policy development by enabling manufacturing companies to predict property changes due to environmental degradation factors. PP and PET were the main subjects of this investigation as these plastic types are abundant in the

oceans and also vastly different in terms of their properties (Lebreton et al., 2017; Heo et al., 2013). In 2018, packaging accounted for 39.9% of the European demand by segment. In addition to that, PP was the most popular resin type at 19.3% with PET at 7.7% (PlasticsEurope, 2019).

1.5 Thesis outline

Section 2 of this document presents some background information on plastics and their production routes. This is followed by the definition of microplastics as well as the ways according to which plastic material is typically characterised. Thereafter the chemistry and some properties of specifically PP and PET are addressed. Degradation pathways and mechanisms are described with specific preference given to the oxidative and hydrolytic routes. The last part of this section covers some factors influencing degradation. The experimental planning, materials and equipment, procedures, analytical techniques, and data interpretation is expanded on in Section 3. The results and discussion are provided in Section 4 with the conclusions and recommendations in Section 5.

The appendices consist of supplementary material (Appendix A), experimental data (Appendix B), and ANOVA tables (Appendix C). It should be noted that Appendix B is presented electronically as a macro-enabled spreadsheet. Please refer to the attached .xlsm file where necessary.

2. Literature review

2.1 Plastics and production

Plastic is the general descriptive term used for a wide range of synthetic or semi-synthetic materials. During production, natural products are often used as raw material and include cellulose, coal, natural gas, and crude oil. Typical production starts with the distillation of crude oil where it is separated into groups of lighter fractions. These fractions consist of hydrocarbon chain mixtures differing in size and molecular structure. Naphtha is a specific fraction that is a particularly important compound for plastic production (PlasticsEurope, 2020).

Plastics are synthesised via the polymerisation reactions (polycondensation or polyaddition) of monomers and are generally classified into two groups: thermoplastics and thermosets (Singh and Sharma, 2008). Thermoplastics are linear chain macromolecules in which atoms and molecules are joined end-to-end into a series of long, single carbon chains. The bi-functionality necessary to form a linear macromolecule from vinyl monomers can be achieved by opening the unsaturated double bond and the reaction proceeding by a free-radical mechanism (Singh & Sharma, 2008). This type of polymerisation process is known as addition polymerisation with example products including polyethylene (PE) and polypropylene (PP). Conversely, thermoset plastics are formed by step-growth polymerisation under controlled conditions allowing bi-functional molecules to condense inter-molecularly with the liberation of small by-products including H_2O and HCl at each reaction step (Singh & Sharma, 2008). In this group, the monomers undergo some chemical changes (condensation) on heating and convert themselves into an infusible mass irreversibly.

Over the years, plastic popularity has increased sharply with consumers preferring plastic material above some metallic counterparts. This is most likely due to its associated benefits, including high versatility, high durability, low cost, and ease of storage and transportation. The downside is that their extreme durability makes them virtually indestructible, especially in the environment. Most plastic resin is produced explicitly for the packaging industry and has a relatively short lifetime. These short-lived plastics routinely end up in litter channels, in the oceans, as well as in municipal solid waste. Jambeck et al. (2015) linked global data on solid waste, population density, and economic status, and estimated that in the year 2010, 4.8-12.7 million metric tonnes of land-based plastic entered the ocean. Without waste management infrastructure improvements, the cumulative quantity is predicted to increase an order of magnitude by 2025.

Even with a conservative waste-to-debris conversion rate estimate, the total amount of oceanic plastic waste is expected to grow from 50 Mt in 2015 to 150 Mt by 2025 (Jambeck et al., 2015).

2.2 Microplastic definition

In the aquatic environment, MPs are made up of particles that differ in size, specific density, chemical composition, and shape (Duis & Coors, 2016). MPs are minute ubiquitous plastic particles smaller than five millimetres (5 mm) in size that originate from two sources: those manufactured explicitly for industrial or domestic application such as exfoliating facial scrubs, toothpaste, and resin pellets (*primary microplastics*); and those formed by the breakdown or fragmentation of larger plastic items under degrading conditions such as UV radiation and mechanical forces (*secondary microplastics*) (GESAMP, 2015).

2.3 Material characterisation

According to Andrady (2015), several measurable plastic properties might change as a result of degradation. Some of these properties are directly relevant to the performance of everyday products made from them (Singh & Sharma, 2008). In some cases, changes at the molecular level are monitored to detect early stages of degradation. The most widely investigated characteristics of common plastics are as follows:

- Changes in spectral characteristics that indicate oxidative degradation or photodegradation. For polyolefins, the relative intensity of the carbonyl absorption band (FTIR spectrum), might be monitored. Spectral results from previous work are discussed in Section 2.5.1.
- A decrease in the average molecular weight of the plastic. This is generally measured using gel permeation chromatography (GPC) and solution (melt) viscosity.
- Loss in bulk mechanical plastic properties; this includes tensile-, compression-, or impact-properties.
- Loss in surface properties of the material including; discolouration, micro-cracking, and flaking.

Table 2.1 summarises some of the typical plastic characteristics known to influence the behaviour of their MPs in the marine environment. Understanding these characteristics is crucial to developing an understanding of environmental MP behaviour.

Table 2.1. Plastic characteristics influencing their microplastic behaviour [Adapted from Andrady, 2017].

Characteristic	Influence on MP behaviour	Comments
Density	The buoyancy in seawater dictates the initial location of the MP in the water column.	General density ranges of plastic classes are known but can change due to fillers and surface foulants.
Partial crystallinity	The degree of crystallinity influences oxidative degradation and subsequent fragmentation due to weathering.	Typical crystallinity ranges are available, but these can change based on the degradation- and processing-history.
Oxidative resistance or weatherability	Chemical structures determine how easily plastic material would oxidise in the environment. Extensive oxidative degradation typically results in fragmentation.	Incorporation of stabilisers and additives may result in the ease of oxidation (as suggested by chemical structure) to be significantly different in compounded plastics.
Biodegradability	Determines the rate of mineralisation and potential partial removal of plastics from the water column or sediment.	Ordinary chemicals are generally bio-inert. However, exceptions do exist in synthetic as well as biopolymers.
Residual monomer	Toxicity of leaching residual monomers (bisphenol A [BPA] or phthalate plasticisers) in MPs to marine organisms via ingestion.	Residual monomer and toxicity levels in conventional plastics are reliably known.
Transport properties	Bioavailability of residual monomers, additives, and POPs sorbed by the MPs depend on their leaching rates in the gut environment.	These properties are initially known for virgin resins but can change due to changes in crystallinity varied by sample history and additives.
Additives	Toxicity and concentration of additives in MPs may contribute to adverse impacts on ingesting species.	Chemistry, levels of use in plastics, and toxicities are generally known. However, levels for endocrine disruptors are not reliably known.
Surface properties	Fouling rates of floating debris determine the weathering and sinking rates of MPs.	Fouling rates and surface properties of conventional plastics are known.

2.4 Polymer chemistry and properties

2.4.1 Polypropylene (PP)

PP is produced via chain-growth polymerisation of the monomer propylene. It forms part of the polyolefin family and is widely used in applications that require toughness, flexibility, lightweight, and heat resistance (Encyclopedia Britannica, 2017). PP is the second-most widely produced plastic and is often used for packaging and labelling. Isotactic polypropylene (i-PP) is produced at low temperatures and pressures via Ziegler-Natta catalysts. PP softens at higher

temperatures with a melting point of approximately 170°C. PP is the commodity plastic with the lowest density, and at room temperature, it is resistant to fats and almost all organic solvents, besides strong oxidants. Due to the tertiary carbon atoms, PP is chemically less resistant to degradation than PE (Koltzenburg et al., 2014). The demand for PP is rapidly increasing, and therefore it is one of the most common types of MPs found in the marine environment. The repeating unit of the polymer PP is shown in Figure 2.1.

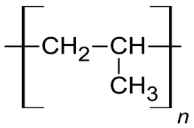

Figure 2.1. Repeating unit of the polymer polypropylene (PP).

2.4.2 Poly(ethylene terephthalate) (PET)

PET is produced from ethylene glycol and dimethyl terephthalate (DMT) or terephthalic acid (TPA). In the former, the reaction is transesterification while the latter involves an esterification reaction. Today more than 70% of global PET production is based on the esterification of TPA (Rieckmann & Volker, 2003). PET is the most common thermoplastic polymer of the polyester family and is the fourth most widely produced. It is primarily used in fibres for clothing as well as containers for liquids and foods. PET may exist as an amorphous or semi-crystalline polymer, depending on its processing and thermal history. The repeating unit of the polymer PET is shown in Figure 2.2.

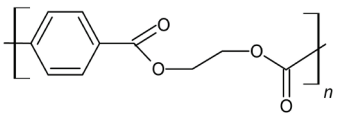

Figure 2.2. Repeating unit of the polymer poly(ethylene terephthalate) (PET).

Some important properties of PP and PET microplastics are shown in Table 2.2 below.

Table 2.2. Plastic properties of common MPs [Adapted from Andrady, 2017].

Property	**PP**	**PET**
Chemical formula	$(C_3H_6)_n$	$(C_{10}H_8O_4)_n$
Glass transition (°C)	-25	+69
Density (g/cm^3)	0.90	1.29-1.40
Crystallinity (%)	30-50	10-30
UV/ oxidation resistance	Low	Good
Strength (psi)	4500-5500	7000-10500
Surface energy (MJ/m^2)	33	45.1

From Table 2.2 above, it is evident that the glass transition temperature (T_g) for PP is much lower than for PET. This temperature is a valuable property when considering the end use of the polymer. When plastics are used below their T_g, their physical properties change in a manner similar to those of a glassy or crystalline state. Conversely, when they are used above their T_g, they behave like flexible (elastic) material. The T_g of a polymer is the temperature below which molecules have little relative mobility. The value however varies and cannot be exact as it depends on the strain rate, and cooling or heating rate during manufacturing (Baur et al., 2016).

The density of PP (0.90 g/cm^3) is also lower than that of PET (1.29-1.40 g/cm^3). This gives an initial indication of the sinking or floating behaviour. Assuming the density of seawater to be in the range of 1.02-1.03 g/cm^3 (Brown et al., 1989), PP particles would supposedly float while PET would sink. For PP the crystallinity ranges of common MPs are also higher than for PET. Crystallinity is thoroughly discussed in Section 2.6.2.1. Percentage crystallinity is an indication of the structural order of the crystalline and amorphous regions of the plastic. This property influences oxygen permeability and is directly correlated to density.

PP also has lower UV/oxidation resistance than PET. This is due to the tertiary carbon atoms in PP whereas PET has stabilising aromatic rings. The stability of plastic is also highly influenced by other factors such as additives, stabilisers, and chromophoric groups. In terms of strength, PET is generally more robust than PP and also has higher surface energy.

2.5 Degradation pathways and mechanisms

Degradation is defined as an irreversible process leading to a significant change in the structure of a material, typically characterised by a change of properties (e.g. integrity, molecular mass or structure, mechanical strength) and/or by fragmentation, affected by environmental conditions proceeding over a period of time and comprising of one or more steps (ISO, 2019).

There are different processes (and mechanisms) according to which degradation can take place, and in general, it is classified by the agency leading to it. For example, degradation by the action of light and oxygen is known as photo-oxidative degradation. Some degradation processes and their causing agents are shown below in Table 2.3.

Table 2.3. General degradation processes and causing agents [Adapted from Andrady, 2011].

Degradation process	**Causing agent**
Photo-oxidative degradation	Action of light (usually sunlight)
Thermo-oxidative degradation	Slow breakdown at moderate temperatures
Hydrolytic degradation	Reaction with water
Thermal degradation	Action of high temperatures
Biodegradation	Action of living organisms (normally microbes)
Mechanical degradation	Action of forces by waves, tides, and sand

The following sections will cover some of the degradation processes specifically relevant to this study. Since the main focus of this investigation was on degradation due to UV radiation, photo-oxidative degradation will preferentially be considered and receive the most emphasis.

Nevertheless, it is acknowledged that this may not necessarily be the only process involved and therefore potential for other processes (thermo-oxidative and hydrolysis) will also be addressed. In an attempt to be as environmentally relevant as possible, relatively low temperatures were used during the experiments. No living organisms were purposely added to the solutions or exposed to the plastic material. Samples were also not subjected to abrasion (by sand) or mechanical forces (by vigorous stirring and shaking). For these reasons, thermal-, bio-, and mechanical-degradation will not be considered.

2.5.1 Photo-oxidative degradation

This section will focus specifically on photo-oxidative degradation since oxygen was present during all experimental runs. Only in an inert environment (nitrogen, argon, or under vacuum) would pure photodegradation occur. General photo-oxidation will be described according to three steps: initiation, propagation, and termination, which make up the auto-oxidation cycle as in Scheme 2.1. Thereafter plastic specific reaction schemes will be depicted.

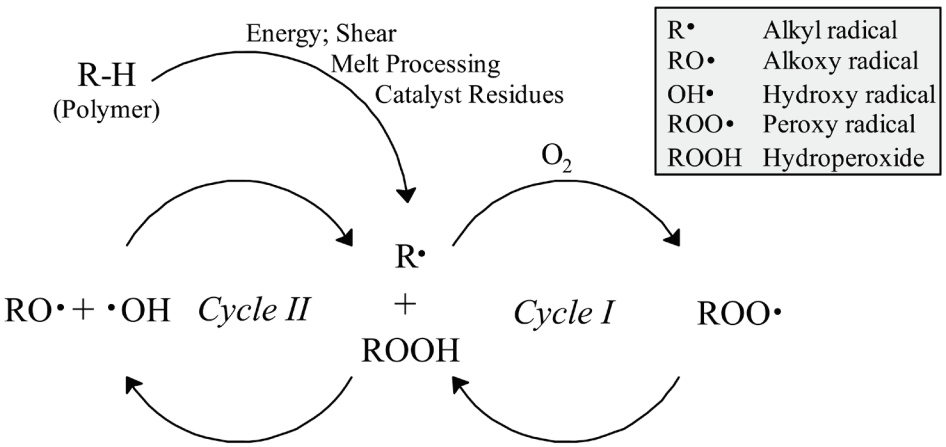

Scheme 2.1. Simplified Ciba Cycle for degradation of polyolefins [Adapted from de Goede (2006)].

Initiation typically involves the formation of free radicals; these radicals may form when the polymer absorbs high energy (short-wavelength) UV light which results in bond breakage. Propagation takes place when free radicals react with molecular oxygen producing polymer oxy-, and peroxy radicals, as well as secondary radicals causing chain scission. Finally, termination occurs due to reactions between different radicals, terminating the process, and ultimately resulting in crosslinking. The following section obtained from Rabek (1995) describes the above-mentioned steps in more detail.

During initiation, polymers (PH) containing intra-molecular chromophoric groups and/or light-absorbing inter-molecular impurities (RH), can produce radicals in the presence of air (oxygen) under UV or visible irradiation:

$$PH \xrightarrow{hv\,(O_2)} P^{\cdot} + HO_2^{\cdot} \qquad RH \xrightarrow{hv\,(O_2)} R^{\cdot} + HO_2^{\cdot} \qquad PH + R^{\cdot} \rightarrow P^{\cdot} + RH$$

Where $P^{\cdot}$ denotes the alkyl radical and $HO_2^{\cdot}$ the hydroperoxyl radical. If hydroperoxyl radicals are formed, they can react with one another to produce hydrogen peroxide (H_2O_2), which can be further photolysed into hydroxyl ($HO^{\cdot}$) radicals, which in turn react with polymer (PH) to produce polymer alkyl ($P^{\cdot}$) radicals:

$$HO_2^{\cdot} + HO_2^{\cdot} \rightarrow H_2O_2 + O_2 \qquad H_2O_2 \xrightarrow{hv} HO^{\cdot} + {}^{\cdot}OH \qquad PH + HO^{\cdot} \rightarrow P^{\cdot} + H_2O$$

Thus far, there is no direct proof indicating the participation of $HO^{\cdot}$ and $HO_2^{\cdot}$ in the initiation step. The relative importance of various possible mechanisms for photoinitiation involving ketone groups, hydroperoxides, catalyst residues, singlet oxygen, atomic oxygen, and ozone is debated to this day. However, without substantially influencing the course, rate, or extent of chain propagation, this debate remains irrelevant (Rabek, 1995).

The most important reaction in the propagation sequence involves the formation of polymer peroxy radicals ($POO^{\cdot}$) from the reaction between polymer alkyl radicals ($P^{\cdot}$) and oxygen:

$$P^{\cdot} + O_2 \rightarrow POO^{\cdot}$$

This reaction is swift but diffusion-controlled. The following step is the abstraction of a hydrogen atom by the polymer peroxy radical ($POO^{\cdot}$) to generate a new polymer alkyl radical ($P^{\cdot}$) and polymer hydroperoxide ($POOH$).

$$POO^{\cdot} + PH \rightarrow P^{\cdot} + POOH$$

The propagation step is very much dependent on the efficiency of the decomposition (photolysis and/or thermolysis) of polymer hydroperoxides ($POOH$) during which new free radicals such as polymer oxy radical ($PO^{\cdot}$) and hydroxyl radical ($HO^{\cdot}$) are formed:

$$POOH \xrightarrow{hv\ or\ \Delta} PO^{\cdot} + {}^{\cdot}OH$$

This reaction is mainly initiated by an energy transfer process from a carbonyl group (CO) to a hydroperoxide group (OOH) and is dependent on the so-called cage recombination reaction. Polymer oxy radicals ($PO^{\cdot}$) and very mobile hydroxyl radicals ($HO^{\cdot}$) abstract hydrogen from the same, or a neighbouring, polymer (PH) chain:

$$PO^{\cdot} + PH \rightarrow POH + P^{\cdot} \qquad HO^{\cdot} + PH \rightarrow P^{\cdot} + H_2O$$

Polymer oxy radicals ($PO^{\cdot}$) can also undergo several other chemical reactions (considered chain branching reactions) including:

- β-scission reactions that result in the fragmentation of the polymer chain together with the formation of end carbonyl (or end aldehyde) groups and end polymer alkyl radicals.

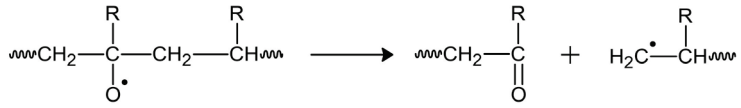

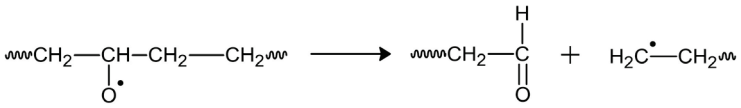

- Formation of in-chain ketone groups.

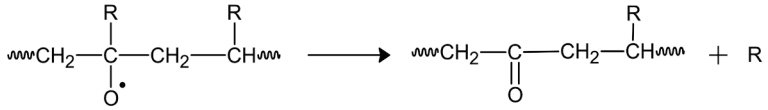

- Radical induced hydroperoxide decomposition.

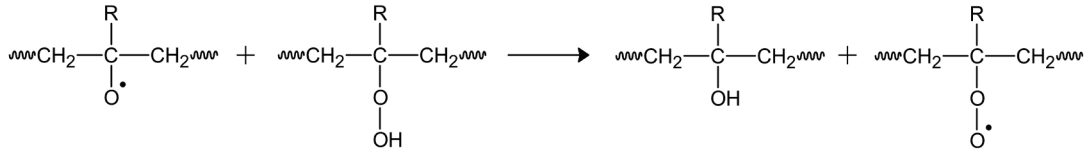

- The reaction between two polymer alkoxy radicals producing a carbonyl and hydroxyl group simultaneously by disproportionation.

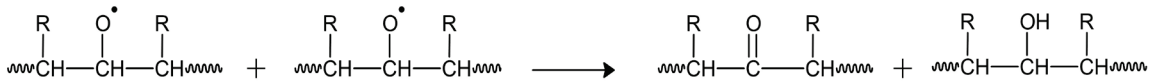

The formation of ketonic groups contributes significantly to further mechanisms of oxidative degradation. These ketonic groups are often formed during polymer manufacturing at high temperatures.

The degradation sequence is terminated when radical species recombine. These radical recombination reactions are usually between two bimolecular species, or between low molecular radicals - such as hydroxyl ($HO^{\cdot}$) and hydroperoxyl ($HO_2^{\cdot}$) - and other available radicals. Some of the main termination reactions are shown below.

$$P^{\cdot} + P^{\cdot} \rightarrow P - P \qquad P^{\cdot} + POO^{\cdot} \rightarrow POOP \qquad POO^{\cdot} + POO^{\cdot} \rightarrow POOP + O_2$$

The next section will consider the reaction mechanisms for plastic investigated explicitly in this study. In order to be concise, depictions of the complete reaction mechanisms (from initiation to termination) will not be included. However, some of the most essential reaction schemes will be illustrated.

Photo-oxidative degradation of PP

The photooxidation mechanism of isotactic PP is widely reported in literature (Bocchini et al., 2007; Lacoste et al., 1993). Rapid photolysis has been attributed to chromophoric (ketone) groups as well as hydroperoxide groups formed during processing and storage. Impurities such as metallic catalyst residues may also initiate the process (Rabek, 1995). The primary product of combined action of UV radiation and oxygen is tertiary hydroperoxides (POOH). These hydroperoxides decompose to produce alkoxy ($PO^{\cdot}$) and hydroxy ($OH^{\cdot}$) radicals which are able to easily abstract tertiary hydrogen atoms from a polymer backbone and propagate chain oxidation. Alkoxy radicals can also undergo β-scissions with scission of C-C bonds (either in the main polymer backbone or methyl-backbone bond) (Bocchini et al., 2008).

Two types of ketone groups, in-chain and at the chain ends, can be responsible for scission processes that occur by the Norrish I and II photochemical reactions. Successive oxidation of the products continues producing carboxylic acids, esters, peresters, and lactones. These products are often witnessed by the presence of a broad carbonyl band around 1800-1600 cm^{-1} from FTIR spectroscopy. Chemical modifications due to photooxidation are easily monitored by infrared (IR) spectroscopy. Analysis typically shows the formation of products in the carbonyl range (ketones and carboxylic acids), as well as in the hydroxyl region, corresponding to hydroperoxides and alcohols. Scheme 2.2 below illustrates this process.

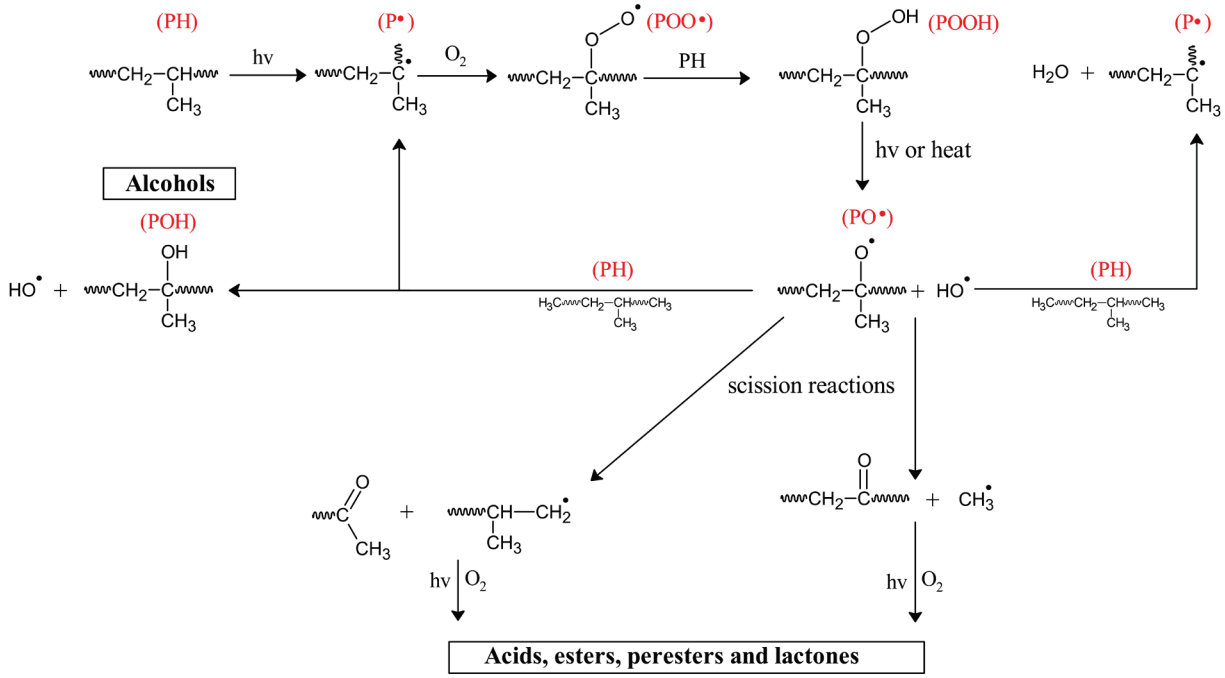

Scheme 2.2. Photooxidative degradation of PP [Adapted from Bocchini et al. 2008].

Pegram & Andrady (1989) studied the weathering of conventional plastic material in air and in seawater. Degradation was measured by tensile property determination. It was statistically concluded that the degradation rate was lower in seawater than in air. PP tape exposed on land, lost 90% of its initial ultimate extension, while tape exposed at sea only lost 26%.

Wu et al. (2018) observed the photodegradation of three types of plastic pellets PE, PP, and polystyrene (PS) exposed to UV radiation in three different environments: simulated seawater, ultrapure water, and in air. FTIR analysis showed the development of new peaks at 3300 cm^{-1} (OH) and 1712 cm^{1} (C=O) for all three plastic types in air and ultrapure water, while only carbonyl groups were found in pellets from simulated seawater. Chemical weathering increased with exposure time. Pellets from the air environment underwent higher degradation than those from the aqueous solutions, and authors believed it was related to the level of oxygen exposure. Photo-oxidative degradation was more effective in air than in water. In addition to that, ultrapure water resulted in higher degradation than seawater, which was suggested to be as a result of salinity differences. The empirical equation for the refraction index of seawater describes an increase in refractive index with an increase in salinity (Quan & Frey, 1995). This translates to light travelling slower through water with higher salinities. Overall, degradation occurred due to photo-oxidation caused by free-radical chain reactions.

Khoironi et al. (2020) investigated the degradation of PP samples immersed at different depths in seawater. Photodegradation was identified by monitoring carboxylic acid, aldehyde, alcohol, ester, ether, and ketone groups between 1457 and 2832 cm^{-1} as in Sowmya et al. (2014). Oxidative degradation was considered by the formation of carbonyl groups between 1630 cm^{-1} and 1850 cm^{-1}. Results indicated the formation of new carbonyl groups at 1720 cm^{-1} as well as reductions in organic carbon content. At the seawater surface, samples underwent photo-oxidative degradation while at depths of 50 cm and 70 cm, photo- and biodegradation were the prevalent mechanisms, respectively.

Ojeda et al. (2011) studied the natural weathering of linear polyolefins (PE and PP). It was mentioned that the durability of polyolefins might be significantly shorter than centuries since in less than one-year, the mechanical properties of all samples deteriorated to virtually zero. Degradation was described to be due to severe oxidative degradation that resulted in substantial reductions in molar mass, accompanied by a significant increase in carbonyl content. PP samples degraded much faster than high-density PE (HDPE) and linear low-density PE (LLDPE), which was mainly attributed to the frequency of tertiary carbon atoms in its chain. The melting and crystallisation temperatures of PP decreased with exposure time; this resulted from an increase in crystal defects occurring with oxidative degradation such as oxygenated groups, double bonds, chain ends, and branch sites. These defects result in smaller crystals with more imperfections. The degree of crystallinity of PP samples decreased, whereas that of HDPE and LLDPE increased.

A paper by Severini et al. (1988) considered the environmental degradation of PP films. It was found that a continuous reduction in mechanical properties occurred after 700 hours of exposure. Crystallinity changed irregularly and thermal oxidation strength decayed in the initial stages of degradation. Data were reported on the absorbance of the carbonyl groups, molecular weight, and quantum yield. The linear relationship between molecular weight and C=O absorbance led authors to believe in a degradation mechanism based mainly on β-scission reactions of macroalkoxy radicals formed by the photodecomposition of hydroperoxides.

Rabello & White (1966) investigated the photodegradation of PP containing a nucleating agent. PP bars containing the nucleating agent showed a more substantial reduction in mechanical properties with UV exposure, and after prolonged exposure, a partial recovery was observed for samples with, and without the incorporated additive. This ability to recover its mechanical properties was ascribed to the development of a fragile degraded layer that was unable to propagate surface cracks into the nondegraded interior. Photodegradation rates were similar for

both samples. Increased crystallinity during UV exposure was attributed to the chemi-crystallisation effect and detected with X-ray diffraction (XRD) and DSC. For exposures exceeding eighteen weeks, molecules contained a large number of chemical irregularities (carbonyl and hydroperoxide groups) that prevented further increases in fractional crystallinity, and a plateau value was obtained.

Another study by Iñiguez et al. (2018) looked at UV degradation of four different plastic types (Nylon, PE, PP, and PET) in marine-like conditions. Results showed mechanical properties being affected with samples weakening; becoming less elastic and more rigid. PP and PET were the most affected. Cracks, flakes, granular oxidation as well as a loss of homogeneity on the sample surfaces were observed with scanning electron microscopy (SEM) and atomic force microscopy (AFM). The authors described photo-oxidative degradation to be the main reason for crack formation.

De Bomfim et al. (2019) investigated different degradation conditions on waste PP espresso capsules. For the accelerated weathering conditions (UV and humidity), samples showed continuous mass loss suggesting that humidity was not absorbed by the hydrophobic PP surface. Samples became yellow and fragile. Black samples suffered partial pigment discolouration primarily due to chromophoric groups forming on the plastic surface. PP samples also showed decreases in crystallinity as obtained from DSC analysis. In terms of FTIR, naturally weathered samples indicated the disappearance of bands at 1745 cm^{-1} (C=O) and 1648 cm^{-1} (C=C). These findings suggest breakage of a double bond resulting in the formation of free-radicals. Samples exposed to UV radiation indicated new bands at 3306 cm^{-1} (O-H) and 560 cm^{-1} (due to TiO_2 pigment). It was concluded that UV exposed samples suffered critical surface damage due to the presence of chromophoric groups such as C=O and O-H.

Photo-oxidative degradation of PET

A comprehensive summary of the photodegradation and photooxidation of PET is provided by (Fagerburg & Clauberg, 2003). The authors illustrated different degradation paths, including direct photodegradation (Norrish I and II reactions), photothermal, and finally photo-oxidative degradation. For this discussion, preference is given to the oxidative routes. The first reaction involves radical abstraction (by any radical present in the matrix), which reacts with oxygen to form a hydroperoxide radical. The hydroperoxide radical is converted to hydroperoxide via hydrogen abstraction. This path has been suggested as a mechanism for glycol oxidation. The hydroperoxide of the glycol unit decomposes, thermally or photolytically, resulting in scission

reactions forming products such as carboxyl radicals and aliphatic aldehydes in which the latter could undergo hydrolysis to form glyoxal. Additional hydrolysable products formed by scission include an anhydride of formic acid and a terephthalic acid half chain end. Ultimately photo-oxidative degradation products from this path include glyoxal, formaldehyde (oxidised to formic acid), methyl ester, and glycolic and oxalic acids.

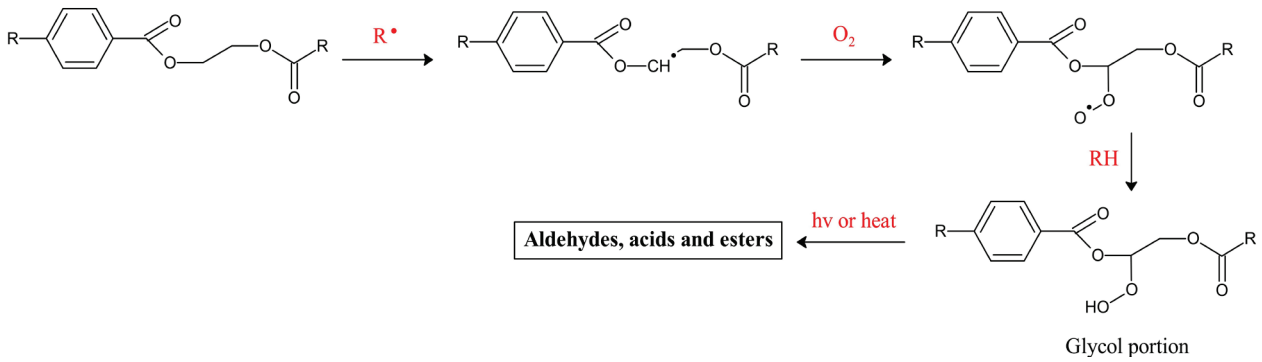

Scheme 2.3. Photooxidation reaction 1 of PET [Adapted from Fagerburg & Clauberg, 2003].

A different reaction path is a ring-oxidation reaction and requires the presence of a hydroxyl radical as in Scheme 2.4. It is easily seen how one can produce the reported hydroxyterepthalic moiety. A repeat of this oxidation would produce the reported 2,5-dihydroxyterepthalate. At this point, it is worth noting that the dihydroxy compound is the first identifiable compound that has colour. It is proposed that this compound could give rise to quinone. Another route (not showed) involves phenyl radicals and simple hydrogen abstraction of cleaved ester rings producing benzene.

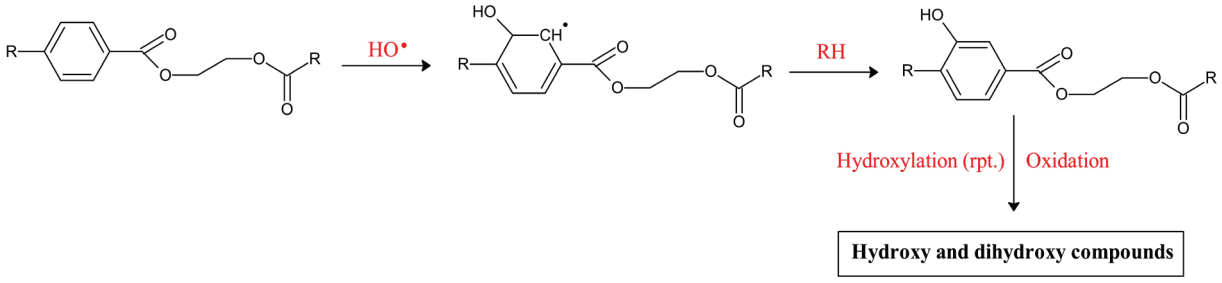

Scheme 2.4. Photooxidation reaction 2 of PET [Adapted from Fagerburg & Clauberg, 2003].

Allen et al. (1991) found no significant relationship between chain scission and light-induced crystallinity of PET. Despite observing high degrees of chain scission after prolonged UV exposure, crystallinity was found to have increased by only 5%. The dominating degradation process was established to be hydrolysis which is discussed in Section 2.5.3.

Allen et al. (1994) considered the degradation of amorphous PET bottles and sheets under different environmental conditions (soil, humidity, and UV radiation). The rate of chain scission was measured (by viscometric analysis), as well as end-group analysis (using FTIR), and crystallinity (via density measurements at different temperatures). It was concluded that the difference in end group concentrations during UV exposure was contributed to the Norrish type II hydrogen abstraction mechanism. The authors also suggested that initial crystallinity significantly influenced photolytic degradation as degradation was more severe in amorphous and low crystalline samples.

Photodegradation of PET with UV irradiation of wavelength 312 nm was investigated by Fujimoto & Fujimaki (1995). GPC measurements showed no significant change in M_w and M_n of the samples. Dynamic mechanical analysis (DMA) revealed the formation of a three-dimensional (3D) network for PET. From FTIR-ATR, intensity bands at 1713 cm^{-1} (C=O of ester) and 1098 cm^{-1} (C-O-C) decreased, and new bands at 3480 cm^{-1} (O-H), 2650 cm^{-1} (C-H of aldehyde), 1760 cm^{-1} (C=O of aldehyde), and 1688 cm^{-1} (C=O of COOH) formed. It was concluded that PET degradation proceeded via a photo-Fries rearrangement leading to the 3D networks, followed by photo-oxidation, that cleaved the main polymer chains.

Weathering of thermoplastic polyester elastomers was studied by Nagai et al. (1997). It was concluded that ether parts of the soft segment in the polymer degraded selectively as ester bonds were formed. In both outdoor and accelerated laboratory tests, chain scission and crosslinking occurred with the amount of crosslinked products significantly higher for accelerated laboratory tests. FTIR analysis showed an increase in the C-O (aliphatic ester) band at 1175 cm^{-1}, as well as the broadening of the carbonyl band near 1720 cm^{-1}. From this result, it was clear that several types of carbonyl groups were formed. It was suggested that the formation of aliphatic ester bonds was caused by the exposure tests.

Scheirs & Gardette (1997) investigated photo-oxidation and photolysis of poly(ethylene naphthalene) using FTIR and UV absorbance spectroscopy. Results indicated that photochemical reactions were restricted to the very outer surface of the polymer within a layer of approximately ten microns. According to the authors, photo-oxidation was responsible for the formation of acidic end groups as major photoproducts. Naphthalate structures were rapidly decomposed by light and the formation of a highly oxidised polymer layer acted as a protective barrier against UV light.

Lee et al. (2012) performed a two-dimensional (2D) correlation analysis on FTIR results obtained from photodegradation of PET films. This led to the identification of photoproducts, such as

esters, peresters, and benzoic acids. Photodegradation was described to strongly influence spectral changes of the ester linkages, as well as their adjacent CH_2 groups. Spectral changes of CH_2 groups preceded changes in terephthalate groups. FTIR intensity bands at 1716 cm^{-1} (C=O) decreased, while those at 1785 cm^{-1} (perester derivative) and 1695 cm^{-1} (benzoic acid) increased, with increasing UV exposure.

Hurley & Leggett (2009) observed surface property changes, including a decrease in contact angle and an increase in friction coefficient, upon degradation. X-ray photoelectron spectroscopy (XPS) analysis showed increased oxygen concentration at the surface, which was attributed to the reaction between radicals and atmospheric oxygen as well as the increase in ester and carbonyl content. It was suggested that photodegradation progressed through radicals (formed via Norrish type I reactions), leading to carboxylic acid and aldehyde groups.

Savchuk & Neverov (1982) showed that the rate of photo-oxidative induced crystallisation was higher in amorphous than in crystalline polymers. The initial polymer orientation was found to affect its extent of degradation.

Yadav et al. (2011) demonstrated outdoor and indoor testing of PET fibres and evaluated their mechanical properties. Microhardness testing revealed increased hardness accompanied by deterioration of tensile properties as solar and artificial exposure was increased. It was also stated that exposed samples depicted a neck formation in a stress-strain curve, whereas unexposed samples did not show this behaviour. This was attributed to inhomogeneity in the structure that set in a result of radiative exposures.

2.5.2 Thermo-oxidative degradation

De Goede (2006) described the thermo-oxidative degradation of unstabilised isotactic PP. The process is similar to photo-oxidative degradation as in Section 2.5.1 and involves the auto-oxidation cycle comprising of initiation, propagation, and termination.

Initiation involves the formation of alkyl radicals (tertiary or secondary) under the influence of shear, heat, or photo-initiation. These radicals follow different routes, but as mentioned earlier, the tertiary radical is predominantly formed. Tertiary alkyl radicals react with oxygen to form tertiary peroxide which will then be converted to a hydroperoxide. Hydroperoxide then decomposes via two avenues; (i) reacting with hydrogen to form tertiary alcohol, (ii) β-scission to form ketone, and macroalkyl radicals. At this point, the main mechanistic difference between photo-, thermo-oxidation is revealed. In the former, photochemical Norrish reactions are

responsible for the further reaction of the formed ketone species while in the latter it is not the case.

The primary chain end by scission can be oxidised further to form an aldehyde or alcohol and water. The main degradation products of thermo-oxidative degradation of PP include hydroperoxides, alcohols, ketones, carboxylic acids, and lactones. Aldehydes are highly reactive and can further be oxidised to form peracid groups. Termination of thermo-oxidation of i-PP can take place via several reactions. PP degrades preferentially via chain scission reactions. However, several other disproportionation reactions may take place. During decomposition, terminal vinylidene groups are formed.

Philippart & Gardette (2001) compared the mechanisms of thermo-and photo-oxidation of isotactic PP. It was found that in thermo-oxidative conditions above 95°C, the formation of oxidation products involves hydrogen abstraction by peroxy radicals, leading to hydroperoxides as primary products. In photo-oxidation at 60°C, two reactions compete: hydrogen abstraction and recombination of peroxy radicals by a non-terminating reaction with the latter producing molecular oxygen and radical species. Nevertheless, the nature of oxidation products was independent of the mechanism of the reactions of peroxy radicals. Oxidation products formed involved the rearrangements of the alkoxy radicals ($PO^{\cdot}$) that were produced either by hydroperoxide or unstable tetroxide decomposition.

The thermo-oxidative degradation of PET involves reaction with oxygen at elevated temperatures (usually above T_g) (Mueller, 2000). This process starts with the formation of a hydroperoxide at the methylene group in the diester linkage of the PET chain (Zimmerman, 1984). It is also believed to follow a free radical mechanism leading to chain cleavage and the formation of carbon and oxygen radicals, carboxyl, hydroxyl, and vinyl ester end groups. Secondary radical reactions can also lead to the formation of branched chains (Zimmerman & Becker, 1976). Previous tests of PET in air at 130°C for 200 hours did not lead to any evidence of thermal oxidation (Fagerburg & Clauberg, 2003).

2.5.3 Hydrolytic degradation

Hydrolysis is a process where a polymer reacts with water which physically changes its polymeric chains by splitting them into two (Booth et al., 2017). This process is not limited to the surface of the polymer (as photodegradation) since water can permeate through the bulk of the material. Hydrolytic reactions are typically catalysed by an acid, base, or enzyme with the former two

resulting in a product with a carboxylic acid end group. It is also accompanied by an increase in hydroxyl end groups, and there is no discolouration of the product or evolution of volatile products (Mueller, 2000).

Under acidic or basic conditions, the rate of hydrolysis is increased (Allen et al., 1991). Polyesters undergo random hydrolytic ester cleavage, and its duration is determined by the initial molecular weight as well as the chemical structure of the polymer (Pitt et al., 1981). Hydrolysis is influenced by several factors, including shape, morphology, crystallinity, relative humidity, and temperature, but bond stability remains one of the most important (McIntrye, 1985). This process decreases with increasing hydrophobicity and molecular weight. In addition to that, polymers with higher crystallinities also undergo slower hydrolysis due to crystallites acting as barriers not allowing water and oxygen to permeate through. The opposite is true for amorphous and porous structures.

Polyolefins (PP and PE) are not susceptible to hydrolytic degradation, while those with hydrolysable ester or amine groups (PET and PU) are. Hydrolysis is autocatalytic (accelerated by increased concentration of carboxyl end groups), but its relative rate is much slower than photodegradation. For PET, hydrolysis is the most important degradation process at low temperatures (Edge et al., 1991).

Neutral pH levels in seawater retard the rate of hydrolysis as no strong alkaline, or acidic conditions are present. However, the further degradation proceeds and more polymer chains are cleaved, the more carboxylic acid groups are formed. This decreases the pH locally within the material, consequently increasing the rate of hydrolysis (Hosseini et al., 2007).

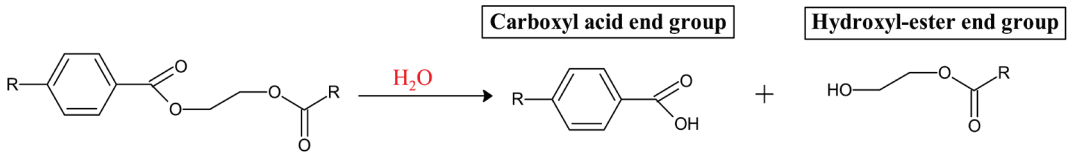

Scheme 2.5. Hydrolysis of PET [Adapted from Gewert et al. 2015].

2.6 Factors influencing degradation

This section covers some general factors known to influence degradation. Initially, environmental factors will be addressed. These include, but are not limited to, UV radiation, temperature, oxygen, and water. It should be mentioned that degradation often relies on several of these factors working together. Thereafter the influence of polymer specific properties will be discussed. These include material properties such as crystallinity, molecular weight, functionality and so on. As degradation occurs, polymer properties are subject to change and further influence the way in which

degradation proceeds. The last topic of discussion entails some degradation expectations, specifically due to polymer type. This study considered plastic material significantly different in terms of chemical composition and chain configurations which accordingly suggests different responses to degrading conditions as well.

2.6.1 Environmental conditions

2.6.1.1 UV radiation

UV radiation determines the useful lifetime of plastic products in outdoor exposures (Andrady et al., 1998). The damage inflicted on polymers exposed to UV radiation is generally intensity-dependent, and degradation at UV wavelengths is described to be highly efficient. The synergistic effect of solar UV radiation and high temperatures particularly results in accelerated deterioration. Degradation due to increased UV levels will invariably be determined by: (i) the spectral irradiance distribution of the UV source and the surrounding temperature, (ii) the spectral sensitivity and dose-response characteristics of the material and (iii) the efficacy of stabilisers under spectrally altered light conditions (Andrady, 2006).

Increased UV intensities result in increased rates and extents of degradation. To visualise why this is the case, it is useful to consider photons as reagents in a photochemical reaction (Daglen & Tyler, 2010). By increasing the intensity, the concentration of photons (reagents) is increased. This translates to more photons impinging on polymeric surfaces and in turn more light being absorbed. Absorbed light further initiates radical reactions and, in some cases, overcomes the bond energy holding molecular structures intact. Increased reaction (degradation) rates due to increased reagent concentrations correspond to what would typically be the case for an elementary reaction. It is worth noting that the effect of UV intensity is also closely correlated to the concentration of chromophoric groups (metal residues, carbonyl, and hydroperoxides) as these species are mainly responsible for light absorption.

In general, disregarding spectral sensitivity of the polymer, lower wavelengths exert more damage per incident photon. This has been proven by monochromatic experiments where a linear relationship existed between the logarithm of damage effectiveness and the wavelength of exposure (Andrady et al., 1998).

2.6.1.2 Temperature

Temperature affects the kinetics of all chemical reactions. The temperature dependence of reaction rates is described by the Arrhenius equation and in general higher temperatures result in

accelerated reaction rates. Numerous studies have investigated the effect of temperature during thermal degradation. Plastic lifetime predictions are often made by assuming Arrhenius behaviour and extrapolating results to lower (environmentally applicable) temperatures.

However, studies regarding the effect of temperature during photochemical reactions are mostly inconclusive with quantum yields indicating Arrhenius and non-Arrhenius behaviour. These deviations were suggested to be due to complexities surrounding degradation pathways. For PP and PE, Arrhenius plots are non-linear, suggesting a change in mechanism and/or rate-limiting step with temperature (Celina et al., 2005). Overall, increasing temperatures can have direct and indirect effects on degradation rates; these include increases in kinetic energy, free volume, molecular mobility, and radical diffusivity (Daglen & Tyler, 2010).

Light-induced degradation is accelerated by a factor depending on the activation energy (E_a) of the process. With an activation energy of 50 kJ/mole, for instance, the degradation rate doubles when the temperature is increased by 10°C (Andrady, 2011). Plastic material washed out on beaches are subjected to very high temperatures relative to those afloat in the oceans. This is due to the low specific heat of sand that can easily reach temperatures exceeding 40°C during summer months. The ocean also acts as a heat sink, absorbing solar energy while its temperature remains relatively constant. Dark plastic can undergo a heat build-up, raising its temperature higher than surrounding air which can, in turn, promote its degradation (Shaw & Day, 1994).

The diffusion of oxygen, radicals, and water is also influenced by temperature (Booth et al., 2017). Increased diffusion rates (at higher temperatures) result in higher reaction rates since reactants (oxygen, unreacted radicals, and water) diffuse deeper into the polymer structure and consequently expose larger volumes to degrading conditions.

2.6.1.3 Oxygen

The auto-oxidation cycle can proceed provided oxygen is available to the system. Oxygen availability affects degradation rates of all processes that depend on its presence, e.g. photodegradation which proceeds via photo-initiated oxidative degradation. In the solid-state, oxygen diffusion is often the rate-limiting step in the auto-oxidative degradation of polymers (Davis et al., 2004). This is contingent on sample thickness, morphology, and permeability of the polymer towards oxygen (Pospíšil et al., 2006). Higher oxygen concentrations (partial pressures) would accelerate reaction rates until a different reaction becomes rate-limiting. The availability of oxygen also plays a crucial role in biodegradation and controls the composition of microbial

communities in each environmental matrix (Booth et al., 2017). The marine environment offers lower temperatures, oxygen concentrations, and UV radiation relative to exposure in air. One cubic meter of air contains about 270 g of oxygen, the same volume of marine water in equilibrium with air holds only 5-10 g, depending on temperature and salinity (Muthukumar & Doble, 2014). Consequently floating plastic debris is far less likely to undergo extensive degradation in this environment (Andrady, 2011).

2.6.1.4 Water

Water is essential for degradation processes such as hydrolysis and biodegradation. In the marine environment, water is rarely a limiting parameter but may play a more important role in influencing the rate of degradation on shorelines. Water reduces the intensity of UV light, which means photo-oxidative degradation only occurs in the upper region of the water column. This was shown experimentally by Khoironi et al. (2020) for PP who studied environmental degradation at different depths. At the ocean surface, moisture and high humidity levels promote light-induced degradation since photo-soluble stabilisers may leach out of the plastic matrix. This reduces the effectiveness of stabilisation and promotes degradation.

2.6.2 Polymer properties

2.6.2.1 Crystallinity

Polymer crystallinity is typically measured by DSC, XRD, or Raman spectroscopy and refers to the arrangement of molecular chains to produce an ordered atomic array (Callister & Rethwisch, 2015). These chains fold and form ordered regions called lamellae, which compose of larger spheroidal structures named spherulites (Puoci, 2014). Due to their size and complexity, polymer molecules are often only partially crystalline (semi-crystalline), having crystalline regions dispersed within the remaining (often dominant) amorphous material.

Chain disorders or misalignments result in amorphous regions since twisting, kinking, and coiling of chains prevent strict ordering of chain segments (Callister & Rethwisch, 2015). Amorphous regions are responsible for material flexibility. The density of a crystalline polymer is greater than an amorphous one of the same molecular weight and material. This is due to chains being more tightly packed, forming the crystalline structure. Crystallinity depends on the rate of cooling during solidification and also on chain configurations. Excessive branching and crosslinking may prevent crystallisation due to imposed restrictions on chain alignment.

Several polymer properties are influenced by their degree of crystallinity. Increased crystallinity results in material being stronger and more resistant to softening by heat, but excessive degrees of crystallinity may render material brittle (Andrady, 2017). Increased crystallinity also results in greater hardness, density, and tensile strength. The permeability of oxygen and water is reduced in polymers with rigid and compact crystalline structures. Conversely, amorphous structures allow these reactants to enter more readily and penetrate deeper (and in larger volumes) within the material to initiate the degradation cycle. It is therefore believed that degradation in the amorphous regions will proceed more rapidly than in the crystalline regions.

Degradation typically involves morphological changes. Often the case when degradation occurs at temperatures above the glass transition temperature of the plastic, chain scissions liberate short-chain segments initially trapped in the entangled network, allowing them to migrate towards lamellae and integrate within the crystalline phase. This process is known as chemi-crystallisation and has been observed in practically all semi-crystalline polymers.

2.6.2.2 Molecular weight

Molecular weight is important as it determines polymer properties and is closely related to polymerisation (Mierzwa-Hersztek et al., 2019). Polymers with higher molecular weights are typically more resistant to degradation. This is because they have lower relative surface areas available for degradation, and most degrading processes occur at the surface, rather than the interior of the plastic. Since degradation often reduces the molecular weight of polymers (due to scission and generation of shorter fragments and small molecules), the increase in available surface area suggests the rate of the degradation process to increase further (Booth et al., 2017).

2.6.2.3 Morphology and hydrophobicity

Morphology is used to interpret the effect of stress on degradation rates (Singh & Sharma, 2008). Higher stress causes morphological changes, including chain straightening in the amorphous regions of polymers. Changes in morphology, especially during the initial period of PP weathering, has been described to facilitate oxygen solubility and contribute to the initiation of oxidation reactions (Niemczyk et al., 2019). These changes modify the macroscopic properties of the material. Generally, after colour changes and crazing at the surface, degradation can lead to embrittlement and plastic disintegration (Gewert et al., 2015). In addition to that surface polarity and morphology of marine plastic debris govern interactions with organisms of biofilms, e.g. in terms of surface adhesion (Ter Halle et al., 2017).

Petrochemical based plastics generally are not easily degraded in the environment because of their hydrophobic character and three-dimensional structure (Yamada-Onodera et al., 2001). Hydrophobicity causes some plastics to sorb marine and atmospheric POPs (Brandon et al., 2016). Recently the bioaccumulation of pollutants due to ingestion has become particularly concerning. Hydrophobicity also significantly reduces hydrolysis, which is dependent on water diffusion. Photo-oxidation of floating debris introduces oxygen to the plastic surface, consequently reducing hydrophobicity and increasing potential for biological degradation.

2.6.2.4 Functionalisation

The type of chemical functionalisation exhibited by a polymer will affect the rate of degradation. For example, carbonyl groups will increase the rate of photodegradation in polyolefins as they contain chromophores (causing a discolouration of the molecules) (Singh & Sharma, 2008). A higher concentration of chromophores results in more sites being available to absorb a photon and initiate photodegradation. The presence of any metal-metal bonds in the polymer backbone will also induce photodegradability since the metal-metal bond is cleaved homolytically upon irradiation (Meyer & Caspar, 1985).

2.6.2.5 Production route

The production route has also been shown to affect polymer stability. For example, PS formed by anionic polymerisation is more stable towards photodegradation than PS made by free radical polymerisation. This is due to the presence of peroxide residue in the latter, which is highly photolabile. PP made by bulk polymerisation or by Ziegler-Natta catalyst is more susceptible to photodegradation compared to co-polymerised PP (Tang et al., 2005). Alternative production routes can also lead to differences in polymer stereochemistry. PP for instance, can be either atactic, isotactic, or syndiotactic (based on the configuration of the methyl group). Degradation differences between isotactic and atactic PP were studied, and results showed atactic PP to be more stable than isotactic PP (Hatanaka et al., 1999).

2.6.2.6 Additives

Additives are chemicals intentionally added to plastics during their manufacture and processing (Andrady, 2015b). Several organic and metallic compounds are often used as additives for different plastics to provide the material with specific physical and chemical properties. Each additive can theoretically be added to target and modify a specific plastic parameter, thereby customising the overall material properties (Booth et al., 2017).

Additives can be used to enhance material aesthetics, mechanical, thermal, electrical, and optical performance, as well as processability during moulding, extrusion, etc. They are used to modify the long-term behaviour, such as ageing (due to heat, sunlight, weathering, and relative humidity), creep, relaxation, and fatigue (Kyrikou & Briassoulis, 2007).

Since additives are usually inexpensive and straightforward, they are extensively used. Fillers are added to reduce overall production costs and use of raw material. The importance of additives is often overlooked, and in the environment, they could potentially significantly influence degradation. Many additives specifically prevent degradation processes from occurring or retards their progress to ensure a maximum service life of the plastic products (Booth et al., 2017).

In general, stabilisers refer to additives including antioxidants, UV stabilisers, and microbial agents which are specifically designed for their purpose. UV stabilisers protect the polymer from solar UV damage via three strategies: (i) absorbing incident UV radiation using organic (e.g. benzophenones) or inorganic (e.g. rutile titanium dioxide) additives, (ii) quenching the photo-excited species formed in the polymer and (iii) removing free radicals formed in the polymer (e.g. with hindered amine light stabilisers (HALS) (Andrady, 2015b). All of these strategies influence the formation and behaviour of free radicals, derailing the initiation step of photo-oxidative degradation as described earlier in Section 2.5.1.

Antioxidants, such as the aniline group of compounds, terminate the reaction due to the absorption of UV light from sunlight. As a result, these chemical additives will delay, or slow down, the degradation processes of plastics and contribute to their persistence when entering the marine environment. Only once stabilisers are consumed, which may take decades, will plastic material start to degrade more rapidly. In contrast, pro-oxidants used in the production of oxo-degradable plastics act to decompose the material in shorter timeframes (Booth et al., 2017).

2.6.2.7 Thickness

Gardette et al. (2014) investigated the influence of photooxidative degradation on oxygen barrier properties of PET films. It was found that photochemically induced oxidation of PET triggered a decrease in the oxygen permeation coefficient, which affected material properties. This effect was shown to result from crosslinking by the recombination of macroradicals formed by photooxidation. The overall effect confirmed strong thickness-dependency with oxidation only occurring within the first 35 microns of the exposed surface. This implied that, for samples with a thickness larger than the oxidised layer, permeability decreased at the surface whereas that of the core remained unchanged.

Jellinek (1978) discussed thermal barriers and its influence on oxygen diffusion and stated that these barriers ensure light intensity, as well as oxidation rate, to never be completely constant throughout a film. In general, oxidation decreases with increased film thickness (Winslow et al., 1966). Moreover, thicker films undergo longer induction periods and slower oxidation.

2.6.2.8 Surface-Area-to-Volume Ratio (SA/V)

Since microplastics in the marine environment enable the adsorption and transportation of POPs, they act as a vector for the widespread contamination of the aquatic environment with chemical pollutants (Crawford & Quinn, 2016). It is of global concern that the possibility exists in which MPs act and function as mobile reservoirs of toxic, organic compounds. A study reported that 10-50 mm PP pieces were capable of adsorption of polychlorinated biphenyl (PCB) at significant concentrations of 4-117 ng/g. The smaller the plastic, the greater the surface area and thus available sites for adsorption to proceed. It has been demonstrated that smaller plastic has a higher affinity for POPs.

The capacity for adsorption of persistent organic pollutants becomes higher as the size of a plastic piece decreases. The increase in adsorption capacity is a direct result of the increase in surface area and thus an increase in the available sites for chemical adsorption of POPs to take place. Weathering of polymer surfaces causes smooth surfaces to become cracked, chipped, and undulated, thereby increasing the surface area. A weathered plastic surface tends to become more reactive due to damage which increases the surface area and the porosity of the material. Furthermore, the surface of weathered microplastics will exhibit an increase in the oxygen groups, thereby increasing the polarity and affinity for hydrophobic contaminants.

2.6.3 Plastic-type

Since this investigation involved degradation of different plastic types, it is useful to classify them according to two groups: those with carbon-carbon backbones (PPs), and those with heteroatoms in its main polymer chain (PET). Plastics with carbon-carbon backbones are most widely used in packaging and therefore most likely to end up in the environment. Generally speaking, plastics from this group are highly susceptible to photodegradation which is believed to be their most important abiotic degradation pathway (Gewert et al., 2015). Conversely, plastics with heteroatoms in their backbone offer increased thermal stability and potential degradation pathways include hydrolysis as well as photodegradation to some extent.

2.6.3.1 Polypropylene (PP)

PP has a high concentration of tertiary carbon atoms. These atoms result in increased susceptibility to abiotic degradation as they form more stable radicals during hydrogen removal. For this reason, PP requires both primary, and secondary antioxidants during processing. Once these antioxidants are consumed, abiotic degradation occurs (Ojeda et al., 2011).

Although PP does not contain unsaturated double bonds and is expected to be immune to photoinitiated degradation (should not absorb at UV wavelengths), the presence of impurities or structural abnormalities allows oxidative degradation to occur. These impurities (chromophores) permit the formation of PP radicals that react with oxygen. During radical reactions, both chain scission and/or crosslinking is possible with the former usually more dominant. The main effects of degradation of PP, is the reduction of molecular weight, the formation of new functional groups on the surface (especially carbonyl, peroxides, and hydroperoxides), and physical changes including crazing and embrittlement (Gewert et al., 2015).

2.6.3.2 Poly(ethylene terephthalate) (PET)

PET contains heteroatoms in its main polymer chain. The aromatic rings increase the thermal stability of this plastic-type. In the marine environment, hydrolytic and photodegradation are the main pathways. Photodegradation results in either cleavage of the ester bond (forming carboxylic acid and vinyl end-groups), or radicals eventually resulting in carboxylic acid end groups. These carboxylic groups have a promoting effect on thermo-oxidative degradation and therefore also on photo-oxidative degradation (Gewert et al., 2015). As in the case with carbon-carbon backbone polymers, PET may also undergo photo-induced auto-oxidation reactions.

When exposed to water, PET is highly susceptible to hydrolytic degradation. Despite being very slow at room temperature, this degradation form has been described to be the most important for PET (Edge et al., 1991). The rate of hydrolysis increases in acidic or basic conditions, and therefore the process becomes autocatalytic once carboxylic acids are formed. The main effects of PET degradation include discolouration (yellowing), decrease in molecular weight, crystallinity changes, embrittlement, chain scission, and the formation of degradation by-products including CO, CO_2, hydroperoxides, and crosslinks (Gok, 2016).

3. Experimental

3.1 Methodology

The following section outlines the methodology and experimental plan followed to achieve the objectives specified in Section 1.3. All experimental runs took place under atmospheric pressure, and the laboratories were at ambient temperatures.

3.1.1 UV pre-treatment

A decision was made to pre-treat plastic material with UV radiation in dry conditions as discarded plastic waste typically spend some extended duration on land before being transported to the ocean via rivers and wastewater channels. The objectives of the pre-treatment stage were to accelerate material degradation and add a known form of degradation history to the plastic pieces prior to further testing. During pre-treatment, two levels of irradiation (130 W/m^2 and 65 W/m^2) were investigated. UV intensity was varied by adjusting the number of lamps in use, and fresh feed material was used throughout as a control.

The peak solar UV irradiance (290-390 nm) was measured in Stellenbosch during May of 2019 and found to be about 40 W/m^2. Solar UV irradiance data for South Africa are limited and therefore available data for solar irradiance (entire spectrum) were extrapolated. According to the Department of Renewable Energy (2020), the annual 24-hour global solar irradiation average is approximately 220 W/m^2 for South Africa.

To confirm this, irradiance data were generated - specific to the Cape Town region - via the Global Solar Atlas from the World Bank (2020). It was found that the average daily irradiance for Cape Town is approximately 217 W/m^2. This value covers the entire electromagnetic spectrum, where the main interest in this investigation lies in the UV region. Assuming UV light account for 5% of the total (Henderson, 1970; Rabek, 1995; Andrady, 2015b), an average daily UV irradiance would be roughly 10.9 W/m^2. Since UV lamps were only in use for 12-hours per day, the investigated irradiance levels were therefore 3 and 6 times higher than the daily levels transferred from the sun (based on a 24-hour daily dose).

By adjusting the distance from samples to UV source and ensuring adequate ventilation, the temperature was kept in a band between 30-40°C. Relative humidity was not controlled, and experimental runs were dry (i.e. ambient relative humidity). During each pre-treatment run, four

shapes from each of the three different plastic types were investigated. The plastic types included black polypropylene (BPP), clear polypropylene (CPP) and PET. Please refer to Section 3.2 for more details. Table 3.1 below summarises the fixed parameters for the UV pre-treatment experiments.

Table 3.1. Fixed parameters for UV pre-treatment.

Fixed parameter	Fixed setpoint	Motivation
Distance to lamp(s)	40 cm	Distance required to minimise temperature effects while ensuring destructive irradiance levels.
Temperature	30-40°C (monitored)	Moderate temperature at which UV radiation was assumed to be the most significant factor.
Air flowrate	5 L/min	Reduced the chamber temperature by displacing warm air and providing an oxidative environment for chemical reactions to occur.

Two pre-treatment runs were conducted. Each run commenced for six-weeks during which UV irradiation was cycled for 12 hours (on/off). Ten samples of each plastic-type and shape were drawn fortnightly and analysed shortly thereafter. Sufficient samples were processed by each pre-treatment run to accommodate further downstream experiments. Table 3.2 illustrates the experimental design for the pre-treatment stage.

Table 3.2. Experimental design for material pre-treatment.

Run Order	UV Irradiance (W/m^2)	Plastic-type	Shape[1]
1	65	BPP	LR
2	65	BPP	SR
3	65	BPP	LC
4	65	BPP	SC
5	65	CPP	LR
6	65	CPP	SR
7	65	CPP	LC
8	65	CPP	SC
9	65	PET	LR
10	65	PET	SR
11	65	PET	LC
12	65	PET	SC
13	130	BPP	LR
14	130	BPP	SR
15	130	BPP	LC
16	130	BPP	SC

[1] Shapes included: large rectangular (LR) (40x10 mm), small rectangular (SR) (8x4 mm), large circular (LC) (Ø 12 mm) and small circular (SC) (Ø 6 mm).

Run Order	UV Irradiance (W/m^2)	Plastic-type	Shape[1]
17	130	CPP	LR
18	130	CPP	SR
19	130	CPP	LC
20	130	CPP	SC
21	130	PET	LR
22	130	PET	SR
23	130	PET	LC
24	130	PET	SC

3.1.2 UV beaker tests

The UV beaker tests were used to study the effect of UV radiation on the degradation of pre-treated and fresh material in aqueous environments. During these tests, two solution media (seawater and demineralised water) were introduced. The same UV chamber as the one for the pre-treatment was used for the beaker tests. Each experimental run continued for six weeks. Samples were placed in 375 mL glass jars containing water and sampled fortnightly to track degradation over time. Water was replaced at each sampling interval to retain salinity. Wet samples were gently rinsed with demineralised water and dried at ambient conditions for 24 hours. Thereafter samples were weighed and stored in dark conditions at 4°C prior to further analysis, as per procedure followed by Gewert (2018).

Table 3.3 below summarises the fixed parameters for the UV beaker tests.

Table 3.3. Fixed parameters for UV beaker tests.

Fixed parameter	Fixed setpoint	Motivation
Distance to lamp(s)	40 cm	Distance required to keep irradiation constant and minimise temperature effects. Enabled comparability to results from the pre-treatment.
Temperature	30-40°C (monitored)	Moderate temperature at which UV radiation was assumed to be the most significant factor.
Air flowrate	5 L/min	Main function was to reduce the chamber temperature by displacement of warm air.
Water volume	200 mL	Maintained plastic material at a constant height and therefore constant UV irradiation.
Plastic shape	Small circular	Spatial availability only allowed for one shape to be investigated during the beaker tests.

The UV beaker tests allowed conclusions regarding the effect of UV irradiance, degree of UV history, and solution medium to be made. Eight runs involved fresh (untreated) material immersed

in demineralised water. These runs enabled comparability and the effect of solution medium to be evaluated. The experimental design for the UV beaker tests is shown below in Table 3.4.

Table 3.4. Experimental design for UV beaker tests.

Run Order	UV Irradiance (W/m^2)	Plastic-type	UV History (W/m^2)	Solution Medium[2]
1	65	BPP	0	SW
2	65	BPP	0	DW
3	65	BPP	65	SW
4	65	BPP	130	SW
5	65	CPP	0	SW
6	65	CPP	0	DW
7	65	CPP	65	SW
8	65	CPP	65	DW
9	65	CPP	130	SW
10	65	PET	0	SW
11	65	PET	0	DW
12	65	PET	65	SW
13	65	PET	130	SW
14	130	BPP	0	SW
15	130	BPP	0	DW
16	130	BPP	65	SW
17	130	BPP	130	SW
18	130	CPP	0	SW
19	130	CPP	0	DW
20	130	CPP	65	SW
21	130	CPP	65	DW
22	130	CPP	130	SW
23	130	PET	0	SW
24	130	PET	0	DW
25	130	PET	65	SW
26	130	PET	130	SW

3.1.3 Temperature beaker tests

The temperature beaker tests were used to study the effect of thermal exposure on the degradation of pre-treated and fresh material in aqueous environments. Similarly to the UV beaker tests, two solution media (seawater and demineralised water) were introduced. The temperature was controlled via an LOM 150 incubator purchased from *United Scientific*. Fresh (untreated) material was used as a control variable during these experimental runs. Each run continued for six weeks.

[2] Solution mediums included: seawater (SW) and demineralised water (DW).

Samples were immersed in 375 mL glass jars containing water and exposed to different temperatures. Ten samples of each plastic-type, UV history, and solution medium were drawn on a fortnightly basis to monitor and track degradation over time. Water was replaced at each sampling interval to retain salinity. Wet samples were rinsed with demineralised water and dried at ambient temperature for 24 hours. Thereafter samples were weighed and stored in dark conditions at 4°C prior to further analysis. The experimental design for the temperature beaker tests is shown in Table 3.5 below.

Table 3.5. Experimental design for temperature beaker tests.

Run Order	Temperature (°C)	Plastic-type	UV History (W/m^2)	Solution Medium
1	25	BPP	0	SW
2	25	BPP	0	DW
3	25	BPP	65	SW
4	25	BPP	130	SW
5	25	CPP	0	SW
6	25	CPP	0	DW
7	25	CPP	65	SW
8	25	CPP	65	DW
9	25	CPP	130	SW
10	25	PET	0	SW
11	25	PET	0	DW
12	25	PET	65	SW
13	25	PET	130	SW
14	60	BPP	0	SW
15	60	BPP	0	DW
16	60	BPP	65	SW
17	60	BPP	130	SW
18	60	CPP	0	SW
19	60	CPP	0	DW
20	60	CPP	65	SW
21	60	CPP	65	DW
22	60	CPP	130	SW
23	60	PET	0	SW
24	60	PET	0	DW
25	60	PET	65	SW
26	60	PET	130	SW

3.2 Materials

3.2.1 Reference material

The feed material was obtained from a company named Zibo Containers (Pty) Ltd. It was decided to investigate their products as they are representative of typical single-use packaging containers widely used by consumers. They service some of the leading retail stores, including Checkers and Woolworths. One PET and two PP (black and clear) sheets were kindly supplied and prepared. Zibo procures resin from different suppliers with PET mostly imported from China, while PP is locally sourced from Safripol and Sasol. The company uses masterbatch as pigment for its products. PET is classified as amorphous and PPs as unfilled homopolymers that were clarified during nucleation. PET is adhesive, and sheets are often dosed with 0.5% anti-block, especially rolls that are required for printing. In addition to that, a thin layer of food approved silicone is applied to the outside of the PET sheets. Thicknesses were measured to be 0.32±0.003 mm, 0.33±0.002 mm, and 0.50±0.002 mm for PET, BPP, and CPP respectively.

3.2.2 Feed preparation

It was decided to investigate three different plastics as well as four different shapes. These shapes included: small circles (6 mm dia.), large circles (12 mm dia.), small rectangles (8x4 mm), and large rectangles (40x10 mm). Small circles were punched with a perforator. Small rectangles were obtained using a comb binder machine. Large circles were punched with a hand-held cylindrical punch, and large rectangles cut precisely with a guillotine. Samples were placed in brown envelopes and stored at 4°C in dark conditions as in Gewert (2018).

3.2.3 Plastic characterisation

The plastic material was initially characterised by weight, functional groups, degree of crystallinity, thickness, and microhardness. In terms of weight, twenty samples of each plastic-type and shape were weighed using a four decimal analytical balance. Individual weights were recorded, and final values reported as the means plus the standard error. The initial functional groups were determined using Fourier transform infrared (FTIR) spectroscopy from the Department of Polymer Science at Stellenbosch University. This allowed a baseline to be set for comparison of the development and changes in functional moieties. Average initial spectra are shown in Figures 4.9, 4.10, and 4.14 for BPP, CPP, and PET, respectively. Fresh material also underwent microhardness tests to provide an initial estimate of the mechanical properties

associated with each type of plastic. Initial microhardness values were 12.11±0.14 kg-f/mm^2 for BPP, 12.12±0.71 kg-f/mm^2 for CPP, and 12.77±0.07 kg-f/mm^2 for PET. Differential scanning calorimetry (DSC) was used to characterise the initial degrees of crystallinity for the different plastics. Figure 4.4 indicates these determined values. The DSC instrument used was from the Department of Chemistry at the University of Stellenbosch. More information on the analytical techniques and data interpretation is provided in Section 3.5.

3.2.4 Seawater

Seawater was obtained from the Gordon's Bay area in the Western Cape, South Africa. Seawater was transported to the Department of Process Engineering and stored in cool dark conditions until required for use. The pH of seawater used was measured to be 8.07. This falls within the typical pH range of 7.9 – 8.2, as described by Riley & Skirrow (1975). The conductivity was determined to be 17.37 mS. The salinity and dissolved oxygen concentration of water from this location have been measured to range between 35 – 35.2 PSU and 4.5 – 6 mg/L, respectively (Laird et al., 2017).

3.3 Equipment

3.3.1 UV pre-treatment and beaker tests

Both the dry pre-treatment and aqueous UV beaker tests took place in the constructed UV chamber. This stainless-steel cubic chamber had a total volume of 125 L and was equipped with two OSRAM Supratech HTC (400-221) UV lamps each mounted onto its own heat sink. The electrical circuits for each of these high-pressure metal halide lamps consisted of a 35-400 W ignitor (produces a 4 kV electric pulse required to ignite the mercury vapour gas in the lamp), a 400 W ballast (transformer is required to keep the current constant during voltage fluctuations), and a standard R7s lamp holder. These components were purchased from *RS Components*, and *ACDC Dynamics,* respectively. The lamps used in this investigation were also used by Gewert (2018), and the spectral distribution is described to correspond almost exactly with the reaction profile of photosensitive plastics (Osram GmbH, 2013). The lamps emit both UVA (315-380 nm) and UVB (280-315 nm) radiation, but the quartz bulb absorbs UV radiation below 250 nm; therefore, no ozone is generated.

The UV chamber was also fitted with an adjustable steel grid that enabled distance control to-and-from the UV source (intensity follows the inverse square law and therefore varying distances could be used to adjust irradiation and reduce temperature).

To ensure no heat build-up in the chamber, a six-point manifold was installed to sparge cool compressed air through the system at constant flowrate. In addition to that, a small axial computer fan was also installed at the bottom-back side of the chamber and two vents at the top-backside corners. A schematic representation of the UV chamber is shown in Figure 3.1.

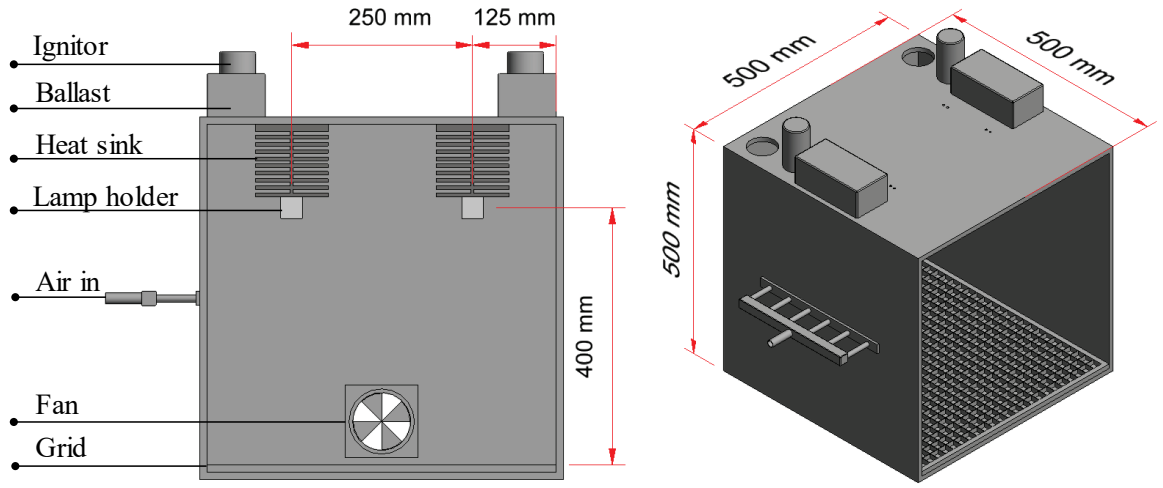

Figure 3.1. Schematic representation of the constructed UV degradation chamber.

3.3.2 Temperature beaker tests

To investigate potential for thermo-oxidative degradation an LOM-150 incubator was purchased from *United Scientific*. This 150 L multipurpose model can shake, incubate, and refrigerate. It has a temperature range of 0°C-70°C that is controlled with a PID controller to an accuracy of ±0.1°C. Samples were placed in glass jars (containing aqueous solutions) and added to the incubator where they were exposed to specific temperatures for predetermined periods.

3.4 Experimental procedure

3.4.1 UV pre-treatment tests

Following sample preparation (different shapes and sizes), UV pre-treatment experiments were conducted. Samples, sorted according to type and shape, were placed in aluminium pans. Care was taken to ensure equal spacing and no overlapping between adjacent samples. Thereafter the UV chamber was started up. This involved switching on the required number of lamps, opening the compressed air flow, as well as switching on the axial computer fan. The temperature was monitored with a mercury thermometer during this time, and once stabilised, sample pans were added to the chamber. This time instance signified the start of the test, t=0 weeks. Every second day, pans were rearranged to ensure equal light distribution and samples were turned over.

Samples were inspected weekly for any visual signs of degradation (crack formation, colour shifts, and bending). Using a metal tweezer, ten random samples of each plastic-type and shape were drawn at each sampling interval. These samples were immediately weighed and stored at 4°C prior to further analysis. After the final sampling of each run, the chamber was shut down, lamps inspected for any damage, and debris removed from any surfaces.

3.4.2 UV beaker tests

The procedure for the UV beaker tests was similar to the pre-treatment with some minor modifications. In this case, glass beakers were filled with 200 mL aqueous solution (either seawater or demineralised water). Samples were placed into the beakers using a metal tweezer. Special care was taken not to damage any samples in the process. Thereafter the lids of the beakers were tightly closed. Beakers were laid down in aluminium trays. The chamber was then started up exactly as described earlier. Once the chamber temperature stabilised, trays containing the beakers were placed inside the chamber. This instance signified the start of the test, t=0 weeks. Beakers were rearranged every second day to ensure equal light distribution. Beakers were gently twirled in cases where samples adhered to the beaker walls. Samples were monitored weekly for any visual signs of degradation. At each sampling interval, water was drained and replaced. Samples were gently rinsed with demineralised water and ten random samples (of each plastic-type, UV history, and from each solution medium) were drawn for analyses. Drawn samples were dried for 24 hours at ambient conditions; thereafter weighed and stored at 4°C prior to further testing. The remaining samples were carefully added back to the beakers and the UV chamber for further exposure. After completion of the final sampling, the chamber was shut down, beakers were cleaned, debris removed, and lamps inspected.

3.4.3 Temperature beaker tests

For the temperature beaker tests, samples were prepared and handled similarly as during the UV beaker tests. The incubator was switched on, and the desired set point temperature selected. Once this set point was reached, pans containing the beakers were added to the incubator. This time instance signified the start of the test t=0 weeks. Samples were investigated weekly for any physical signs of degradation. At each sampling interval, water was drained and replaced. Samples were gently rinsed with demineralised water, and ten samples (of each plastic-type, UV history, and from each solution medium) were drawn for further analysis. The remaining samples were immersed in replaced solutions and immediately added back to the incubator.

Samples drawn for further analysis were dried at ambient conditions for 24 hours, thereafter weighed, and stored at 4°C prior to further testing. After completion of each run, the incubator was switched off, and beakers were cleaned.

3.5 Analytical techniques and data interpretation

3.5.1 Mass loss

Measuring changes in mass is the simplest and most direct way to quantify the extent of degradation (Chamas et al., 2020). Since degradation predominantly takes place at the surface, the rate of mass loss is closely related to (and usually proportional to) the surface area of the plastic piece (Moore & Saunders, 1998). Reductions in mass are typically due to volatilisation or solubilisation of converted plastic material to small molecules including CO_2 and H_2O. However, overall mass loss convolutes the liberation of small molecules with flaking of larger, insoluble pieces, including microplastics (Andrady, 2011).

To determine percentage mass loss, the initial weights of the dry samples had to be recorded. This was done by making use of a Sartorius 4-decimal analytical balance. Twenty samples of each plastic-type and shape were weighed, and the standard error was calculated as the population standard deviation divided by the square root of the sample size. Mass loss (%) was calculated at each sampling interval, according to Equation [1] below.

$$Mass\ loss\ (\%) = \frac{W_i - W_f}{W_i} \times 100 \qquad [1]$$

Where $W_i\ and\ W_f$ represent the initial and final (at sampling interval) mass values, respectively.

3.5.2 Differential scanning calorimetry (DSC)

Calorimetry is a useful technique that forms part of a group of techniques called thermal analysis (Raka & Bogoeva-Gaceva, 2008). This technique is based on the detection of enthalpy (or specific heat) changes of a sample with temperature. Thermal transitions, as a function of temperature and time, allow quantitative and qualitative information to be extracted.

For this investigation, a Q200 DSC instrument equipped with a specific sensor was used. Samples were weighed (5-10 mg) and sealed in aluminium pans. Pans were then heated (from ambient) at a specific rate (10°C/min) to a ceiling temperature of 200°C for PP and 300°C for PET.

An empty pan was used as a reference and the system was operated under continuous nitrogen flow of 20 mL min^{-1}. Parameters, including temperatures (onset and peak) as well as melting

enthalpies, were determined using the integration function of *TA Universal Analysis* software. Depending on the individual baselines, integrations were either linear, sigmoidal-horizontal or sigmoidal-tangential. Melting enthalpies were used to calculate percentage crystallinity as in Equation [2] below.

$$\% \, Crystallinity = \frac{\Delta H_m}{\Delta H_m^{ref}} \times 100 \qquad [2]$$

Where ΔH_m depicts the melting enthalpy per unit mass (J/g) of the sample and ΔH_m^{ref} the theoretical value of the melting enthalpy per unit mass of a 100% crystalline polymer. For PP and PET, the reference enthalpies used were 207 J/g and 140 J/g, respectively (Karger-Kocsis, 1995; Wunderlich, 1973).

3.5.3 Fourier-transform infrared spectroscopy (FTIR)

FTIR is an analytical technique used to identify organic (and in some cases inorganic) materials. This technique measures the absorption of infrared radiation by the sample versus wavelength. The location and intensity of infrared absorption peaks indicate molecular components and their corresponding structures.

When plastic is irradiated with infrared radiation, molecules are energised into a higher vibrational state. The wavelengths at which a specific molecule absorbs light is a function of the energy difference between the at-rest and excited vibrational states and is specific to its molecular structure (Pecheva, 2017).

The FTIR spectrometer uses an interferometer to manipulate the wavelength from a broadband infrared source. A detector measures the intensity of transmitted or reflected light as a function of its wavelength. The signal obtained from the detector is known as an interferogram which is processed using Fourier transforms to obtain a single-beam infrared spectrum. FTIR spectra are usually presented as intensity plots versus wavenumber. Intensity can be plotted as percentage light transmitted, or absorbed, at each wavelength.

For this investigation, the Thermo Nicolet iS10 spectrometer was used and consisted of a Smart iTX ATR sampling attachment equipped with a diamond crystal. An incident angle of 45° was used for all measurements. Spectra were collected at a resolution of 4 cm^{-1} with 32 scans collected for each spectrum and a wavenumber range of 400 cm^{-1} – 4000 cm^{-1}. The option for automated background subtraction was also available. Thermo Scientific *OMNIC* software was used to analyse spectral data.

To monitor chemical degradation changes, it was decided to consider two main groups of degradation products. The first being the formation of carbonyl (C=O) functional groups, these are typically indicative of oxidative degradation taking place, and represent degradation products such as ketones, aldehydes, esters, lactones, and acids. Although carbonyl group tracking is a well-established and accepted way of tracking degradation of carbon-carbon backbone polymers, for PET the hydroxyl (-OH) groups were also considered.

Nevertheless, both carbonyl and hydroxyl regions were monitored for the PPs and PET in this study as both plastics may have formed degradation products visible within these regions. Two indices were defined and used to quantify changes in the above-mentioned functional groups, namely the carbonyl index (CI) and the hydroxyl index (OHI). These indices are shown in Equations [3] and [4] and were calculated in two ways. Firstly, from areas under the absorbance curve between a specific wavenumber range, and secondly by focussing on the peak itself and measuring its height.

$$CI = \frac{Abs_{(C=O)}}{Abs_{(ref)}} \qquad [3] \qquad\qquad OHI = \frac{Abs_{(OH)}}{Abs_{(ref)}} \qquad [4]$$

In most literature, only one of the methods is used. It was believed that considering both methods in tandem might have resulted in useful information. For example, if an index calculated from areas increased, while the same index calculated by heights decreased, it can be deduced that the peak flattened as well as broadened. This would imply that although intensity decreased, new degradation products might have formed with different peaks falling within the same region. The overlapping of spectral IR peaks is a common problem that has been reported in various literature (Francois-Heude et al., 2015). This limitation also makes the interpretation semi-quantitative.

The carbonyl frequency range used in this study was between 1540 cm^{-1} and 1870 cm^{-1} with the peak centred at around 1725 cm^{-1} for the PPs and 1710 cm^{-1} for PET. The hydroxyl range used was 3800-3050 cm^{-1} for the PPs and 3700-3020 cm^{-1} for PET. These ranges were selected based on literature, as well as after close inspection of spectra specific to this study.

To successfully calculate index values from Equations [3] and [4], reference areas and peak heights had to be calculated for the denominator term. These references would typically represent molecular structures unaltered by oxidation. Those used in this study are summarised in Table 3.6. There are, of course, numerous other peaks that could have been selected as potential references.

Table 3.6. Summary of reference peaks for FTIR analyses.

Plastic	Reference peak	Region	Description	Source
BPP	1456 cm^{-1}	1400-1500 cm^{-1}	Methylene ($\delta_S CH_2$) scissoring peak	(Ter Halle et al., 2017; Longo et al., 2011)
CPP	1456 cm^{-1}	1400-1500 cm^{-1}	Methylene ($\delta_S CH_2$) scissoring peak	(Ter Halle et al., 2017; Longo et al., 2011)
PET	1576 cm^{-1}	1590-1540 cm^{-1}	C=C stretching of aromatic skeleton	(Nagai et al., 1997)

Through macro programming, *OMNIC* was used directly to correct spectral baselines (by high-order polynomial fitting), calculate heights and band areas, and perform arithmetic calculations to obtain index values. Generated datasets were then imported to *Minitab* statistical software, where box plots were used to identify and remove outliers.

3.5.4 Vickers microhardness

Hardness is the measure of the material's resistance to localised plastic deformation (Callister & Rethwisch, 2015). Hardness tests are performed more frequently than other mechanical tests as they are inexpensive and straightforward, non-destructive, and enable other mechanical properties to be estimated from hardness data, such as tensile strength. For this investigation, Vickers microhardness tests were performed using the UHL VMHT-001 instrument. The procedure involved a small diamond indenter with a pyramidal geometry that was forced into the surface of the specimen. The resulting impression was then observed under a calibrated microscope and measured manually. The measurement is converted to a hardness value by Equation [5] where F is the applied load (kg-f) and d the average diagonal distance (mm) across the indentation (Pilař et al., 2015).

$$HV = 1.8544\ F/d^2 \qquad [5]$$

For this investigation an indentation load of 300 g-f was applied at a speed of 50 $\mu m/s$ for a total application time of 15 s.

3.5.5 Analysis of variance (ANOVA)

The result section of this document was structured in a manner that allowed for key variables to be evaluated individually. In order to comment on the significance of a particular effect, one-way ANOVA tests were employed. All analyses were conducted via *Minitab* statistical software, and complete results are tabulated in Appendix C. These tests were used to determine whether there were statistically significant differences among the final means of different populations.

During these analyses, the null hypothesis was that all level means were equal. The alternative hypothesis was that one (or more) of the means differed from the other. By considering the determined p-values, it was possible to accept or reject the null hypothesis. For instances where the p-value was less than or equal to the selected α-value (0.05), it could be concluded that the specific effect of interest resulted in a significant difference in the final means. Conversely, if the p-value was greater than the α-value, then the effect was found not to have resulted in significant differences at this level of confidence.

4. Results and discussion

4.1 UV pre-treatment

As discussed in Section 3.1.1, the main objectives of the pre-treatment stage were to accelerate degradation and add a known form of degradation history to the plastic pieces prior to further testing. These experiments represented the initial period plastic material typically spend on land before ending up in wastewater channels and eventually the ocean. Plastics of different shapes, types, and sizes were considered and exposed to two different UV irradiance levels. The following sections will focus on the analytical results obtained from the dry UV pre-treatment experiments. The complete ANOVA results for the pre-treatment stage are presented in Section C.1 of Appendix C.

During these experiments, some physical observations were made as degradation occurred. In as early as two weeks of exposure, microcracks started developing on the surfaces of CPP samples with samples becoming brittle (easily broken when applying minor force). CPP also showed colour shifts (from transparent clear to chalk-white) and in some instances minor bending. For BPP the same crazing effect was not seen with the naked eye, only later on under microscope. BPP samples showed colour shifts (from glossy black to matte black) accompanied by occasional bending as well. PET only showed minor yellowing, an effect likely attributed to quinone degradation products arising from oxidation reactions which has been reported in previous literature (Fagerburg & Clauberg, 2003) and described in Section 2.5.1.

4.1.1 Mass loss

During degradation, plastic material may exhibit mass loss. This likely stems from volatile or soluble components released from the polymer matrix or from a physical process where fragments break away from larger segments by means of erosion or surface ablation. Mass loss could also be as a result of non-covalently bonded additives like plasticisers or flame retardants leaching out of the polymer into a potential surrounding solution medium. For the pre-treatment stage, ten random samples (of each plastic-type and shape) were drawn at each sampling interval. Samples were weighed and their average mass values used in Equation [1] to determine percentage mass loss. The following sections will consider the effects of UV irradiance, shape, and plastic-type, on the mass loss observed during the pre-treatment experiments.

4.1.1.1 Effect of UV irradiance (all plastic)

To describe the effect of UV irradiance on mass loss, samples weighed from the 65 W/m^2 experiment were compared to those from the 130 W/m^2 experiment. The main effect of UV irradiance, as well as the different trends observed for the specific plastic types and shapes, are summarised in Figure 4.1. The p-values indicated on these graphs represent the degree of significance in differences between the final (week 6) measurements for the specific effect of interest. Tabulated ANOVA results are included in Appendix C.

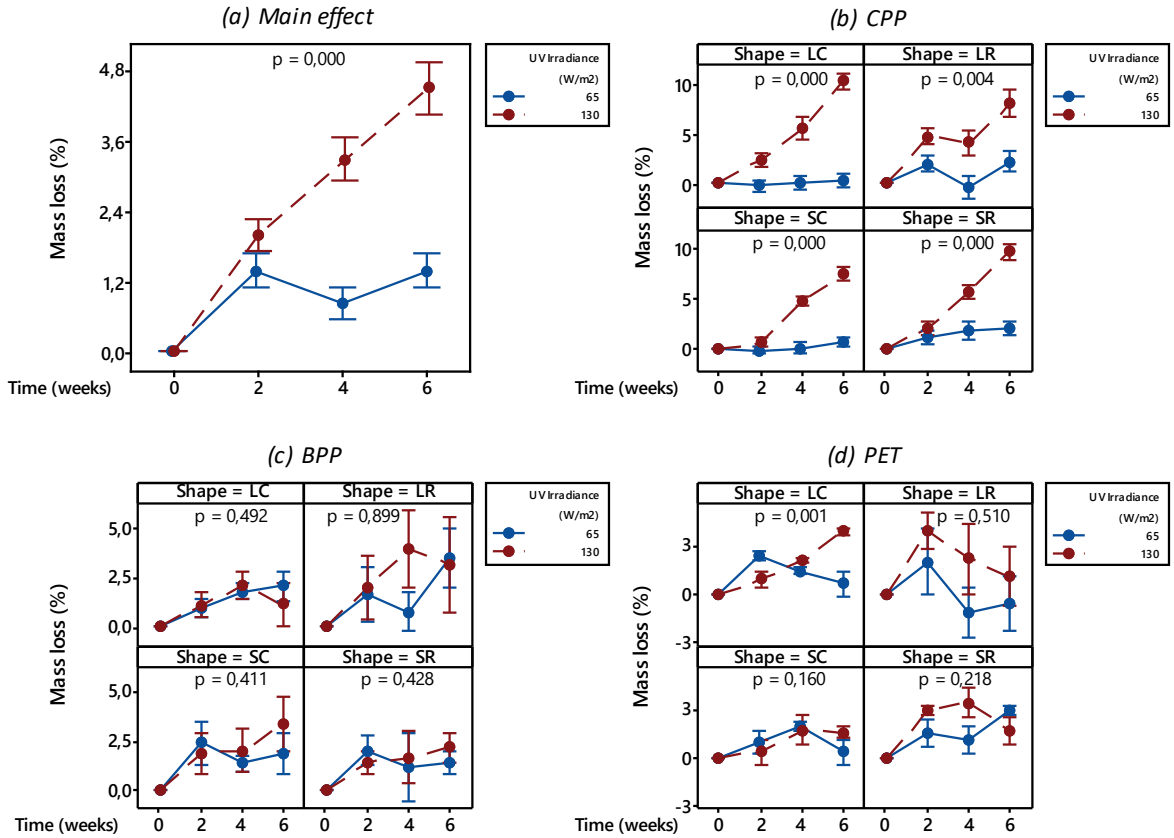

Figure 4.1. (a) Main effect of UV irradiance on mass loss (%) over time (weeks); (b) Mass loss (%) over time (weeks) for CPP per shape; (c) Mass loss (%) over time (weeks) for BPP per shape; (d) Mass loss (%) over time (weeks) for PET per shape.

From Figure 4.1 (a) the overall effect of UV irradiance on mass loss is prominent. The higher irradiance (130 W/m^2) resulted in increased rates and extents of mass loss relative to the lower irradiance (65 W/m^2). Ultimately the 130 W/m^2 run resulted in 3.3 times more mass loss than the 65 W/m^2 run. In terms of mass loss rate, it was found that for the first two weeks of degradation, the rate was 1.4 times higher for the higher irradiance in comparison to the lower one.

Figure 4.1 (b) indicates the mass loss over time for CPP (of different shapes) exposed to different irradiances. Between the different plastics, only CPP resulted in a regular trend. The increased

UV irradiance resulted in significant increases in mass loss as exposure time progressed. On average, it was found that for CPP, the higher UV irradiance resulted in 6.9 times the final mass loss obtained from the lower irradiance.

The mass loss trends for differently shaped BPP samples are shown in Figure 4.1 (c). In this case, it seemed that for the larger shapes (LC and LR), the final mass loss percentages were higher for the 65 W/m^2 irradiance than the 130 W/m^2 irradiance. For both of these shapes, this was not the case within the first four weeks of degradation, and from the p-values, it is evident that these final differences were not significant. Conversely, the smaller shapes (SC and SR) indicated that the higher irradiance resulted in increased final mass loss. Overall, for BPP it was found that the 130 W/m^2 irradiance resulted in 1.1 times the mass loss obtained for the 65 W/m^2 irradiance.

Figure 4.1 (d) shows the mass loss over time for differently shaped PET samples exposed to the two investigated UV irradiances Again, there were some discrepancies as time progressed, but overall, three of the four shapes indicated that the higher irradiance level resulted in increased mass loss with only LC reflecting a significant difference. Taking the week six averages for the different shapes, it was found that overall, the higher irradiance resulted in 2.5 times the mass loss of the lower irradiance.

To conclude, the overall effect of UV irradiance on mass loss was significant. This finding was mostly driven by results obtained for CPP. During pre-treatment, increased UV irradiance resulted in increased rates and extents of mass loss. An explanation for this is that an irradiance increase translates to an increase in electromagnetic energy reaching the polymers' surface. This energy increase ensures more light being absorbed, creating higher molecular excitation states and increased radical formation, initiating degradation reactions. These reactions subsequently lead to chain scission or direct cleavage of the bonds that are responsible for holding the polymer (and its additives) intact. Once these bonds are broken, the polymer falls apart, additives are released, and mass loss increases. CPP resulted in the most significant response when compared to the other plastics and possible reasons for this finding are described in Section 4.1.1.3, where plastic-type is specifically addressed.

4.1.1.2 Effect of shape (all plastic)

This section aims to describe the effect of shape on mass loss during exposure to UV radiation from the pre-treatment experiments. To evaluate this effect, mass loss percentages of differently shaped samples were compared. The main effect of shape, as well as specific trends obtained on a per-plastic basis and at different UV irradiances, are shown below in Figure 4.2.

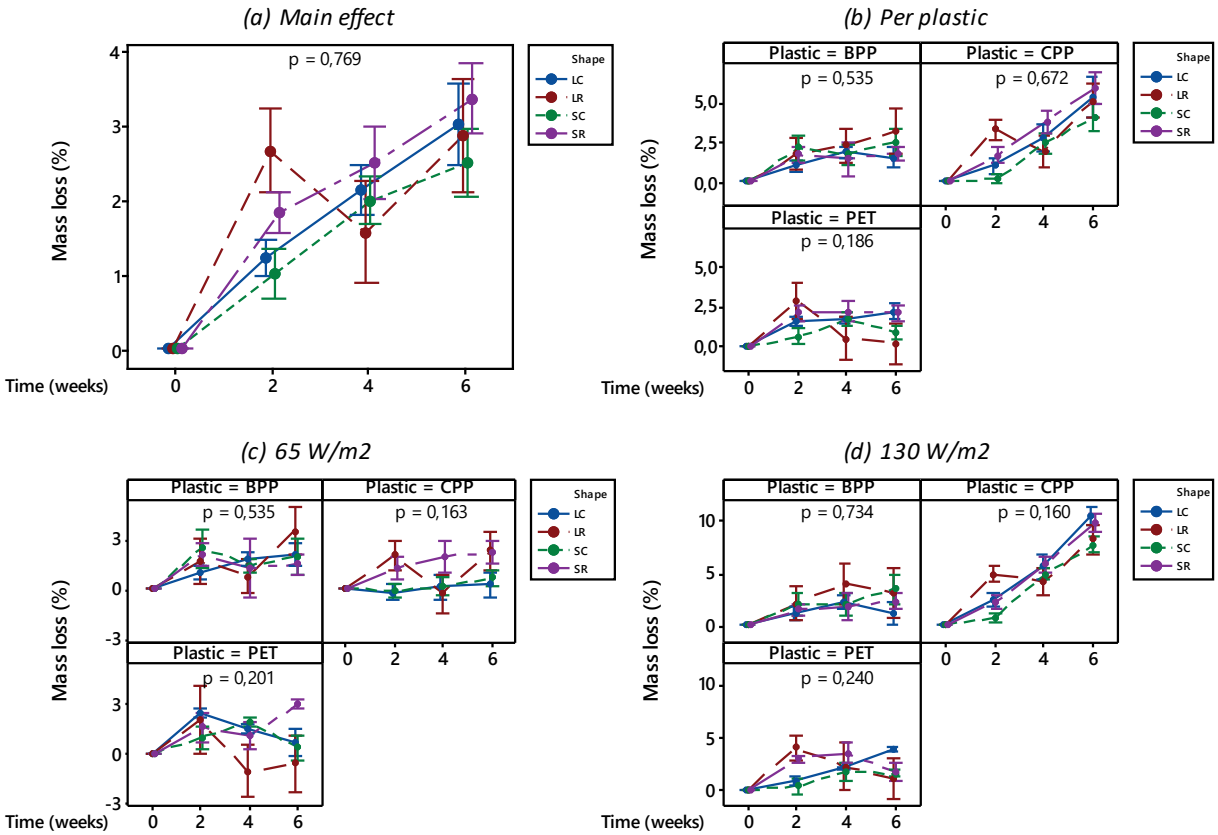

Figure 4.2. (a) Main effect of shape on mass loss (%) over time (weeks); (b) Mass loss (%) over time (weeks) per plastic; (c) Mass loss (%) over time (weeks) for the 65 W/m^2 irradiance; (d) Mass loss (%) over time (weeks) for the 130 W/m^2 irradiance.

From Figure 4.2 (a) the overall effect of shape on mass loss initially seems irregular. Closer inspection reveals that as time progressed, mass loss occurred in decreasing order from SR to LC to SC. This trend held for those three shapes, but LR changed irregularly over the degradation period. Ultimately SR, LC, LR, and SC resulted in mass losses of 3.4%, 3%, 2.9%, and 2.5% respectively. The determined p-value of 0.769, however, indicates that overall different shapes did not result in significantly different final mass loss percentages. Table C.2 in Appendix C contains the complete ANOVA results for this effect.

When considering the results on a per-plastic basis as in Figure 4.2 (b) it is evident that for BPP, LR resulted in the highest mass loss of 3.2% and LC the lowest of 1.5%. For CPP it was found that SR resulted in the highest mass loss of 6% and SC the lowest of 4%. Results for PET showed almost no difference between LC and SC with the highest mass loss at around 2.3% and the lowest reported for LR at 0.2%.

These irregular trends remained apparent in Figure 4.2 (c) and (d). At both irradiances, no clear distinction on mass loss between the different shapes could be established. The overlapping of

standard error bars, as well as all the p-values being larger than 0.05, confirm the insignificant effect of shape on mass loss. This finding suggests that when considering UV induced degradation of different plastic shapes, minor differences in mass loss (instead of exclusively due to shape) might have been attributed to (i) differences in the incident light angles falling onto plastic samples, (ii) heterogeneity as degradation is expected to preferentially take place in the amorphous regions, with these regions not being equally distributed among the different shapes and (iii) differences in samples thickness influencing oxygen diffusion to the polymer interior.

It is however known that particle shape strongly influences settling behaviour. In the marine environment, this would translate to material finding itself at different locations in the water column while continuously being subjected to different currents. UV irradiance and temperature are strong functions of these locations and degradation behaviour of differently shaped plastic pieces would consequently be different. Therefore, it can be concluded that in the marine environment, and depending on depth, sample shape would indirectly influence mass loss due to UV degradation. A report by Ter Halle et al. (2016) suggested that shape influences fragmentation behaviour in the ocean and that small pieces (with low aspect ratios) fragment faster because their isotropic motion inhibits biofilm development.

4.1.1.3 Effect of plastic-type (all plastic)

This section considers the effect of plastic-type on mass loss during the UV pre-treatment where material was exposed to different irradiances. To evaluate this effect, mass loss over time for the different plastic types (per shape and UV irradiance) were compared. These results are summarised in Figure 4.3.

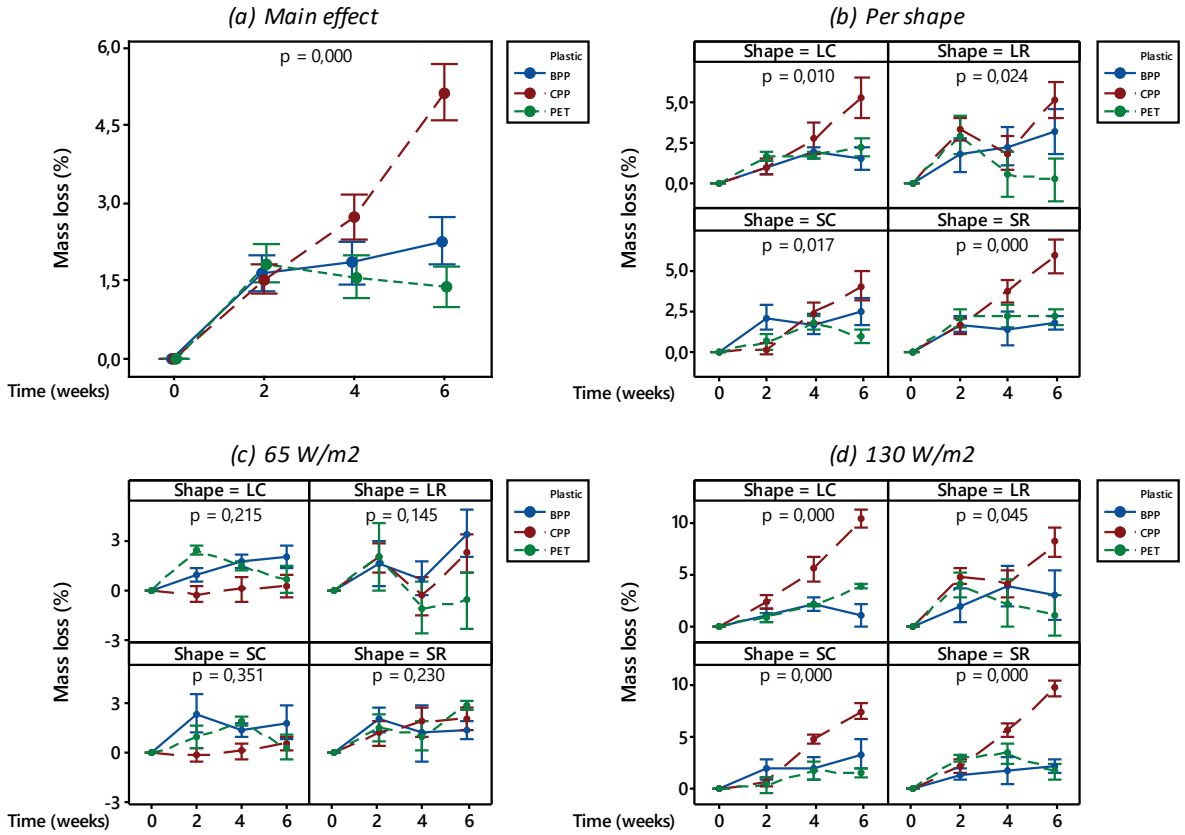

Figure 4.3. (a) Main effect of plastic-type on mass loss (%) over time (weeks); (b) Mass loss (%) over time (weeks) per shape; (c) Mass loss (%) over time (weeks) for the 65 W/m^2 irradiance; (d) Mass loss (%) over time (weeks) for the 130 W/m^2 irradiance.

In Figure 4.3 (a) the overall main effect of plastic-type on mass loss (%) for the pre-treatment is shown. For the first two weeks of degradation, the mass loss behaviour was quite similar between the different plastic types. Thereafter the trends deviated; CPP continued losing weight, BPP also continued losing weight, albeit more moderately, and PET showed a reduction in mass loss. The overlapping error bars for PET between weeks two and six suggest that this mass increase was not significant. Ultimately CPP resulted in the highest mass loss of 5.1%, followed by BPP at 2.3% and finally PET at 1.4%.

Figure 4.3 (b) looks more specifically at the mass loss (%), per plastic shape, for the different plastics. For all shapes, it was found that CPP resulted in the highest mass loss, followed by alternating trends for BPP and PET. For LR and SC, BPP resulted in the second-highest mass loss, whereas for LC and SR, PET resulted in the second-highest mass loss.

When considering the lower UV irradiance (65 W/m^2) in Figure 4.3 (c), it was found that for three out of four shapes, BPP resulted in the highest mass loss. Only for SR did PET result in the highest mass loss. It should be mentioned that the y-axis of these figures is more magnified in comparison

to that of the higher irradiance in Figure 4.3 (d) and consequently results (and trends) might appear more emphasised than they actually were. In addition to that, none of the determined p-values indicate significant differences due to plastic-type in the final mass loss values at the lower UV irradiance setting.

Moving over to the higher UV irradiance (130 W/m^2) in Figure 4.3 (d), the dominating effect of CPP was again apparent. For all shapes at this irradiance, CPP resulted in the highest overall mass loss with final extents of BPP and PET changing irregularly. When considering the determined p-values, it is evident that for all shapes, CPP resulted in significantly higher mass loss relative to the other plastics at this irradiance.

Overall, the effect of plastic-type on mass loss was significant. In general terms, different plastics simply degrade differently. In this case, plastic types were classified according to their chemical composition. PPs have carbon-carbon backbones while PET contains heteroatoms in its main chain. It was found that UV induced degradation resulted in significant differences in their mass loss behaviour. These differences could be described by considering compositional differences, specific wavelength sensitives, and additives incorporated into the polymer matrix.

Firstly, owing to the presence of its tertiary carbon atoms, PP is known to be highly susceptible to UV degradation. Due to its stabilising aromatic rings, PET on the other hand, is known to show good UV resistance. Furthermore, the most damaging UV wavelength for a specific plastic depends on the bonds present and therefore maximum degradation occurs at different wavelengths for different plastic types, e.g. it is at approximately 300 nm for PE and 370 nm for PP (Singh & Sharma, 2008). As shown in Figure A.1, the spectral radiation distribution of the lamps used in this investigation indicated a maximum peak intensity at 365 nm. This corresponds well to the highest wavelength sensitivity of PP, which led to the degradation of PP being more pronounced than that of PET.

Considering degradation differences between the polypropylenes (CPP and BPP), the main topic of interest is that of an additive named carbon black. It is believed that carbon black was used as a pigment in BPP. This additive protects the interior by acting as a physical screen absorbing UV light and converting energy to heat. It also acts as a radical trap and a terminator of the free radical chain reactions through which oxidative degradation is propagated (McKeen, 2013). Therefore, BPP did not show the same extreme mass loss as observed for CPP. As mentioned in Section 2.5.1, the termination by radical recombination often results in crosslinking. This is important to keep in mind specifically for BPP and will be elaborated on in the next section for crystallinity.

4.1.2 Crystallinity

As discussed in Section 2.6.2.1, crystallinity affects several plastic properties, including hardness, tensile strength, density, and oxygen permeability. In general, increased degrees of crystallinity makes material tougher, but too high levels may render it brittle. This section will look at the effect of UV irradiance and plastic-type on percentage crystallinity for the UV pre-treatment stage. Percentage crystallinity was determined via DSC as described in Section 3.5.2.

4.1.2.1 Effect of UV irradiance and plastic-type

To evaluate the effects of UV irradiance and plastic-type on crystallinity changes, results from different plastics exposed to different UV irradiance levels were compared. These results are shown in Figure 4.4 below. Although initially redundant, percentage increase is also reported. This increase is relative to untreated material and is a useful metric when comparing sequential degradation as during the beaker tests in Sections 4.2 and 4.3. The irradiance setting of 0 W/m^2 shows the initial crystallinities of untreated material. For this analysis, only small circular shapes were considered. All measurements were triplicates with the means and standard errors reported.

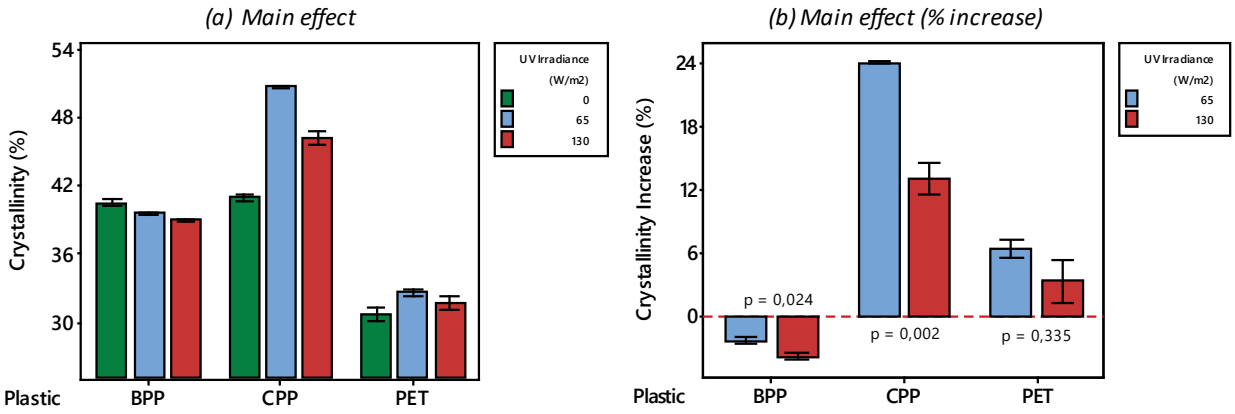

Figure 4.4. (a) Crystallinity (%) results for different plastics exposed to different UV irradiances during the pre-treatment stage; (b) Percentage crystallinity increase (from week 0) of plastics shown in (a).

In Figure 4.4, the crystallinity results from the pre-treatment stage are presented. It is evident that for BPP samples, an increase in irradiance resulted in a decrease in crystallinity. More specifically, the 65 W/m^2 irradiance resulted in a crystallinity decrease of 2.3% and the 130 W/m^2 irradiance in an extended decrease of 3.8%. The difference between these two results was found to be statistically significant, as seen by the determined p-value of 0.024 in figure (b).

For CPP and PET, a different trend was apparent with both irradiances increasing the crystallinity relative to untreated material. For both of these plastics, the lower irradiance (65 W/m^2) resulted

in the highest crystallinity increase with a considerable 24% and 6.4% increase for CPP and PET respectively. The higher irradiance (130 W/m^2) resulted in lower increases of 13% for CPP and 3% for PET. When considering the p-values, it was found that the difference in crystallinity change for CPP was significant, whereas that of PET was not. Tabulated results for these findings are shown in Table C.5 and Table C.6 of Appendix C.

The observation described above might be due to competing effects between crosslinking and chain scission with the former taking place more rapidly at higher irradiance levels. Crosslinking is associated with rigid polymer chains that are unable to rotate and align in an orderly crystalline structure, which consequently decreases crystallinity. Conversely, chain scission results in shorter chain segments that are easily able to align in a crystalline structure, thus increasing the degree of crystallinity. One way to monitor crosslinking is to track changes in the glass transition temperature of the plastic. In cases where crosslinking is taking place, the glass transition temperature would typically increase accordingly (Stutz et al., 1990). The investigated DSC conditions allowed for the glass transition temperatures of PET to be calculated. Thermograms are shown below in Figure 4.5.

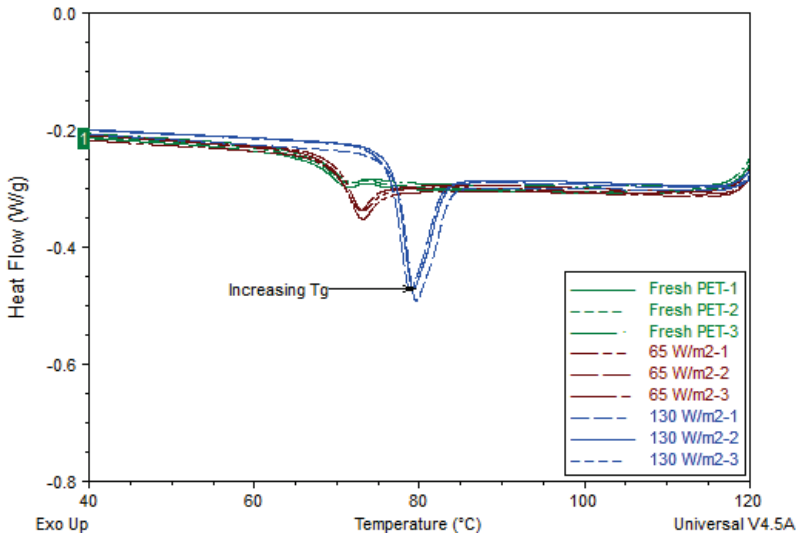

Figure 4.5. Thermograms indicating Tg shifts for PET as a result of UV pre-treatment.

From Figure 4.5, it is clear that an increase in UV irradiance increased the glass transition temperature of PET. From these thermograms, it was calculated that the lower irradiance resulted in an increase of 2.21% whilst the higher irradiance in an increase of 10.8%. These findings prove that initial crosslinking occurred at the higher irradiance, hampering the ability of chains to realign and form an orderly structure and resulting in lower crystallinities being reported. Edge et al. (1991) also reported initial crosslinking of PET during its degradation at temperatures below 90°C.

This effect was described to be associated with an emulsion layer on the film, which impaired oxygen diffusion. Nagai et al. (1997) found crosslinking of PET to be more pronounced in accelerated weathering than during outdoor weathering experiments. The glass transition temperature of PP lies between -10°C and -20°C while the cycles in this study started at 25°C; therefore, the same motivation for the PP could not yet be established.

In terms of plastic-type, it was found that the initial crystallinities of CPP and BPP were very similar at values of 40.9% and 40.4% respectively. PET reflected the lowest initial crystallinity of 30.5%. This confirms that PET was amorphous and provides insight into its processing conditions. The melt was likely quench cooled which resulted in its amorphous structure. More gradual cooling would have produced larger (and more) crystals, thereby increasing the ratio of crystalline to amorphous regions and reflecting higher crystallinities. Crystals larger than the wavelength of light would have also compromised transparency.

Following UV exposure, CPP showed the highest average crystallinity of 48.8%, followed by BPP at 39.2%, and finally PET at 32%. The degree of crystallinity determines the ease of oxidation and fragmentation (Andrady, 2017). This is consistent with the physical observations for CPP as discussed in the introduction of Section 4.1. During degradation, CPP samples initially became whiter, showed crazing (network of microcracks), and became excessively brittle. The major increase in crystallinity for CPP is indicative that its polymer chains had the highest relative mobility, and consequently the highest ability to align in a crystalline structure as exposure time progressed. When considering the overall absolute change in crystallinity, it was found that CPP was the most susceptible, followed by PET, and finally BPP.

4.1.3 Microhardness

Microhardness describes a material's resistance to localised deformation and enables estimations of other mechanical properties, such as tensile strength, to be made. Results from the previous section showed different changes in crystallinity for the investigated plastic types and experimental UV conditions. Flores et al. (2005) illustrated a linear relationship between microhardness and the degree of crystallinity of PET. In general, polymers with increased crystallinities have more densely packed molecular chains, as well as a higher ratio of the crystalline to amorphous domains. Therefore, increased crystallinity is typically associated with increased microhardness.

For this analysis, CPP samples could not be tested as samples were excessively brittle and fractured immediately as the indenter made contact with the surface. Performing the analysis at lower indentation loads was also unsuccessful. The tendency of PP samples becoming too brittle for microhardness determinations has been reported in other literature as well (Pilař et al., 2015). Please refer to Figure 4.6 for images indicating the degree of crack formation and sample failure.

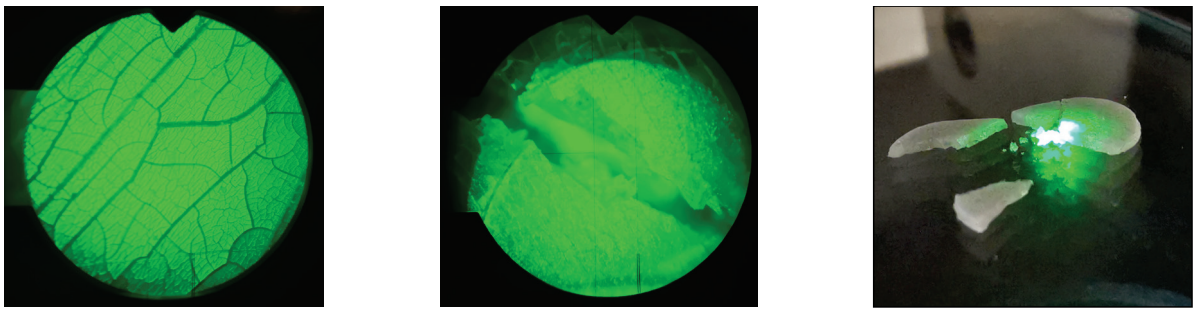

Figure 4.6. Photographs of embrittled CPP that failed during an attempted microhardness test.

Although microhardness was not determined for CPP samples, by considering the crystallinity results in Section 4.1.2 and accepting the relationship between crystallinity and microhardness, it is believed that the microhardness of CPP would have increased significantly as well.

4.1.3.1 Effect of UV irradiance and plastic-type (BPP and PET)

To describe the effects of UV irradiance and plastic-type on microhardness, values for BPP and PET samples exposed to different irradiance levels were compared. Triplicate samples of each plastic type were analysed on different locations of both sides. Figure 4.7 illustrates the average microhardness values of fresh (untreated) material as well as the final values following different UV exposures. The percentage increase relative to untreated material is also presented.

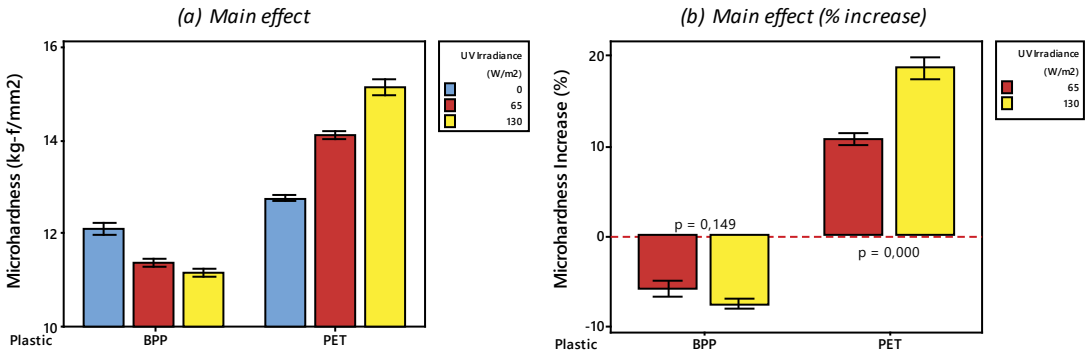

Figure 4.7. (a) Microhardness (kg-f/mm^2) results for different plastics exposed to different UV irradiances during pre-treatment; (b) Percentage microhardness increase (from week 0) of plastics shown in (a).

The first observation when considering Figure 4.7 (b) is that BPP showed a decrease in microhardness, while PET showed an increase as UV irradiance was increased. This corresponds to the trends observed for crystallinity in Figure 4.4 (a). BPP showed a decrease of 2.9% for the low UV irradiance (65 W/m^2) and a decrease of 3.7% for the high UV irradiance (130 W/m^2). Conversely, PET showed an increase of 4.9% for the low UV irradiance (65 W/m^2) and an increase of 8.5% for the higher UV irradiance (130 W/m^2) setting. In this case, it was found that different UV irradiances did not result in significantly different changes in the microhardness of BPP samples, as shown by the p-value of 0.149. However, differences in PET samples were statistically significant. These results confirm the relationship between microhardness and crystallinity for the pre-treatment experiments.

4.1.4 FTIR Indices

As discussed in Section 3.5.3, FTIR spectroscopy was used to identify and track changes in the molecular structures of the investigated plastics. Two regions were considered in this study; the carbonyl region (1870-1540 cm^{-1}) and the hydroxyl region (3800-3050 cm^{-1}). For the exact methodology used to determine the corrected band areas and peak heights, please refer to Section 3.5.3. It is worth noting that the carbonyl indices (CI) and hydroxyl indices (OHI) of BPP and CPP were directly comparable; this was since they were calculated in the same way, by integrating between precisely the same frequencies and using the same reference peak for the denominator in these calculations. PET showed a much sharper (and more intense) carbonyl peak (due to the ester carbonyls in its backbone), and a different unaltered reference peak was selected for its calculations. Therefore, BPP and CPP will be discussed together, with PET in a separate section.

4.1.4.1 Effect of UV irradiance (BPP and CPP)

To describe the effect of UV irradiance on carbonyl group developments, indices from samples exposed to different irradiance levels were compared. Carbonyl indices were determined at each sampling interval for different plastic types and shapes. Triplicate samples were analysed on three different spots on both sides (front and back). The drawn spectra were used to calculate the corrected areas (and heights) and substituted into Equations [3] and [4] to determine the index values. Outliers were statistically identified and removed. Figure 4.8 summarises the effect of UV irradiance on the determined CI values for BPP and CPP. In these figures, the means and standard errors are reported.

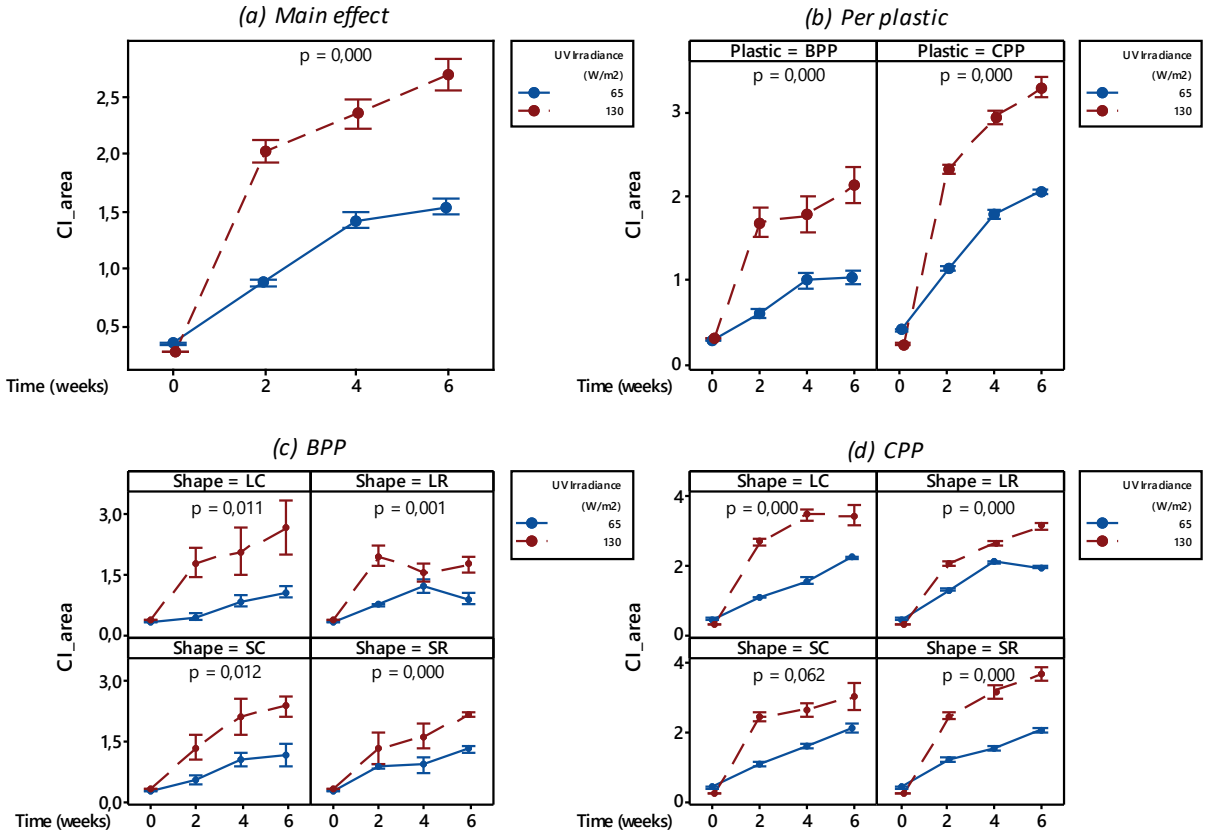

Figure 4.8. (a) Main effect of UV irradiance on carbonyl index over time (weeks) for PPs; (b) Carbonyl index over time (weeks) per plastic; (c) Carbonyl index over time (weeks) for BPP per shape; (d) Carbonyl index over time (weeks) for CPP per shape.

Figure 4.8 (a) depicts the pronounced effect of UV irradiance on carbonyl group development for the two PPs. Increased irradiance resulted in significantly increased rates and extents of carbonyl-containing product formation. Overall, the higher UV irradiance (130 W/m^2) resulted in a 74.5% higher CI value relative to the lower irradiance (65 W/m^2). In terms of the rate at which these groups developed, it is evident that for the higher irradiance, the maximum rate was within the first two weeks of degradation. The lower irradiance indicated a more gradual increase within the first four weeks and then slightly plateaued. When comparing the first two weeks of exposure, the rate of CI growth was 3.3 times higher for the 130 W/m^2 irradiance than the lower 65 W/m^2 irradiance.

For Figure 4.8 (b) that considers the effect of UV irradiance per plastic-type, the same is seen. Both BPP and CPP displayed increased rates and extents of carbonyl group developments for the higher irradiance setting. These figures are further narrowed down in (c) and (d) wherein both cases no discrepancies were present. The effect of UV irradiance on carbonyl group developments for CPP corresponds particularly well to the trends for mass loss in Figure 4.1.

Increased irradiance resulted in more energy transferred to the polymer surface, initiating more radical reactions as more light was absorbed. These reactions then produced carbonyl-containing degradation products, as described earlier in Section 2.5.1. Figures 4.9 and 4.10 below indicate the development and formation of carbonyl peaks for BPP and CPP, following six weeks of exposure to the 130 W/m^2 irradiance, respectively. The spectra shown in these figures are the average spectra of the different investigated shapes.

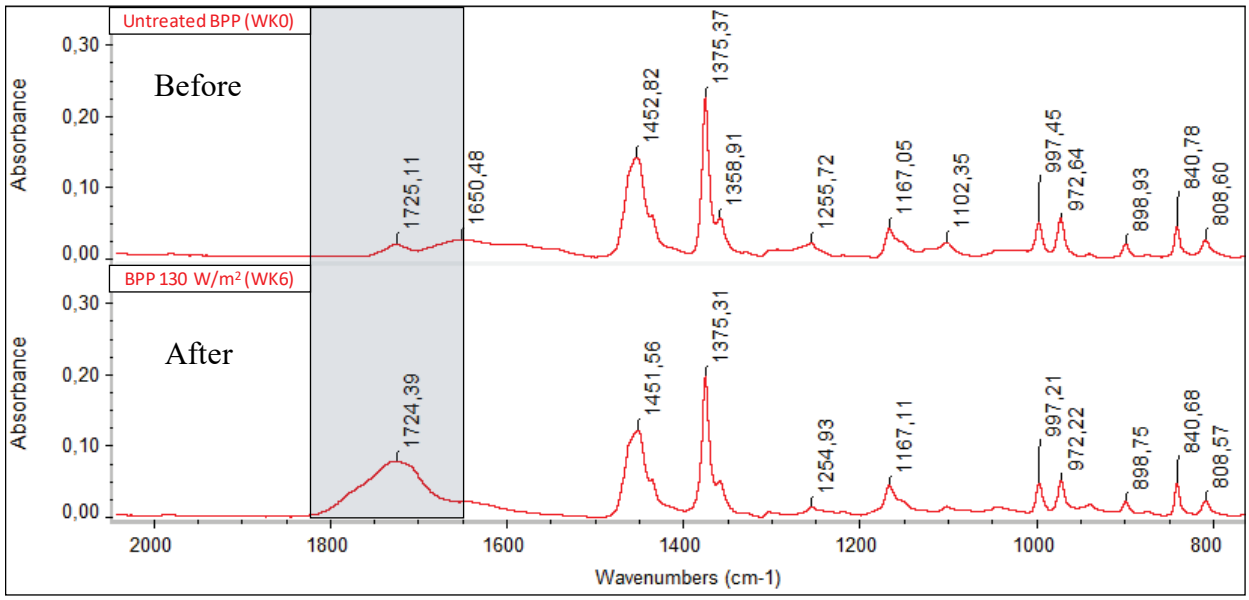

Figure 4.9. Average FTIR spectra of BPP indicating the development of the carbonyl peak following six weeks of exposure to the 130 W/m^2 UV irradiance.

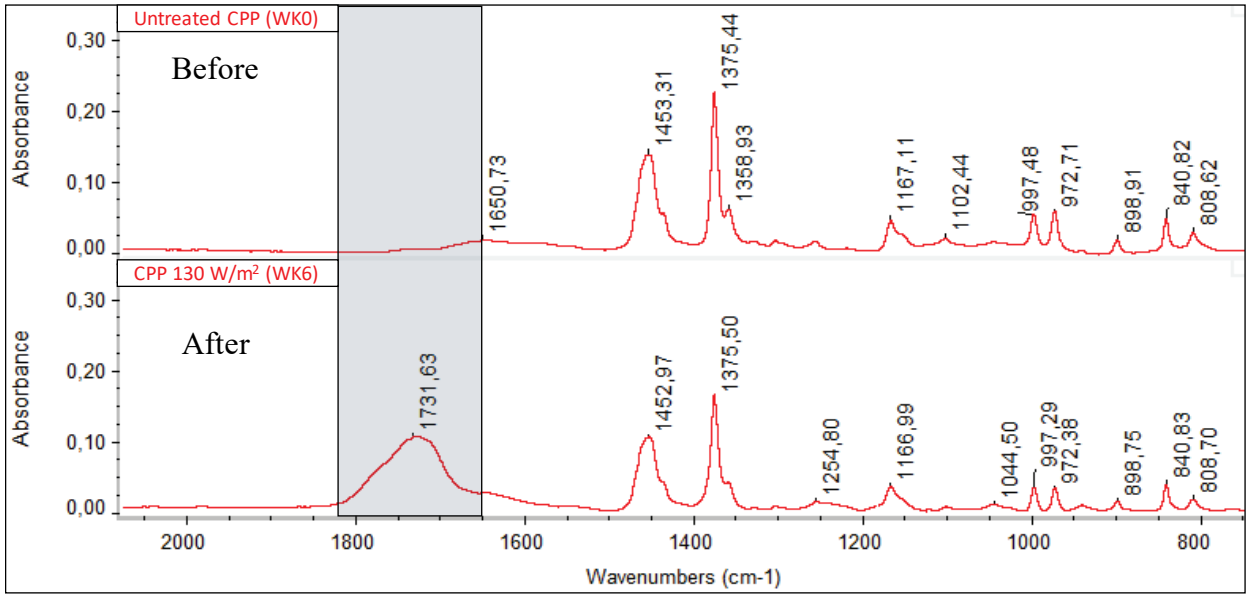

Figure 4.10. Average FTIR spectra of CPP indicating the formation of the carbonyl peak following six weeks of exposure to the 130 W/m^2 UV irradiance.

4.1.4.2 Effect of shape (BPP and CPP)

The effect of shape on carbonyl group development during UV pre-treatment for BPP and CPP is summarised below in Figure 4.11. In these figures, the CI values obtained from different shapes are plotted against exposure time. Values reported are the means and standard errors.

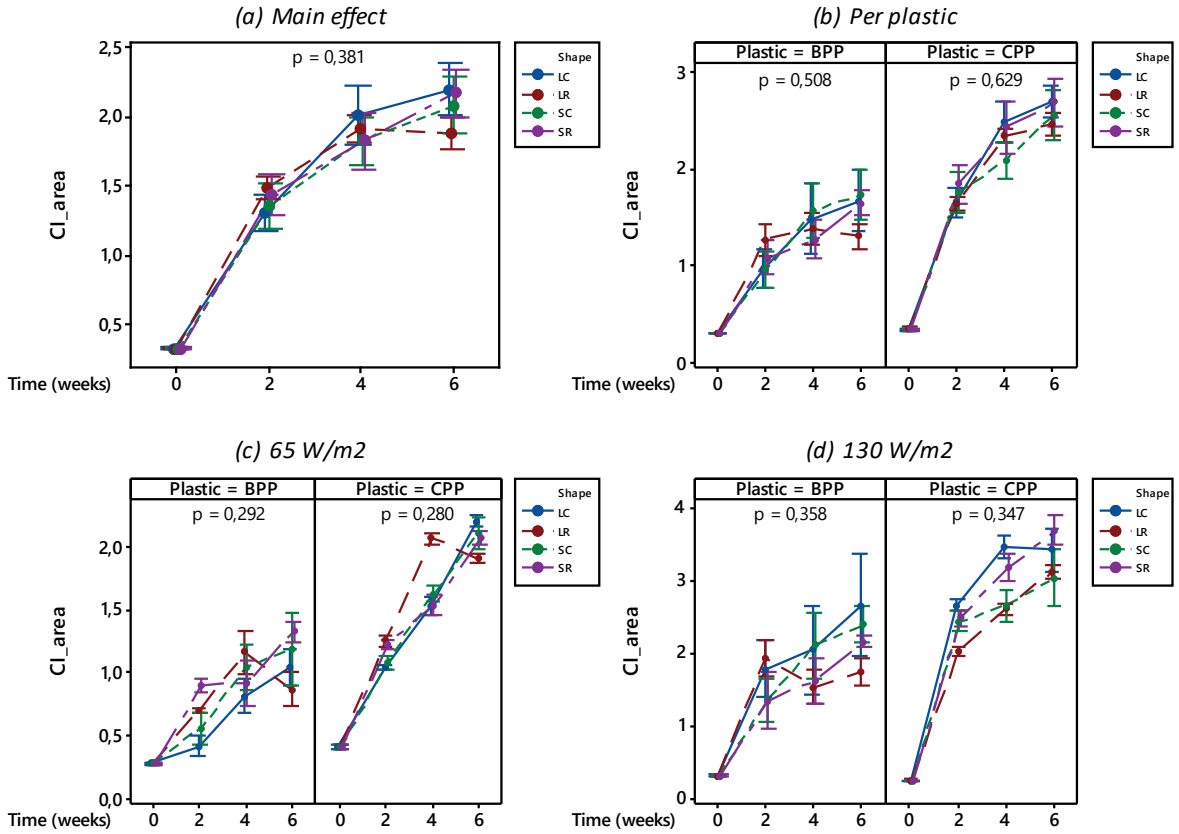

Figure 4.11. (a) Main effect of shape on carbonyl index over time (weeks) for PPs; (b) Carbonyl index over time (weeks) per plastic; (c) Carbonyl index over time (weeks) for the 65 W/m^2 irradiance; (d) Carbonyl index over time (weeks) for the 130 W/m^2 irradiance.

When considering Figure 4.11 (a), it is evident that overall, different shapes did not result in significant differences in the CI values during the UV pre-treatment. Although all shapes reflected increases in their carbonyl content, the uncertainty in the final week six values and overlapping error bars suggests that the effect of shape may be insignificant. This was proven by the determined p-value of 0.381 as in Table C.10. The same was seen for Figure 4.11 (b) through (d) and corresponded to the effect of shape on mass loss as in Figure 4.2. No significant differences were found to arise from different shapes. These findings indicate that oxidation occurred similarly for all shapes. Again, some minor discrepancies might be due to other parameters such as differences in sample thickness (influencing oxygen diffusion), incident UV light angles, and unevenly distributed additives incorporated into the plastic matrices.

4.1.4.3 Effect of plastic-type (BPP and CPP)

To describe the effect of plastic-type on carbonyl group developments, CI values were compared for the different polypropylenes. The results are summarised in Figure 4.12 below. The mean values and standard errors are reported for each sampling interval.

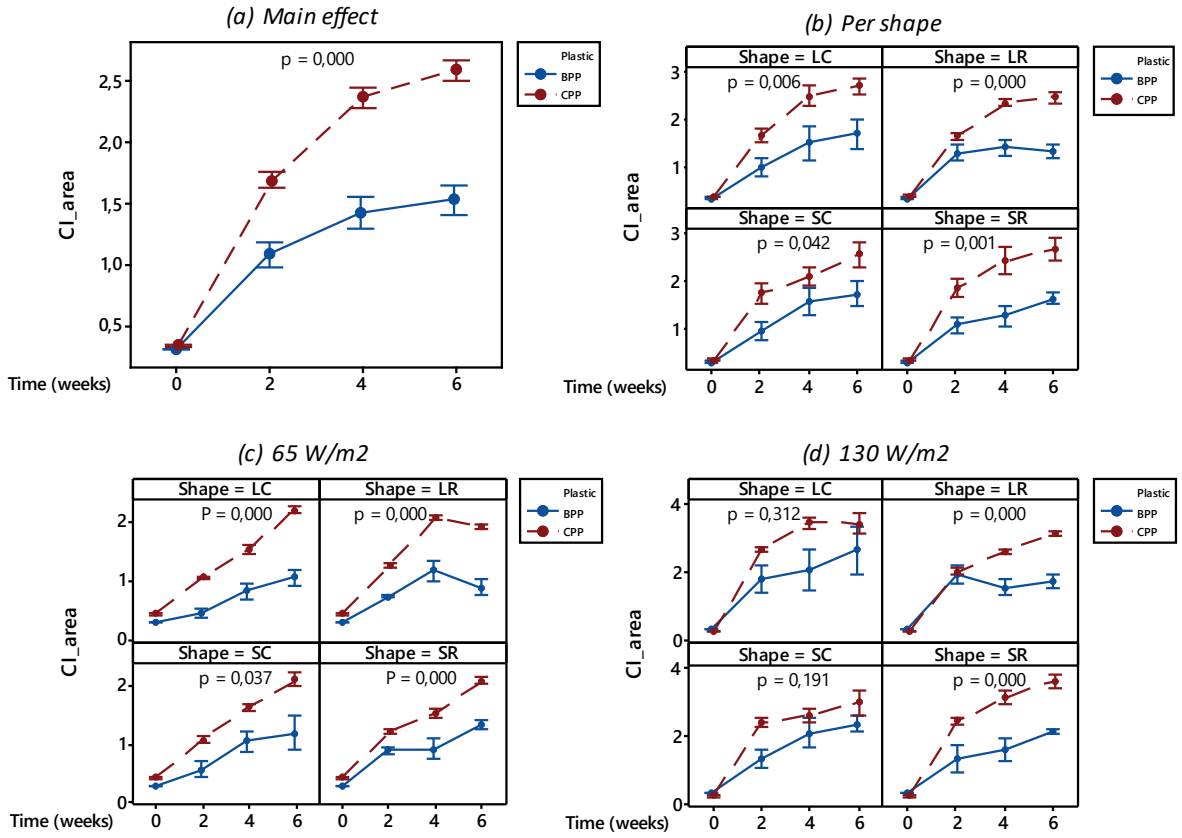

Figure 4.12. (a) Main effect of plastic-type on carbonyl index over time (weeks) for PPs; (b) Carbonyl index over time (weeks) for PPs per shape; (c) Carbonyl index over time (weeks) for the 65 W/m^2 irradiance; (d) Carbonyl index over time (weeks) for the 130 W/m^2 irradiance.

Figure 4.12 (a) indicates the main effect of plastic-type on carbonyl group developments for the PPs during the pre-treatment experiments. CPP showed significantly higher rates and extents of carbonyl formation than BPP. More specifically, this figure indicates that the final CI value for CPP was 70% higher relative to its black counterpart. The same trend was apparent when narrowing down results from Figure 4.12 (b) through (d). Although both plastics were polypropylenes, results suggest that CPP was more susceptible to oxidation than BPP. As mentioned earlier, this was probably due to the absence of carbon black acting as a UV absorber (or radical scavenger) making CPP more susceptible to photo-oxidative degradation.

4.1.4.4 Effect of UV irradiance (PET)

The following section will focus exclusively on PET. As mentioned in the introduction of Section 4.1.4, different frequency ranges were used to determine the indices of PET. In addition to that, carbonyl indices of PET were at least an order of magnitude higher than those of the PPs. This is due to the high number of carbonyl compounds present in the ester groups of the polymer backbone. In addition to only describing the carbonyl indices calculated by band areas, the same was done by considering peak heights. This resulted in an interesting observation where areas increased, but peak heights decreased; i.e. broadening and flattening of the carbonyl peak, which is a known phenomenon during PET degradation. The carbonyl peak was specifically considered for PET as the formation of C=O from carboxylic acids (1675 cm^{-1}) are represented in the region as an energetic shoulder evolving from the existing carbonyl peak (Gok, 2016).

The effect of UV irradiance on carbonyl functional group developments is shown below in Figure 4.13. Results from both band area and height calculations are shown, with means and standard errors reported for each sampling interval.

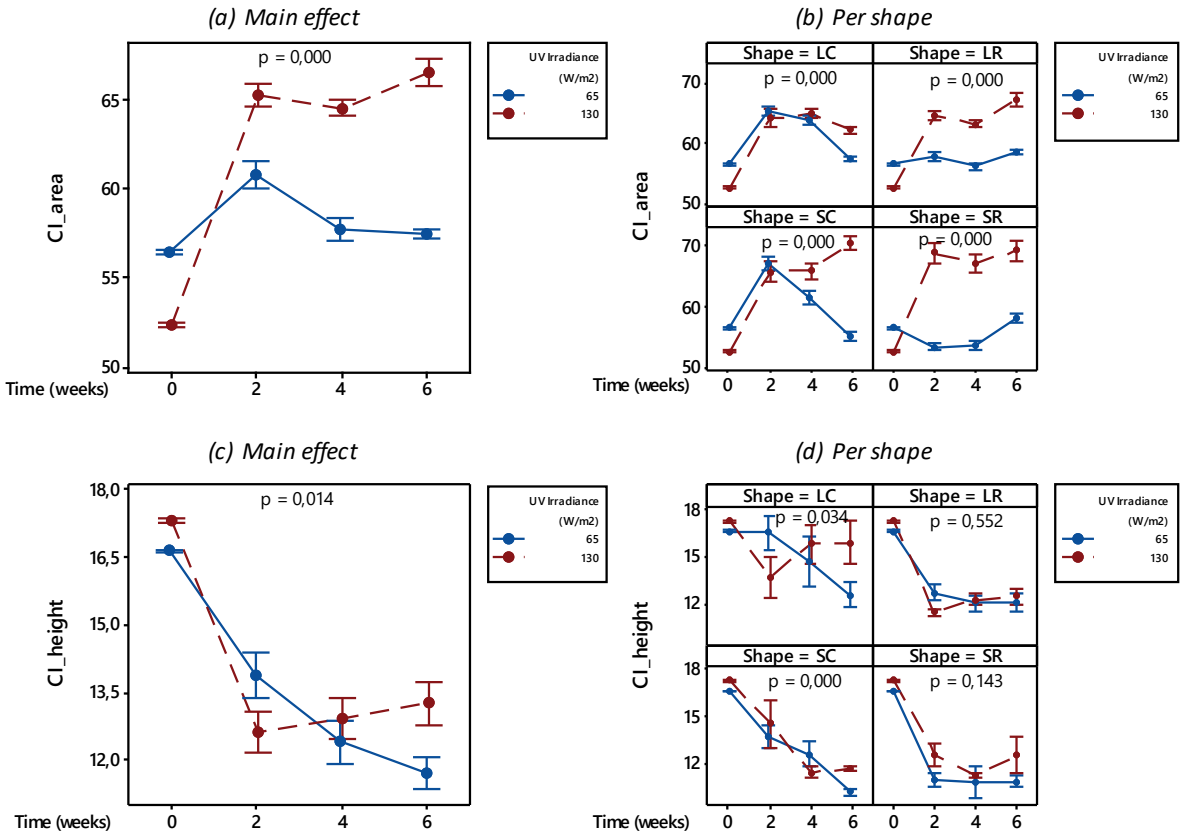

Figure 4.13. (a) Main effect of UV irradiance on carbonyl index (by areas) over time (weeks) for PET; (b) Carbonyl index (by areas) over time (weeks) for PET per shape; (c) Carbonyl index (by heights) over time (weeks) for PET; (d) Carbonyl index (by heights) over time (weeks) for PET per shape.

Considering Figure 4.13 (a) and (c) there is a clear trend indicating the effect of UV irradiance particularly within the first two weeks of degradation. In (a) the initial rate of carbonyl growth (by area ratios), was 2.9 times higher for the 130 W/m^2 irradiance than for the 65 W/m^2 irradiance. Conversely, in (c) the rate of carbonyl index decline (by height ratios), was 1.7 times higher for the 130 W/m^2 irradiance in comparison to the lower 65 W/m^2 irradiance. This band area increase, and simultaneous peak height decrease, indicate the broadening and of the carbonyl peak.

The same argument as for mass loss holds. Higher UV irradiance resulted in more reactions and more degradation products being produced. Assuming degradation took place via the free-radical mechanism, hydroperoxide decomposition resulted in scission reactions forming products including carboxyl radicals (converted to carboxylic acids) and aliphatic aldehydes. The formation of aldehydes or carboxylic acids probably made up the new carbonyl products observed via FTIR resulting in the broadening of the carbonyl peak as described above. The spectra indicating the formation of a new peak and the broadening effect is shown below in Figure 4.14. These spectra are the averages of the different investigated shapes.

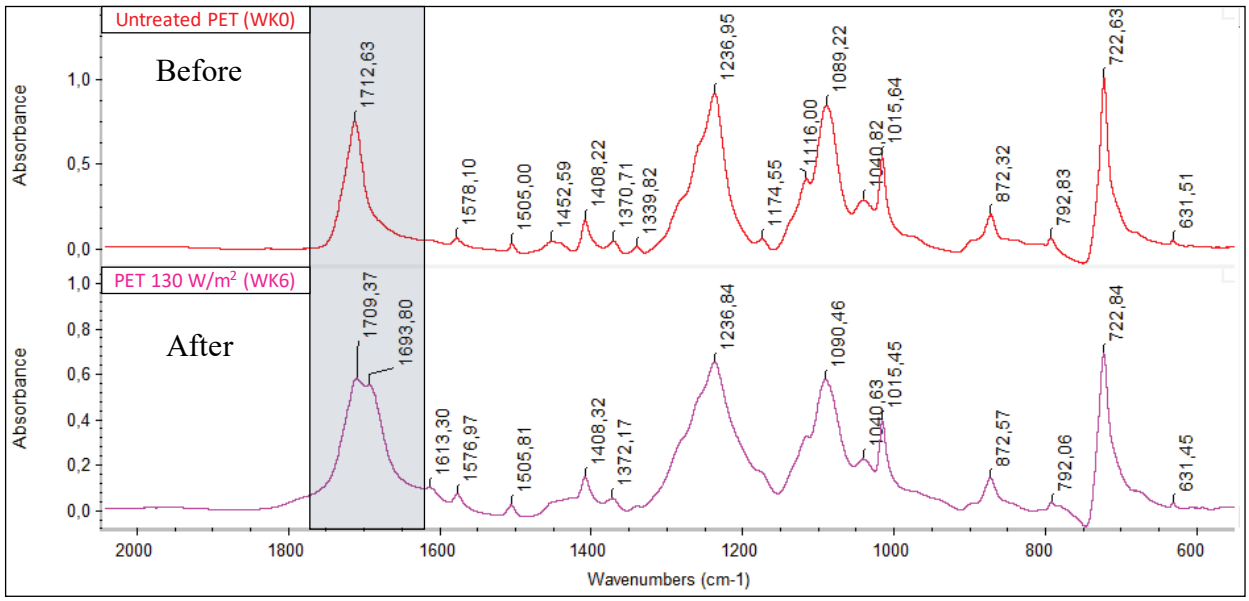

Figure 4.14. Average FTIR spectra of PET indicating the broadening of the carbonyl peak and formation of acids following six weeks of exposure to the 130 W/m^2 UV irradiance.

4.1.4.5 Effect of plastic shape (PET)

Figure 4.15 below is a summary of the effect of shape on carbonyl developments for PET during the UV pre-treatment. Carbonyl indices of different shapes were compared for each sampling interval. The mean values and standard errors are reported.

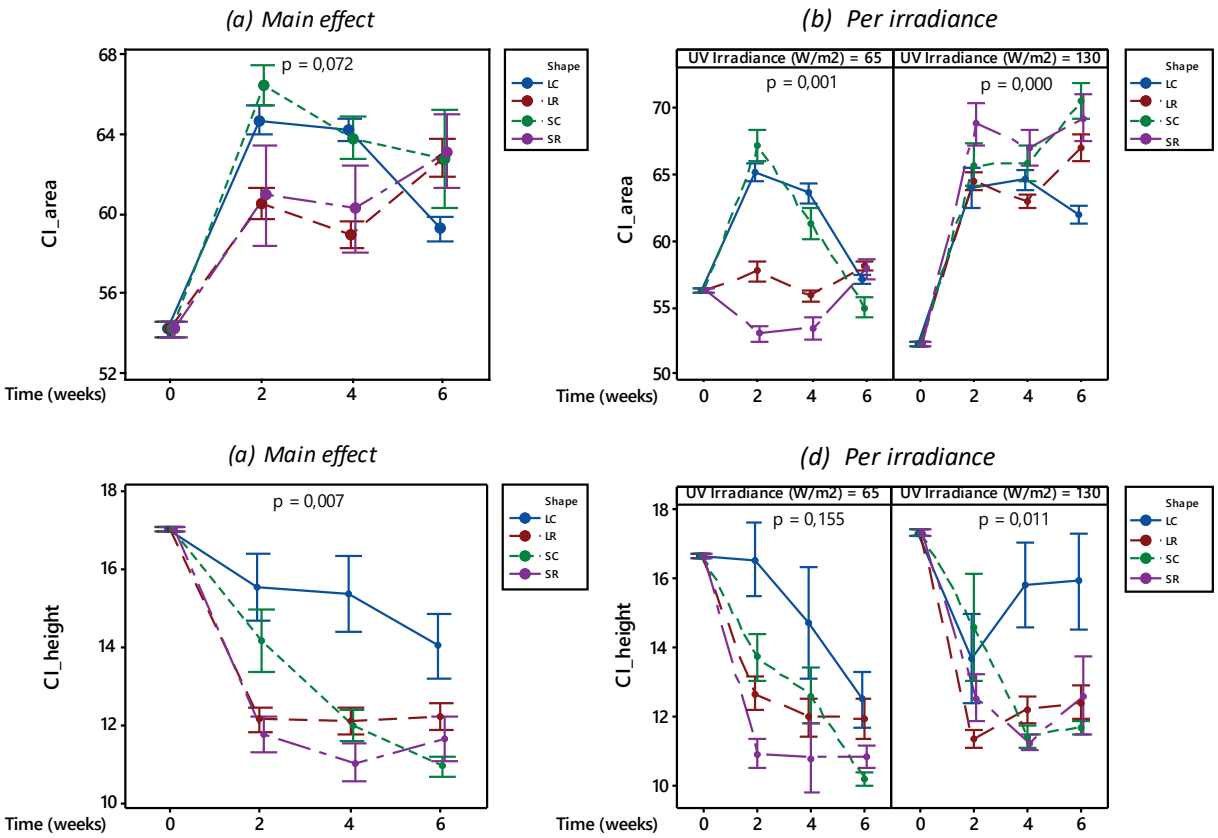

Figure 4.15: (a) Main effect of shape on carbonyl index (by areas) over time (weeks) for PET; (b) Carbonyl index (by areas) over time (weeks) for PET at different irradiances; (c) Carbonyl index (by heights) over time (weeks) for PET; (d) Carbonyl index (by heights) over time (weeks) for PET at different irradiances.

When considering Figure 4.15 (a) and (c), within the first four weeks of exposure, it seemed as if there was a trend apparent between the rectangular and circular shaped samples. Indices for the circular-shaped samples increased more rapidly in terms of area and decreased less so in terms of height. This implies that although the peak intensity remained relatively constant, additional carbonyl-containing products were formed. The same grouping between circular and rectangular shapes was observed in (b) and (d). Nevertheless, when considering only the final CI values, it was found that standard error bars mostly overlapped, with some exceptions in the case of LC and SC. In most instances, these outliers were responsible for the significance as indicated by the determined p-values.

4.2 UV beaker tests

The beaker tests formed part of the second stage of the sequential degradation experiments. These tests represented the period after which plastic material (after spending time on land) has entered the marine environment. This usually takes place via wastewater channels, rivers, and

occasionally spillages from shipping freights. Two types of beaker tests were conducted: one focusing again on UV radiation, and the other on temperature. In this section, the results of the former will be discussed. The same analyses were performed as for the pre-treatment, with some minor adjustments including the drying and rinsing of samples prior to analysis, as well as only focussing on small circular-shaped pieces. Two additional parameters were introduced: the sample's previous UV history (irradiance level of the pre-treatment), and different solution media (either seawater or demineralised water). The complete ANOVA results for the UV beaker tests are presented in Section C.2 of Appendix C.

4.2.1 Mass loss

As material enters the marine environment, it is anticipated that samples might exhibit more mass loss. The same reasons, as mentioned in Section 4.1.1 apply with the additional possibility of hydrophilic degradation products, previously formed on the plastic's surface, dissolving in the solution medium contributing to mass loss. Figure 4.16 shows the main effects of UV irradiance, plastic-type, UV history, and solution medium on mass loss that occurred during the UV beaker tests. The mass loss values reported here are relative to the beginning of the beaker tests.

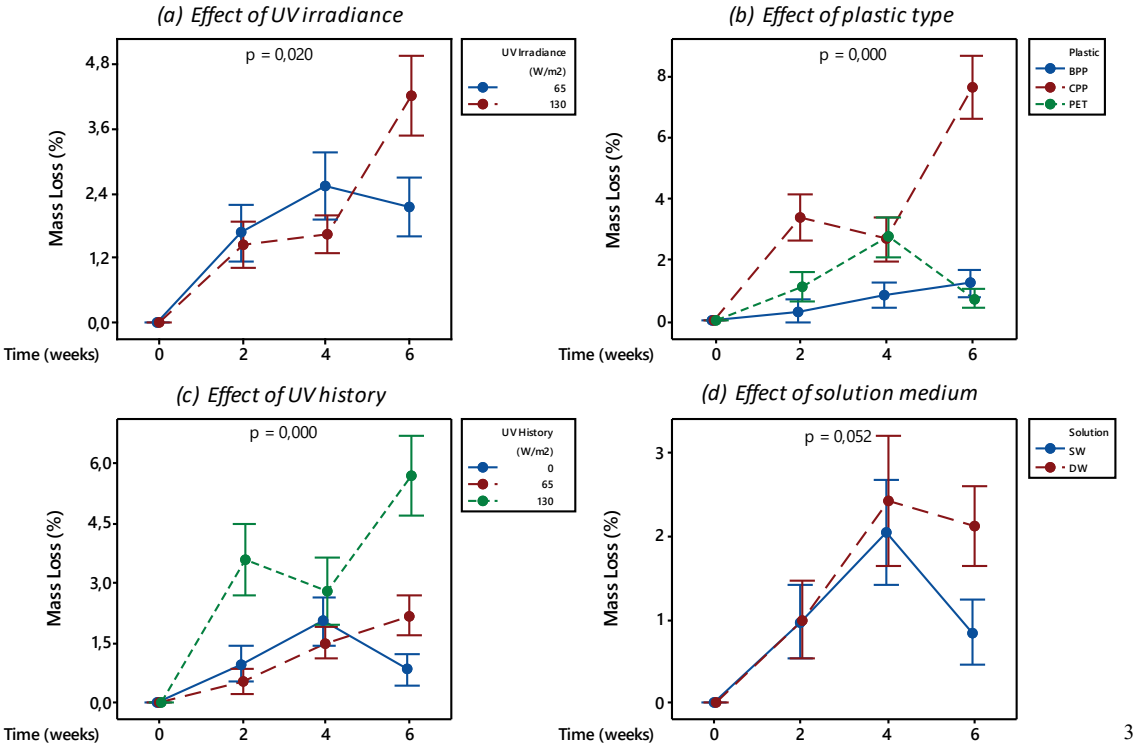

Figure 4.16. Effect of (a) UV irradiance (W/m^2), (b) plastic-type, (c) UV history (W/m^2), and (d) solution medium on mass loss (%) over time (weeks) during the UV beaker tests.

[3] Figure 4.16 (a), (b), and (c) depicts data from samples immersed in seawater while (d) represents data from untreated samples with no previous UV exposure.

Figure 4.16 is a summary of the overall main effects of (a) UV irradiance, (b) plastic-type, (c) UV history, and (d) solution medium. These figures could be further narrowed down per parameter, but overall, they encapsulate the main individual effects sufficiently.

Starting with (a) the main effect of UV irradiance is shown. Within the first four weeks of degradation, the lower irradiance resulted in slightly higher mass loss than the higher irradiance. This trend reversed for the final sampling interval, where the higher irradiance resulted in a significantly increased mass loss. These results indicated that ultimately the higher irradiance resulted in double the mass loss obtained from the lower irradiance. This corresponds to the effect of UV irradiance on mass loss as during the pre-treatment in Figure 4.1 (a). From the p-value of 0.020, the difference in final mass loss due to different UV irradiances was significant. The complete ANOVA results are presented in Table C.14 of Appendix C.

When considering the effect of plastic-type in (b), it is evident that initially, mass loss occurred in decreasing order from CPP to PET to BPP. This is an interesting observation as PET samples seem to have lost more mass when exposed to water than during the dry pre-treatment stage as shown in Figure 4.3 (a). This can likely be attributed to PET being more susceptible to hydrolytic degradation, as discussed in Section 2.6. Ultimately, CPP resulted in a significant 7.7 % mass loss, while the values for BPP and PET were at 1.2% and 0.7 % respectively.

In Figure 4.16 (c) the effect of UV history is illustrated. A clear trend is apparent, indicating samples with the highest previous UV history (130 W/m^2) resulted in the most significant mass loss as degradation time progressed. When comparing the mass loss for material with 0 W/m^2 and 65 W/m^2 histories, it was found that, for the first four weeks of degradation, fresh material (0 W/m^2) lost more mass than those with a 65 W/m^2 degradation history. This changed in the final two weeks with the fresh material (0 W/m^2) increasing in mass. It is believed that overall, an increase in UV history resulted in increased mass loss due to previous degradation already weakening the material surfaces and increasing its surface roughness (i.e. SA/V ratio). This allowed water, UV light, radicals, and oxygen, to permeate deeper into the material body, leading to degradation and eventually disintegration.

Lastly, when considering Figure 4.16 (d) the effect of solution medium on the mass loss of untreated material is illustrated. These results indicate that the rate, and ultimately the extent of mass loss was higher in demineralised water than in seawater. Owing to the presence of dissolved solids (salts and organic matter), seawater absorbs UV light more rapidly, leading to lower radiation levels reaching the plastics' surface. This, along with lower dissolved oxygen

concentrations reduced the degradation effects of this solution medium. The determined p-value of 0.052 was marginally higher than the selected α-value of 0.05. This is an indication that for the selected confidence interval of 95%, the final difference in mass loss due to solution medium was not statistically significant. ANOVA results for this determination are tabulated in Table C.17 of Appendix C.

4.2.2 Crystallinity

Crystallinities were calculated similarly as during the pre-treatment. For discussion purposes, percentage change is also reported. This change is reported as the percentage increase from the initial crystallinity at the start of the beaker tests (week 0) to the final crystallinity at the end (week 6). Importantly, for samples with previous UV histories, the initial (week 0) values are equivalent to the final (week 6) values obtained from the pre-treatment as in Figure 4.4 (a).

4.2.2.1 Effect of UV (irradiance and history)

To describe the effect of UV irradiance and history, samples with different UV histories (coming from pre-treatment) were immersed in seawater and exposed to different UV irradiances. Fresh untreated material with no UV history was also investigated. Triplicate samples were analysed with the means and standard errors reported. Crystallinity results for BPP following the UV beaker tests are shown below in Figure 4.17.

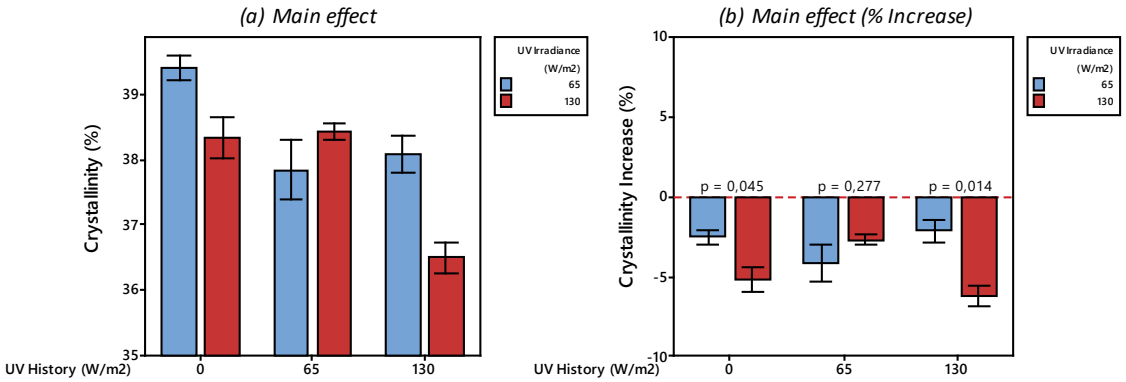

Figure 4.17. (a) Percentage crystallinity (%) over UV history (W/m^2) for BPP samples exposed to different UV irradiances (W/m^2) while immersed in seawater; (b) Percentage crystallinity increase (from week 0) of samples shown in (a) with Figure 4.4 as baseline.

In terms of the UV irradiance, it was found that an irradiance increase resulted in a crystallinity decrease for BPP. During the pre-treatment in Figure 4.4, BPP responded similarly to UV radiation. This was especially the case for untreated samples (0 W/m^2 history) and those coming from the 130 W/m^2 pre-treatment, both of which showed significant differences when considering

their respective p-values. No significant difference was found for samples with a previous UV history of 65 W/m^2. When comparing percentage crystallinity change in Figure 4.17 (b), it was found that for the higher irradiance (130 W/m^2), crystallinities decreased by 5.5% and 6.6% for the 0 W/m^2 and 130 W/m^2 UV histories respectively.

For the effect of UV history, it was found that an increase in UV history resulted in a decrease in crystallinity of BPP. The motivations for these observations remain similar to those for the pre-treatment. It is believed that increased irradiance (during pre-treatment) resulted in increased crosslinking, decreasing the ability of polymer chains to realign in an ordered structure. Moreover, decreased crystallinities due to increased UV histories could also be attributed to an increase in the number of structural defects and other chemical irregularities such as carbonyl and hydroperoxide groups (Rabello & White, 1966). Figure 4.18 below depicts the crystallinity results obtained for CPP following the UV beaker tests. Triplicate samples were analysed with the means and standard errors reported.

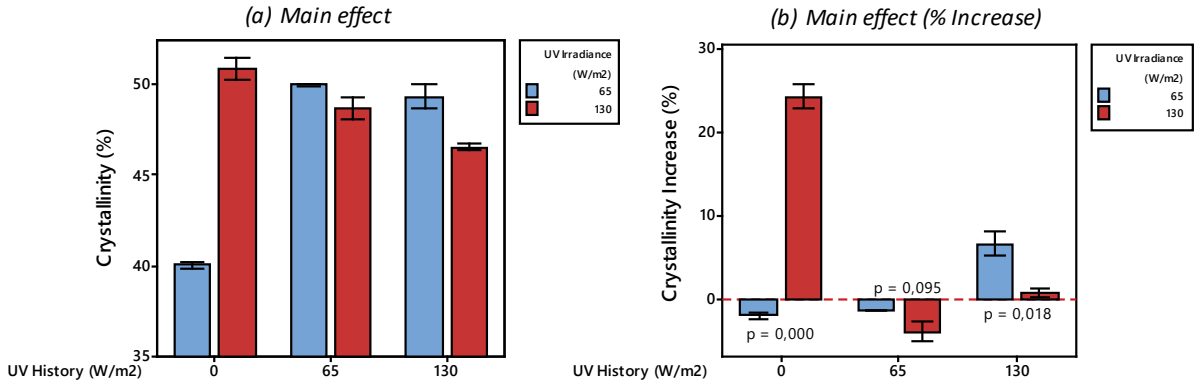

Figure 4.18. (a) Percentage crystallinity (%) over UV history (W/m^2) for CPP samples exposed to different UV irradiances (W/m^2) while immersed in seawater; (b) Percentage crystallinity increase (from week 0) of samples shown in (a) with Figure 4.4 as baseline.

The response for CPP during the UV beaker tests was different than for BPP. From Figure 4.18 (b) it is evident that initially, an increase in UV irradiance resulted in a significant increase in crystallinity. This corresponds to the observations during the pre-treatment in Figure 4.4 for CPP. However, as UV history was increased, the trend changed irregularly. When considering the 65 W/m^2 and 130 W/m^2 histories, it was found that for the former, both irradiance levels decreased the percentage crystallinity whilst the latter reflected increases for both irradiance levels.

This highlights the intricacies introduced by different degradation histories. The crystallinity of CPP initially increased considerably, but as samples were excessively degraded, their weakened surface layers might have eroded and broken down into the solution medium, exposing a fresher,

less crystallised layer to the solution. This is corroborated by the mass loss observed for CPP in Figure 4.16 (b). The same "reverse degradation" effect was also described by Brandon et al. (2016). Figure 4.19 illustrates the crystallinity results obtained for PET following the UV beaker tests. As for the previous two plastic types, triplicate samples were analysed, and the means and standard errors are reported.

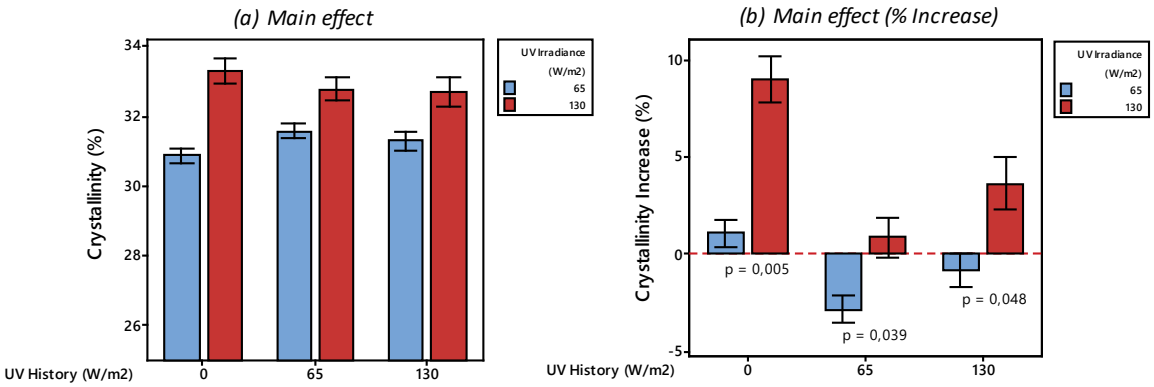

Figure 4.19. Percentage crystallinity (%) over UV history (W/m^2) for PET samples exposed to different UV irradiances (W/m^2) while immersed in seawater; (b) Percentage crystallinity increase (from week 0) of samples shown in (a) with Figure 4.4 as baseline.

PET behaved fairly similarly to CPP, where initially an increase in UV irradiance resulted in a significant increase in crystallinity. Thereafter, when considering samples with previous UV histories, the trend changed; in these cases, the 65 W/m^2 irradiance resulted in a decrease in crystallinity, while the 130 W/m^2 irradiance resulted in an increase. The effect of UV history showed that in general, by increasing the degradation history, the degree of crystallinity is reduced. Again, this might be ascribed to increased crosslinking as well as an increased number of structural defects and chemical irregularities arising from prior treatment.

4.2.2.2 Effect of solution medium

To evaluate the effect of solution medium on crystallinity, samples with no previous UV exposure (0 W/m^2) were immersed in glass beakers containing different aqueous solutions. Beakers were exposed to two different UV irradiances for a total duration of six weeks. After completion of the experiments, crystallinities were determined and results for the same plastics, immersed in different solutions, were compared. Results are shown in Figure 4.20. Triplicate samples were analysed, and the means and standard errors are reported.

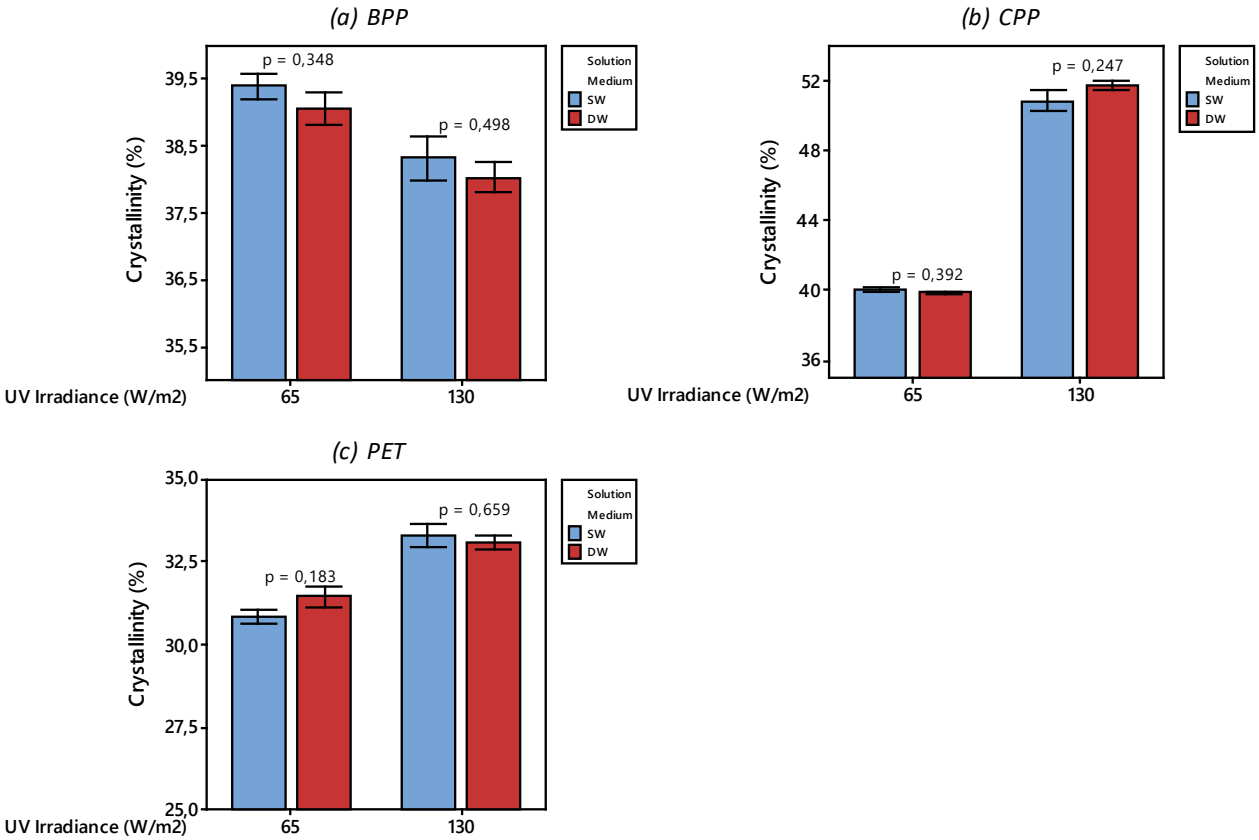

Figure 4.20. Percentage crystallinity (%) over UV irradiance (W/m^2) for different untreated plastic samples (0 W/m^2 UV history) immersed in different aqueous solutions.

Figure 4.20 (a) shows the crystallinities calculated for untreated BPP immersed in different aqueous solutions. From this figure, it is evident that for untreated BPP, an increase in UV irradiance resulted in a decrease in crystallinity. This has been explained previously. In addition to that, demineralised water at both irradiances resulted in slightly lower obtained crystallinities. Assuming a decrease in crystallinity of BPP indicates progressing degradation as seen during the pre-treatment, this finding implies a more pronounced degradation effect in demineralised water than in seawater.

Figure 4.20 (b) illustrates the effect of UV irradiance and solution medium on untreated CPP. In this case, an increase in UV irradiance resulted in a major increase in crystallinity with samples immersed in demineralised water resulting in the overall highest crystallinity at 130 W/m^2. From previous findings, it was evident that CPP showed crystallinity increases when exposed to UV radiation. Based on this, it seems as though demineralised water resulted in a more pronounced effect than seawater.

Finally, when considering untreated PET samples from different solutions in Figure 4.20 (c), it was found that crystallinity was proportional to UV irradiance. Furthermore, at the lower

irradiance level (65 W/m^2), demineralised water resulted in increased crystallinity relative to seawater. At the higher irradiance of 130 W/m^2, the opposite was found with samples immersed in seawater resulting in slightly higher degrees of crystallinity. Overall, although changes in crystallinity were more pronounced for samples immersed in demineralised water, the determined p-values confirmed that none of these differences were statistically significant. Tables C.21 through C.23 contains the results for these statistical analyses.

4.2.3 Microhardness

Microhardness was determined in the same way as for the UV pre-treatment. CPP samples were omitted as full datasets could not be generated due to material failure as described in Section 4.1.3. The percentage increase from the initial microhardness at the beginning of the experiments to the final microhardness at the end is also reported. For samples with previous UV histories, their initial (week 0) values are equivalent to the final (week 6) values from the pre-treatment, as shown in Figure 4.7 (a).

4.2.3.1 Effect of UV (irradiance and history)

To track changes in microhardness, untreated samples, as well as those with previous UV histories (from the pre-treatment), were immersed in glass beakers containing different aqueous solutions. Beakers were exposed to two different UV irradiances. After completion of each experiment, triplicate samples were analysed on multiple spots per sample. The means and standard errors are reported. Figure 4.21 illustrates the microhardness results for BPP following the UV beaker tests.

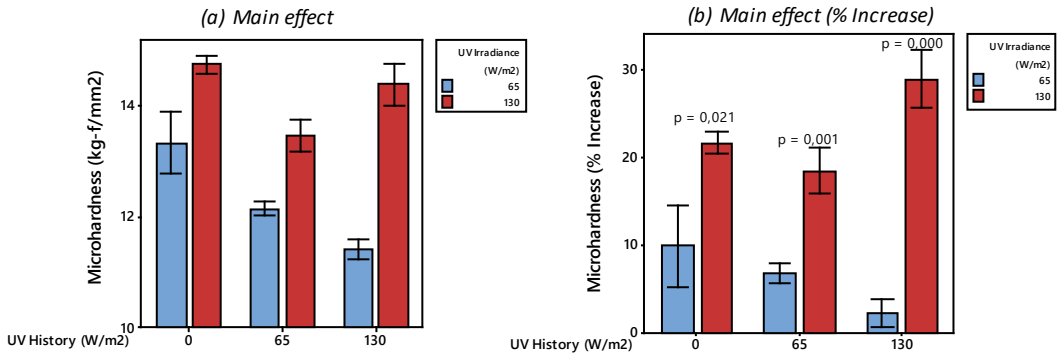

Figure 4.21. Microhardness (kg-f/mm^2) over UV history (W/m^2) for BPP samples exposed to different UV irradiances (W/m^2) while immersed in seawater; (b) Percentage microhardness increase (from week 0) of samples shown in (a) with Figure 4.7 as baseline.

When considering the effect of UV irradiance on the microhardness of BPP, it is evident from Figure 4.21 that irrespective of UV history, an increase in irradiance resulted in significant

increase in microhardness. This is contrary to the results for crystallinity in Figure 4.17 (a). The highest microhardness increase observed, was for BPP samples with a previous UV history of 130 W/m^2. An explanation for this result is that the absorbing and shielding ability of carbon black might have deteriorated due to prolonged exposure to radiation. This exposed previously stabilised polymer segments to destructive radiation that changed its microstructure and led to an increase in hardness. It was observed that by bending exposed BPP samples, a powdered black residue was released. In terms of UV history, it is evident that an increase in UV history generally resulted in a decrease in hardness for BPP. This result corresponds to the results for crystallinity in Figure 4.17. Prolonged exposure increased the number of structural defects, as well as the degree of crosslinking between polymeric chains. Figure 4.22 illustrates the microhardness results for PET following the UV beaker tests.

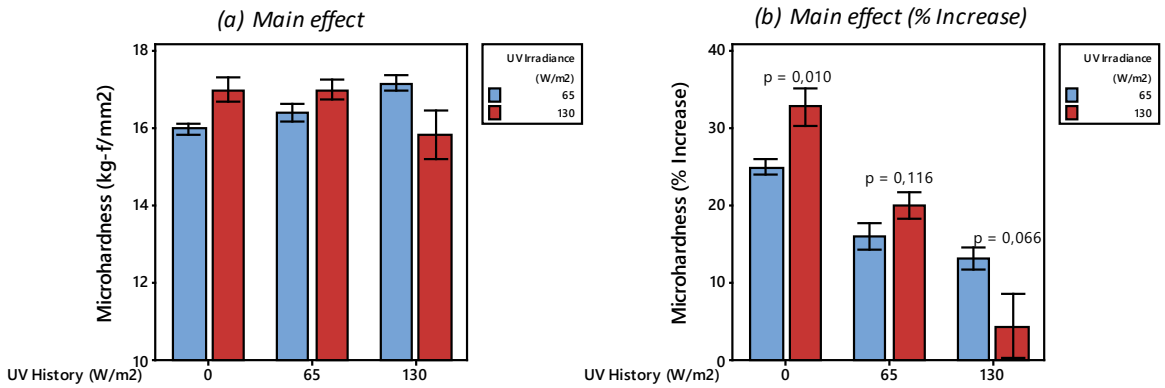

Figure 4.22. Microhardness (kg-f/mm^2) over UV history (W/m^2) for PET samples exposed to different UV irradiances (W/m^2) while immersed in seawater; (b) Percentage microhardness increase (from week 0) of samples shown in (a) with Figure 4.7 as baseline.

In terms of microhardness, Figure 4.22 shows similar trends for PET than those observed for crystallinity in Figure 4.19. Higher irradiance levels resulted in greater microhardness. The only discrepancy being PET with a UV history of 130 W/m^2. In terms of UV history, it is found that increased UV history resulted in smaller increases in microhardness. Material with no prior degradation showed the highest increase in microhardness as well as the only significant effect as reflected by the p-value of 0.010.

4.2.3.2 Effect of solution medium

To investigate the effect of solution medium on microhardness, fresh samples with no previous UV history (0 W/m^2) were immersed in different aqueous solutions. Beakers were exposed to different UV irradiances for six weeks. Final microhardness values of samples immersed in different solutions are reported below in Figure 4.23.

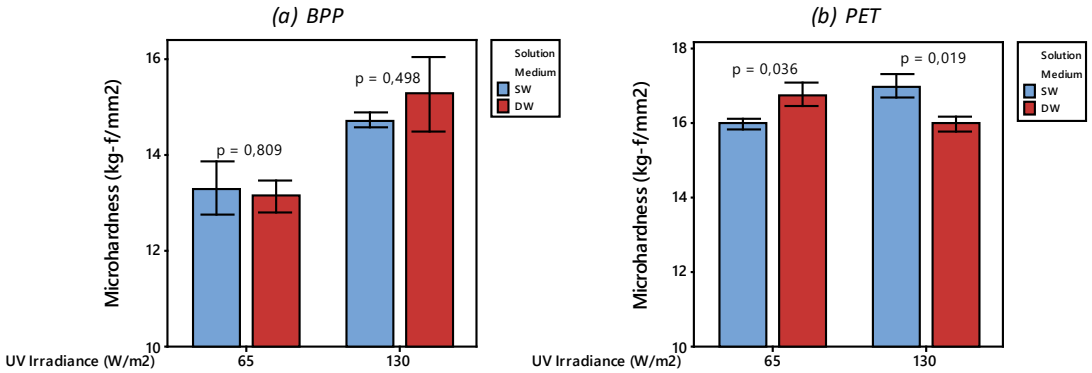

Figure 4.23. Microhardness (kg-f/mm^2) over UV irradiance (W/m^2) for different untreated plastic samples (0 W/m^2 UV history) immersed in different aqueous solutions.

Figure 4.23 looks at the effect of solution medium on microhardness for different plastics exposed to UV radiation. In Figure 4.23 (a) for BPP, it is clear that an increase in irradiance resulted in an increase in microhardness for untreated samples immersed in both solutions. Some irregularities are present at the different irradiances with error bars overlapping at both and p-values being greater than 0.05.

For PET in Figure 4.23 (b) the irregular trend persisted. In this case, however, error bars did not overlap, and differences were determined to be statistically significant. These results suggest that in seawater, PET increases in microhardness with an increase in irradiance, while decreasing when immersed in demineralised water. This might indicate some interaction between the type of solution medium and the UV irradiance of the source. A fundamental explanation for this interaction could not yet be established.

4.2.4 FTIR Indices

Carbonyl and hydroxyl indices were calculated similarly for all plastics as during the pre-treatment. During analysis, it was observed that for PET, the reference peak occasionally shifted, resulting in negative areas and indices to be calculated. This was countered by selecting a different reference peak at ~1508 cm^{-1} (aromatic skeleton vibration of C=C) that was used instead of the ~1576 cm^{-1} peak as in the pre-treatment. Outliers were statistically identified and removed. In this section, results for BPP and CPP will be discussed, followed by results for PET in a separate section.

4.2.4.1 Effect of UV (irradiance and history) for PPs

To investigate the effect of UV irradiance and UV history, carbonyl indices for samples exposed to different irradiances, and with different previous UV histories, were compared. Multiple spectra

were collected by analysing at least three samples on both sides. Results for BPP and CPP samples that were immersed in seawater are presented below in Figure 4.24. The means and standard errors are reported.

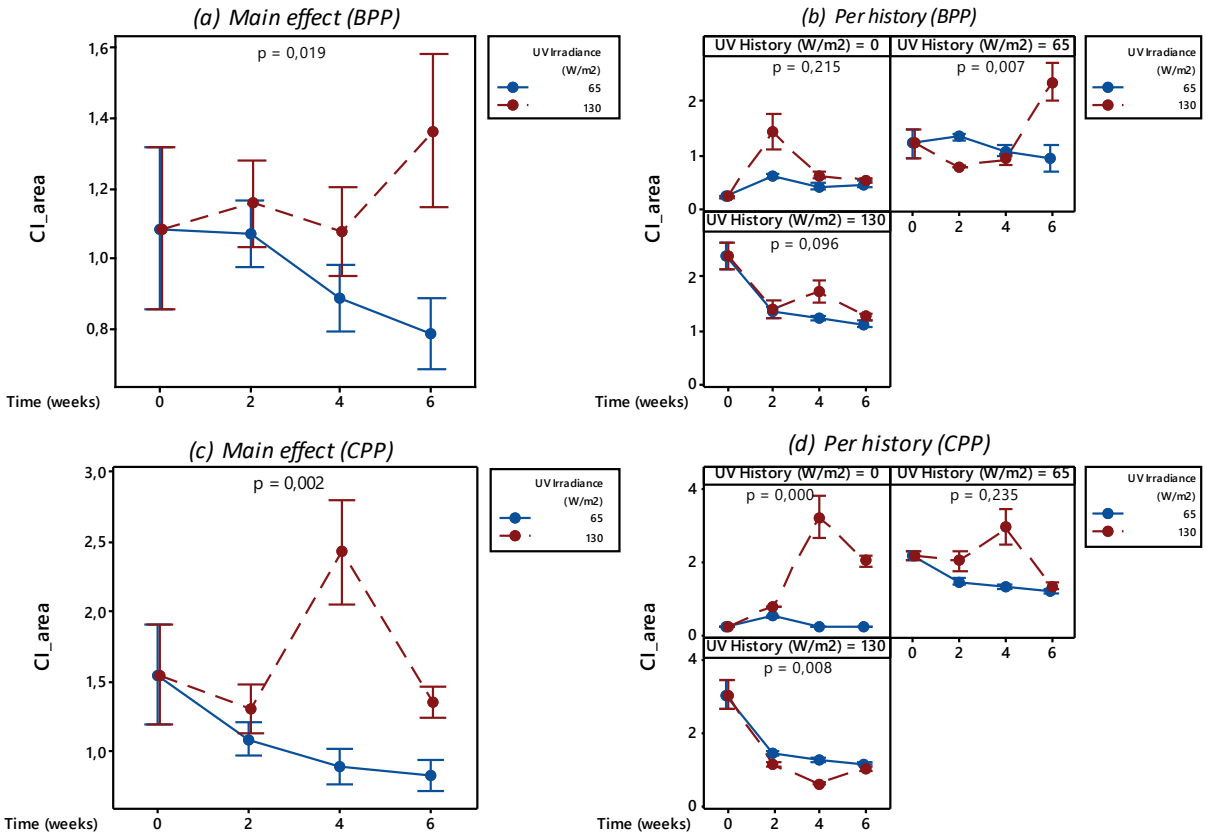

Figure 4.24. (a) Main effect of UV irradiance on CI over time (weeks) for BPP; (b) CI over time (weeks) for BPP with different UV histories; (c) Main effect of UV irradiance on CI over time (weeks) for CPP; (d) CI over time (weeks) for CPP with different UV histories.

From Figure 4.24 (a), it is evident that for BPP, increased irradiance resulted in higher carbonyl indices. This trend corresponds to results from the pre-treatment for BPP shown in Figure 4.8 (b). When considering Figure 4.24 (b), untreated plastic with no previous UV history and those with a UV history of 65 W/m^2 showed an increase in carbonyl index, whilst material with the most severe history of 130 W/m^2 showed a decrease. This indicates that prolonged UV exposure might have resulted in initial carbonyl products degrading further and peaks fading away. In addition to that, the liberation of smaller molecules containing these carbonyl species was believed to also have occurred. Canopoli et al. (2020) described advanced degradation to result in carbonyl group depletion and consequent reduction in the determined indices.

Overall, for CPP in Figure 4.24 (c), it was found that both irradiance settings ultimately resulted in a decrease in carbonyl index. This seems surprising, but again when considering figure (d)

evidence indicates that untreated CPP (with no UV history) resulted in a steep increase in carbonyl index, while samples with previous degradation histories resulted in a decrease. It is believed that specifically for CPP, besides carbonyl degradation products degrading and peaks fading away, the degraded and embrittled surface layer broke down into the solution medium, resulting in a fresher, undegraded layer being analysed. That would explain why the final carbonyl index of CPP with a UV history of 130 W/m^2 was relatively closer to the initial index (week 0) of fresh CPP with no previous UV history.

4.2.4.2 Effect of solution medium for PPs

To evaluate the effect of solution medium on carbonyl index changes, BPP and CPP samples with no previous UV histories were immersed in beakers containing different aqueous solutions. Beakers were exposed to two different UV irradiances for a duration of six weeks. Carbonyl indices were determined at each sampling interval, and values from the same plastics immersed in different solutions were compared.

Over the course of the experiments, CPP samples reflected different colour changes. Initially, samples were clear and almost entirely transparent. High transparency is a common manufacturing requirement and is typically achieved by the introduction of clarifying agents. These agents increase nucleation density, thereby reducing spherulite size which improves the overall transmittance of light. Figure 4.25 below indicates CPP colour shifts following different experiments. Samples became chalk-white following the pre-treatment and yellow following exposure to seawater. These observations indicate clarifying agents potentially leaching out into surrounding medium, or crystallisation altering the crystal sizes, therefore refracting light differently.

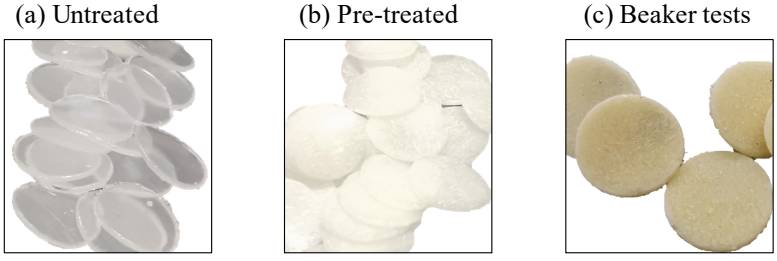

Figure 4.25. Photographs of CPP samples indicating the observed colour change following different degradation conditions.

Results for the effect of solution medium on carbonyl indices for BPP and CPP are summarised below in Figure 4.26. Datapoints represent the mean values and standard errors.

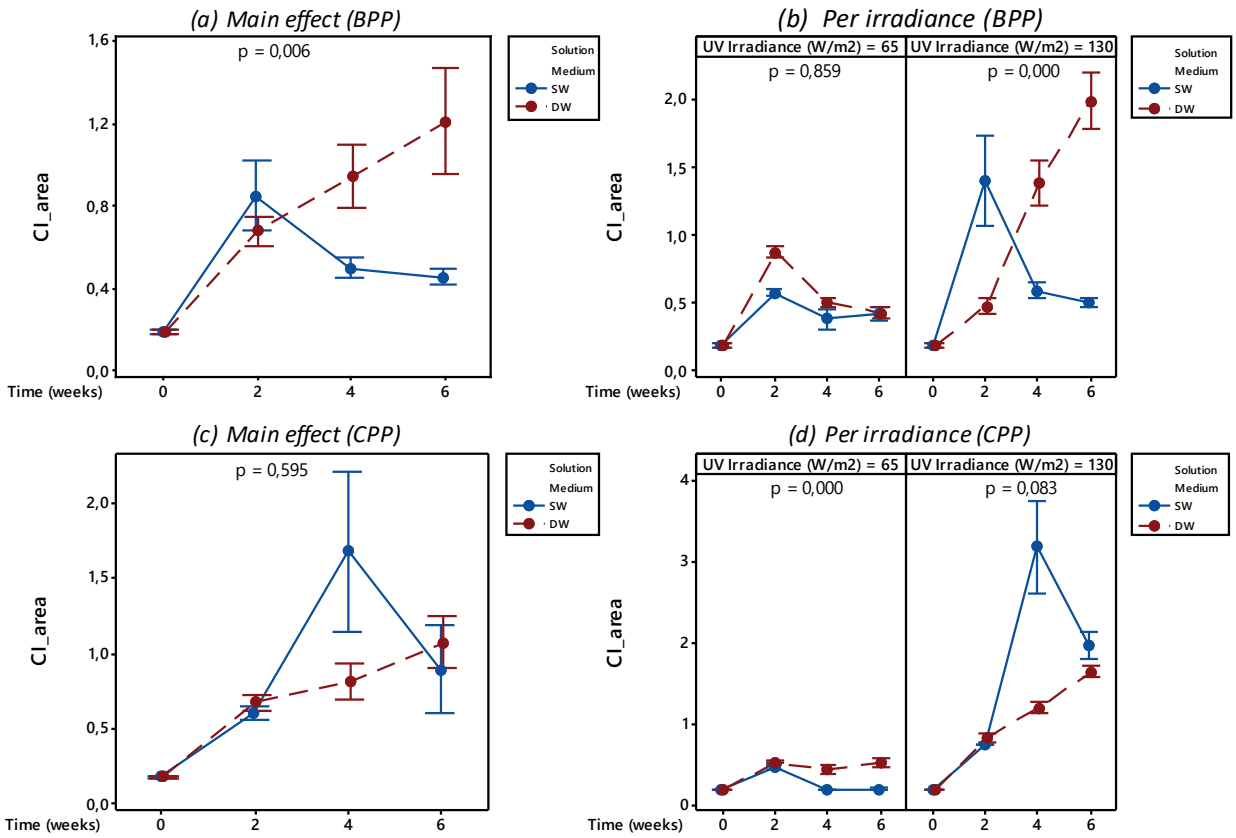

Figure 4.26. (a) Main effect of solution medium on CI over time (weeks) for BPP; (b) Effect of solution medium on CI over time (weeks) for BPP per irradiance; (c) Main effect of solution medium on CI over time (weeks) for CPP; (d) Effect of solution medium on CI over time (weeks) for CPP per irradiance.

From Figure 4.26 (a) the main effect of solution medium on carbonyl groups for BPP is shown. BPP immersed in demineralised water gave rise to higher carbonyl indices than those in seawater. Furthermore, when considering (b), it is evident that this was particularly the case at the higher irradiance level where a significant difference is reported.

For CPP in Figure 4.26 (c), the effect of solution medium was less pronounced. Overall, CPP samples immersed in demineralised water resulted in slightly higher indices than those immersed in seawater. This overall difference, however, was not statistically significant as seen by the p-value of 0.595. By considering (d), a significant difference was found for CPP samples immersed in demineralised water and exposed to the 65 W/m^2 irradiance.

Comparing these results to the pre-treatment as in Figure 4.1, it is revealed the rate and extent of oxidation were lower during the UV beaker tests than during the dry pre-treatment. This finding suggests that material would ultimately degrade faster on land than in the ocean.

4.2.4.3 Effect of UV (irradiance and history) for PET

To investigate the effect of UV irradiance and UV history on chemical changes of PET, samples with different histories were exposed to different UV irradiances while immersed in seawater. Carbonyl- and hydroxyl-indices were determined and compared. The spectral results for PET are summarised in Figure 4.27. In these figures, the means and standard errors are reported.

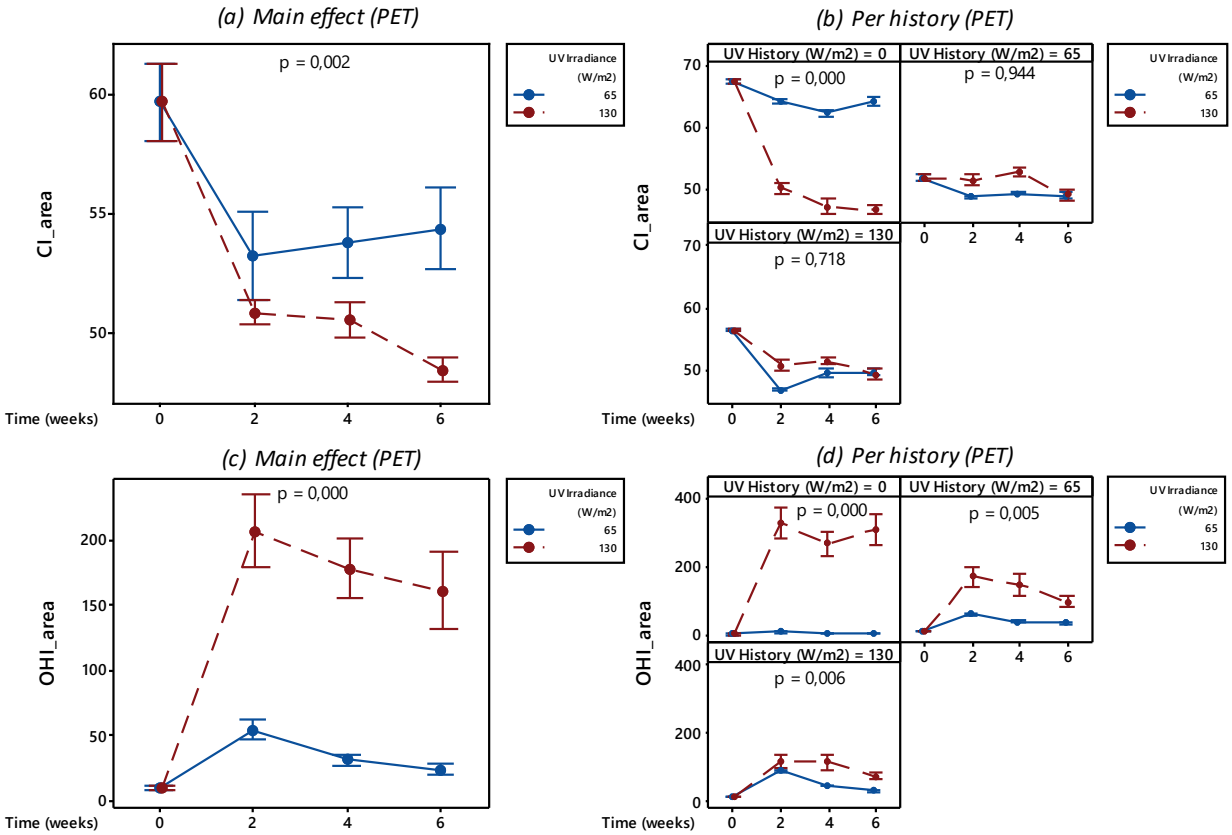

Figure 4.27. (a) Main effect of UV irradiance on CI over time (weeks) for PET; (b) CI over time (weeks) for PET with different UV histories; (c) Main effect of UV irradiance on OHI over time (weeks) for PET; (d) OHI over time (weeks) for PET with different UV histories.

From Figure 4.27 (a) the main effect of UV radiation on carbonyl indices for PET is shown. Both irradiances resulted in decreased carbonyl indices, with the higher irradiance in a steeper decrease. Gok (2016) described the loss of carbonyl groups in PET to be attributed to chain scission whereas the broadening is due to carboxylic acid generation, as seen for the pre-treatment in Figure 4.13 and Figure 4.14. Moving over to Figure 4.27 (b), it is evident that PET with no previous UV history resulted in the most significant change in carbonyl indices, while smaller changes were observed for material with previous exposure.

Figure 4.27 (c) indicates the hydroxyl indices calculated for PET during the UV beaker tests. A clear trend is apparent indicating that the higher irradiance resulted in a significant increase in the

hydroxyl index. These hydroxyl peaks were not observed during the pre-treatment, and it is believed that the introduction of water resulted in additional hydrolytic degradation occurring along with photo-oxidative degradation. This additional pathway probably introduced new products being formed, such as carboxylic acids and/or hydroxyl-esters as in Scheme 2.5. Again, when considering Figure 4.27 (d), it is evident that fresh material showed the most considerable change, while the hydroxyl growth was less pronounced for material that underwent previous UV exposure.

4.2.4.4 Effect of solution medium for PET

To describe the effect of solution medium, carbonyl indices of PET samples immersed in different aqueous solutions were compared. At each sampling interval, at least three samples were analysed on both sides. Indices were calculated and outliers removed. At each sampling interval, the means and standard errors are reported. The results are illustrated in Figure 4.28.

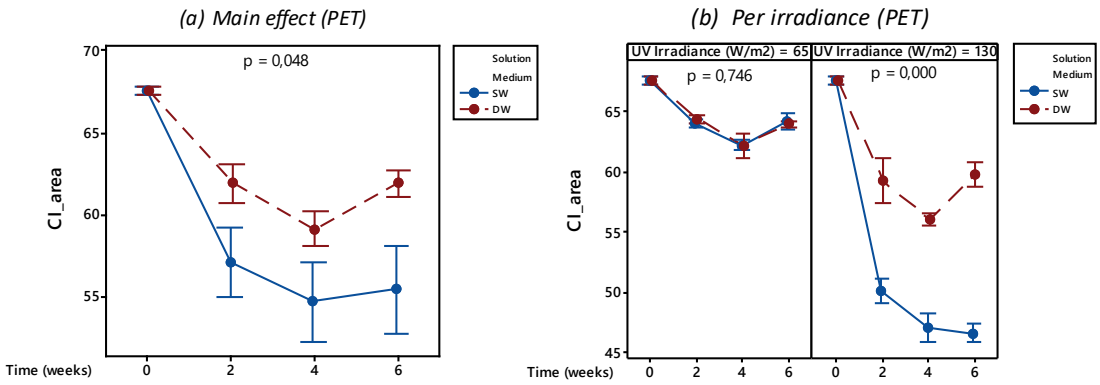

Figure 4.28. (a) Main effect of solution medium on CI over time (weeks) for PET; (b) Effect of solution medium on CI over time (weeks) for PET per irradiance.

From Figure 4.28 (a) it is evident that for both aqueous solutions, the carbonyl indices of untreated PET samples decreased. Overall, samples immersed in seawater resulted in a steeper decrease than those immersed in demineralised water. Moving over to Figure 4.28 (b), it is evident that at the lower irradiance (65 W/m^2), no significant difference between indices from the different solutions was found. However, at the higher irradiance the effect was more pronounced and a significant difference was determined.

This observation was contrary to previous results for solution medium. It was expected that assuming a decrease in carbonyl indices indicate degradation occurring for PET, demineralised water should have resulted in the lowest indices. However, this was not the case in these results. By recalling the findings for the PPs in Section 4.2.4.2, in all instances, plastics that were immersed in demineralised water resulted in higher carbonyl indices. This observation might point

out that carbonyl products remain more preserved in demineralised water than in seawater. Moreover, it might be indicative that PET degrades faster in seawater than in demineralised water. Following the beaker tests, PET samples immersed in seawater reflected a significant colour change from entirely transparent to opaque white. The same colour change was not observed for samples immersed in demineralised water. Figure 4.29 indicates these observations.

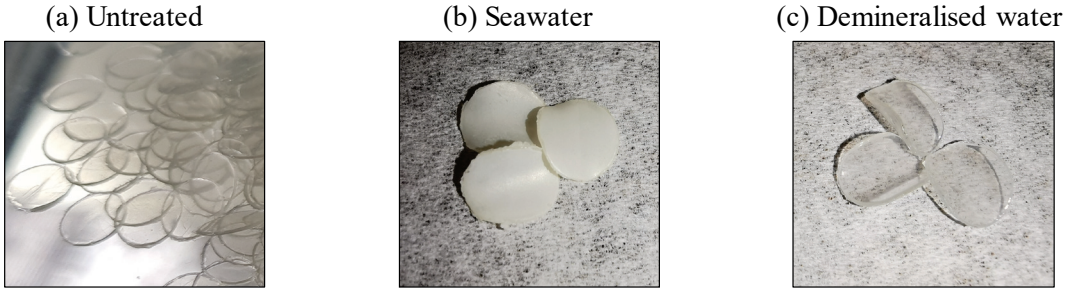

Figure 4.29. Photographs of PET samples indicating colour shifts (changes in transparency) following exposure to different aqueous solutions, (a) untreated PET samples, (b) samples immersed in seawater and (c) samples immersed in demineralised water.

It is known that crystallisation and particularly crystal size influences the transparency of PET. Manufacturing typically requires crystalline regions to be smaller than the wavelength of light since these regions also represent changes in the refractive index. Larger crystallites will scatter light at their interfaces and make PET opaque. Therefore, it can be concluded that more pronounced crystallisation took place in seawater than in demineralised water. This was verified by the findings for crystallinity of untreated (0 W/m^2) PET in seawater as in Figure 4.19.

4.3 Temperature beaker tests

The temperature beaker tests were conducted in conjunction with the UV beaker tests. For these experiments, samples were placed in glass beakers containing different aqueous solutions and exposed to different constant temperatures in an incubator. The idea was to investigate the physical and chemical property changes of plastic material with (and without) previous UV degradation histories when exposed to thermal environments. Two temperatures were investigated: 25°C and 60°C. Each experiment commenced for six weeks, with samples drawn and analysed on a fortnightly basis. The same analyses as during the UV beaker tests were performed. The complete ANOVA results for the temperature beaker tests are provided in Section C.3 of Appendix C.

4.3.1 Mass loss

It was believed that an increase in temperature would increase the reaction kinetics and consequently promote degradation. Ten random samples of each plastic-type, previous UV history, and from each solution medium were drawn on a fortnightly basis. Wet samples were gently rinsed with demineralised water, dried, and analysed shortly thereafter. Equation [1] was used to determine the percentage mass loss at each sampling interval. The effects of temperature, plastic-type, UV history, and solution medium on mass loss for the temperature beaker tests are summarised below in Figure 4.30. The mean values and standard errors are reported.

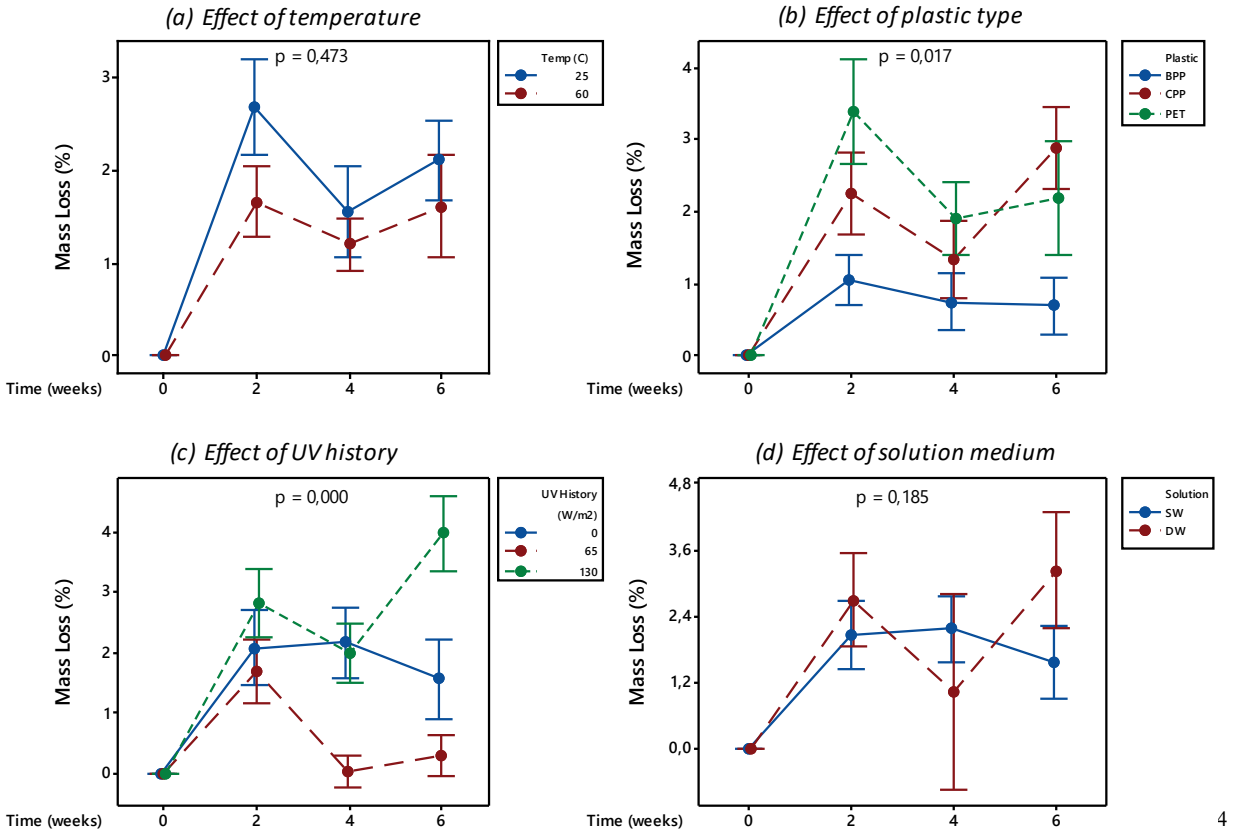

Figure 4.30. Effect of (a) temperature (°C), (b) plastic-type, (c) UV history (W/m²), and (d) solution medium on mass loss (%) over time (weeks) during the temperature beaker tests.

Figure 4.30 shows the effects of the investigated variables on mass loss during the temperature beaker tests. These results could be narrowed down further but are believed to represent the most important findings adequately.

[4] Figure 4.30 (a), (b), and (c) depicts data from samples immersed in seawater while (d) represents data from untreated samples with no previous UV exposure.

Starting with Figure 4.30 (a) the overall effect of temperature is shown. For the entire degradation period, it was found that the lower temperature (25°C) resulted in slightly higher mass loss than the higher temperature (60°C). This result was surprising at first since the higher temperature was expected to increase reaction kinetics and therefore facilitate subsequent mass loss. An explanation for this considers the reduced oxygen solubility in water at higher temperatures. This might have reduced the concentration of available reactant partaking in the oxidative reactions. Weiss (1970) showed that by increasing the temperature of seawater at 1 atm (salinity of 35 PSU) from 24°C to 40°C, the oxygen solubility decreased by 27.5%. Furthermore, the sorption kinetics is expected to have increased at elevated temperatures which may have resulted in salts and other organic material adsorbing to the plastic surfaces reducing mass loss. In general, salts do not adsorb onto polymer surfaces, but as oxidation proceeded, the surface energy could have changed, enabling this to occur. Another possibility is that samples underwent increased swelling when subjected to higher temperatures. This could have resulted in seawater permeating deeper into the polymer interior, and once samples were dried, salt crystals precipitated increasing mass and resulting in lower percentage mass loss. Nonetheless, the overlapping error bars and p-value of 0.473 indicate that the final week six values were not significantly different for plastics exposed to different temperatures.

Figure 4.30 (b) illustrates the effect of plastic-type. For the first two weeks of degradation, PET showed the highest rate and extent of mass loss, followed by CPP, and finally BPP. This finding differs from those of the pre-treatment and UV beaker tests as in Figure 4.3 (a) and Figure 4.16 (b) respectively. Hydrolysis is believed to be responsible for the rapid initial mass loss of PET during these experiments. Ultimately, CPP resulted in the highest mass loss, followed by PET, and finally BPP. For the pre-treatment and UV beaker tests, CPP also resulted in the highest mass loss. From the p-value of 0.017, it is evident that BPP resulted in significantly lower mass loss than the other two plastics.

Moving over to the effect of UV history in Figure 4.30 (c), it was found that material with the highest prior UV history resulted in the highest mass loss, followed by fresh material (0 W/m^2 history), and finally samples with a history of 65 W/m^2. It was expected that plastic with the highest UV history would have resulted in the highest mass loss. This is likely due to previous degradation weakening the material sufficiently to rapidly lose weight during downstream exposures.

In terms of solution medium, Figure 4.30 (d) shows that demineralised water ultimately resulted in higher mass loss than seawater. This was possibly due to demineralised water having a lower density than seawater which improved diffusion into the polymer interior promoting degradation. Additionally, demineralised water also has higher dissolved oxygen concentrations than seawater, as mentioned in Section 2.6.1. This contributes to the radical reactions associated with degradation. However, the determined p-value of 0.185 indicates that the difference in final mass loss between samples immersed in different solution media was not statistically significant.

4.3.2 Crystallinity

Crystallinities were calculated in the same way as for the UV beaker tests. Percentage change is again reported. This change represents the percentage increase from the initial crystallinity at the start of the temperature beaker tests (week 0) to the final crystallinity at the end (week 6). For samples with previous UV histories, the initial (week 0) values are equivalent to the final (week 6) values obtained from the pre-treatment as in Figure 4.4 (a).

4.3.2.1 Effect of temperature and UV history

To evaluate the effect of temperature and UV history on crystallinity changes, samples with different UV histories were immersed in seawater and exposed to two different temperatures. Triplicate samples were analysed after completion of each experimental run. Sample means and standard errors are reported. Figure 4.31 indicates crystallinity results obtained for BPP samples following the temperature beaker tests.

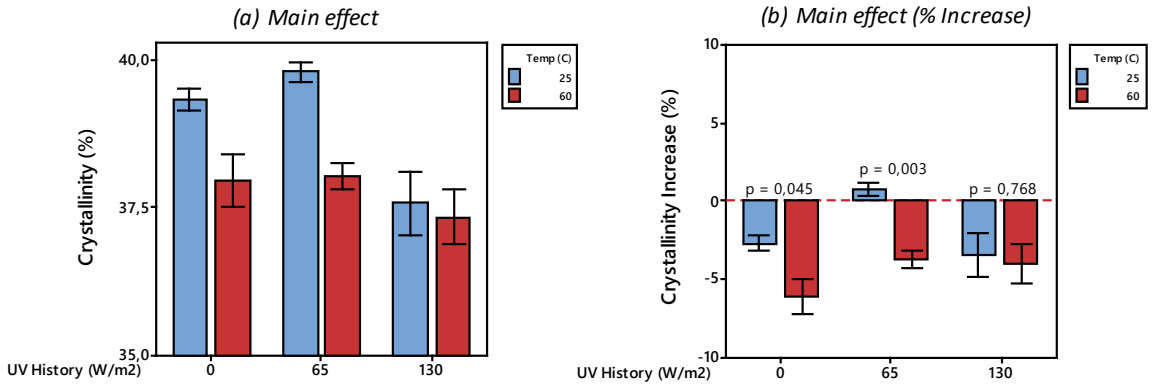

Figure 4.31. (a) Percentage crystallinity (%) over UV history (W/m^2) for BPP samples exposed to different temperatures while immersed in seawater; (b) Percentage crystallinity increase (from week 0) of samples shown in (a) with Figure 4.4 as baseline.

From Figure 4.31 (a) it is evident that for BPP, the higher temperature resulted in lower crystallinities. For the pre-treatment, the degradation of BPP showed reductions in crystallinity. PP has a glass transition temperature somewhere between -20°C and -10°C. Exposing BPP to experimental temperatures such as 25°C and 60°C, both of which were well above its glass transition temperature, further increased its molecular motion, relaxing the polymer chains making them softer and more elastic. This was reflected by the reduced crystallinity. As seen throughout the UV beaker tests, samples with no previous history underwent the most substantial crystallinity change. For the temperature beaker tests the same was seen for BPP samples.

In terms of UV history, Figure 4.31 (b) shows that an increase in UV history resulted in lower decreases in crystallinity. Recalling from the pre-treatment in Figure 4.4 (a) where an increase in UV irradiance resulted in a decrease in crystallinity for BPP, it is almost as if a crystallinity threshold has been reached. Rabello & White (1966) suggested that a large number of chemical irregularities like carbonyl and hydroperoxide groups prevented further increases in the crystallinity of PP and reported that a plateau value was obtained. The crystallinity of untreated BPP material (with no previous UV history) easily decreased with samples becoming more-elastic while those that were already softened did not undergo an equivalent change later on. Figure 4.32 indicates the crystallinity results obtained for CPP samples following the temperature beaker tests. Triplicate samples were analysed with the means and standard errors reported.

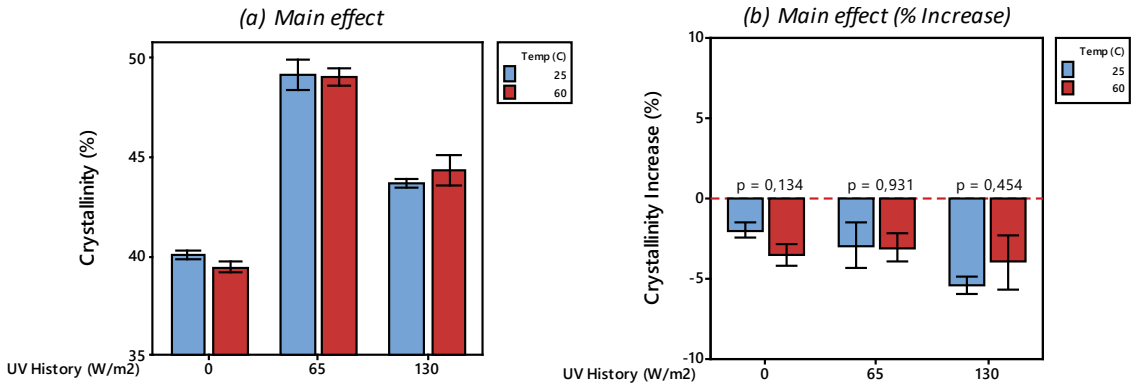

Figure 4.32. (a) Percentage crystallinity (%) over UV history (W/m^2) for CPP samples exposed to different temperatures while immersed in seawater; (b) Percentage crystallinity increase (from week 0) of samples shown in (a) with Figure 4.4 as baseline.

Figure 4.32 indicates the crystallinity results for CPP samples following the temperature beaker tests. Considering (a) it is evident that for CPP, temperature changes did not result in a noticeable trend. For untreated CPP, the 60°C experiment resulted in slightly lower crystallinities than the 25°C experiment. This was an unexpected observation as for all previous UV exposures untreated

CPP showed significant increases in crystallinity. This difference highlights a clear distinction between the effects of UV radiation and temperature on the degradation behaviour of CPP. It is concluded that CPP was more susceptible to degradation by UV radiation than by temperature. For samples with a 65 W/m^2 history, no difference could be attributed to differences in temperature. CPP with a previous history of 130 W/m^2 resulted in a higher crystallinity for the higher investigated temperature. However, from the determined p-values, none of these differences as a result of different temperatures were statistically significant.

When considering the effect of UV history in Figure 4.32 (b), it was found that for samples exposed to 25°C, an increase in history resulted in a decrease in crystallinity. Although more moderate, the same trend was observed for samples exposed to 60°C. The decrease in crystallinity as UV history was increased could most likely be attributed to an increased number of structural defects introduced by previous exposures. These defects inhibited the polymers' ability to undergo further crystallisation. Figure 4.33 below indicates the crystallinity results for PET following the temperature beaker tests. Triplicate samples were analysed with the means and standard errors reported.

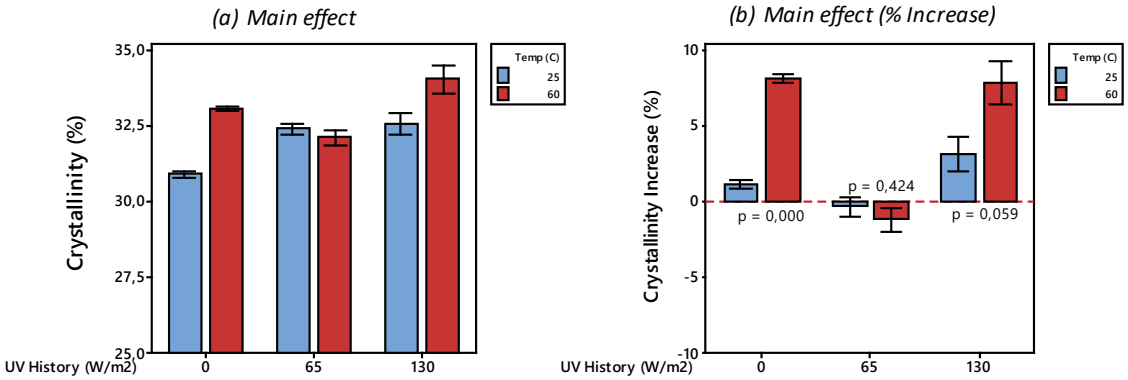

Figure 4.33. (a) Percentage crystallinity (%) over UV history (W/m^2) for PET samples exposed to different temperatures while immersed in seawater; (b) Percentage crystallinity increase (from week 0) of samples shown in (a) with Figure 4.4 as baseline.

For PET in Figure 4.33 (a) it is evident that a temperature increase resulted in a corresponding crystallinity increase. This was particularly the case for untreated PET samples and those with a UV history of 130 W/m^2. Samples with a UV history of 65 W/m^2 showed little difference in crystallinities due to temperature change, with the higher temperature resulting in slightly lower crystallinity. Statistically, this result was not significantly different. Besides this discrepancy, it was expected that the higher temperature would have resulted in increased crystallinities for PET since it was relatively close to its T_g value of 69°C.

Figure 4.33 (b) indicates that the effect of UV history on percentage crystallinity increase. For PET samples exposed to 25°C, increasing the UV history from 0 W/m^2 to 65 W/m^2 resulted in a crystallinity decrease. Increasing the UV history further resulted in a steep crystallinity increase. The same was seen for PET samples exposed to 60°C. Recalling from the pre-treatment in Figure 4.4 (a), the 65 W/m^2 irradiance resulted in higher crystallinity than the 130 W/m^2 irradiance. Again, it almost seems as if there was more 'room available' for crystallinity to increase for untreated samples and those with previous UV exposure of 130 W/m^2.

4.3.2.2 Effect of solution medium

To describe the effect of solution medium, plastic samples with no previous UV histories were immersed in different aqueous solutions and exposed to different temperatures for six weeks. After completion of the experiments, crystallinity values were determined and compared between samples from different solution mediums. Figure 4.34 shows the effect of solution medium on the different plastics following the temperature beaker tests. Samples were analysed in triplicate and the means and standard errors are reported.

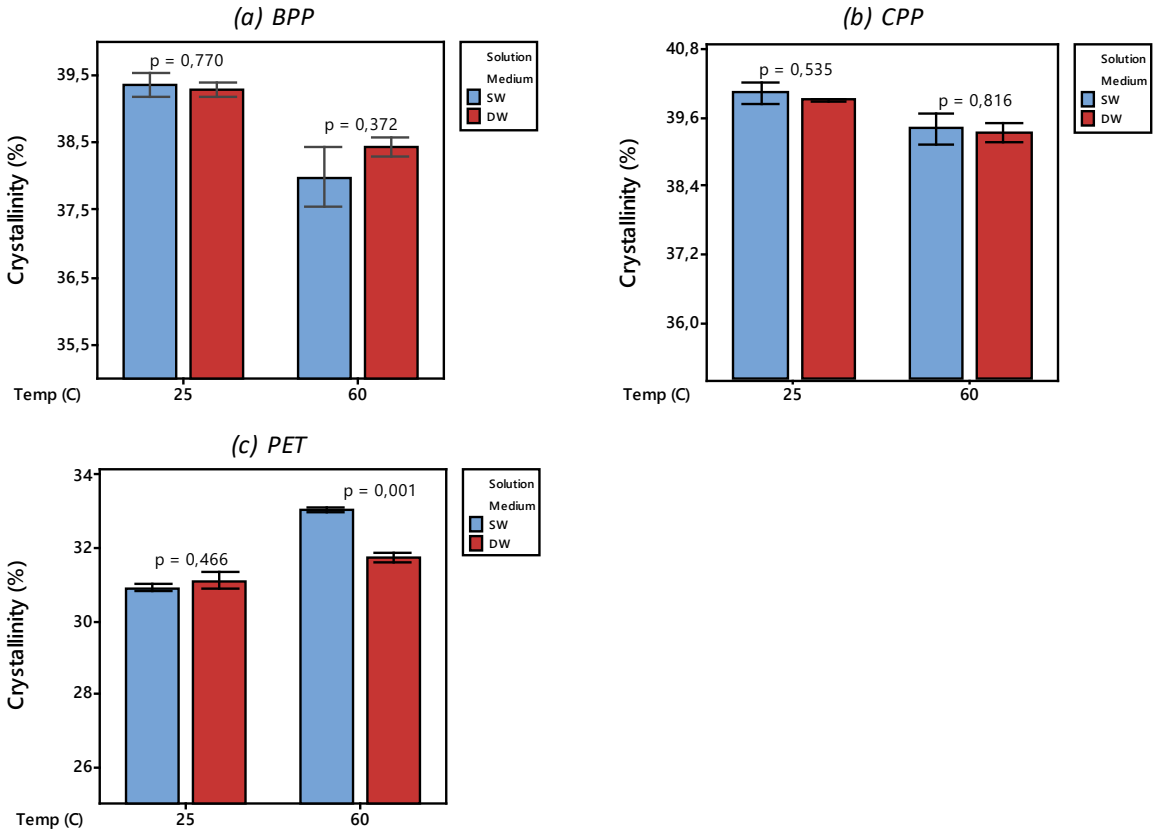

Figure 4.34. Percentage crystallinity (%) over temperature (°C) for different untreated plastic samples (0 W/m^2 UV history) immersed in different aqueous solutions.

For BPP in Figure 4.34 (a) no significant difference was evident for crystallinities determined from each solution medium at the investigated temperatures. This is shown by the overlapping error bars and determined p-values all being higher than 0.05. Therefore, besides increasing temperature reducing the crystallinity of fresh BPP samples, no additional conclusions could be made.

Figure 4.34 (b) shows the crystallinities for untreated CPP samples from different solutions exposed to different temperatures. It appears that at both temperatures, samples from demineralised water resulted in slightly lower crystallinities than those from seawater. With that said, the error bars between the different solutions overlapped at both temperatures suggesting the effect of solution medium on crystallinity changes of fresh CPP samples also to be insignificant. This insignificance was again proven by the determined p-values.

Finally, when considering PET in Figure 4.34 (c), it was found that at 25°C, no significant difference was observed in crystallinities for samples from different solutions. However, at 60°C there was a significant difference indicating seawater resulted in increased crystallinity. Reflecting on the UV beaker tests, this finding corresponds to that of the higher irradiance (130 W/m^2) where seawater also resulted in the highest crystallinity as in Figure 4.20 (c). PET samples exposed to seawater during the temperature beaker tests also turned opaque, which was previously attributed to the formation of larger crystals as a result of crystallisation.

4.3.3 Microhardness

For the temperature beaker tests, microhardness was determined in a similar way as for the UV beaker tests. CPP samples were omitted as complete datasets could again not be generated. Additionally, BPP samples with the highest UV history (130 W/m^2) also became brittle and failed after six weeks of exposure to 25°C in seawater, as seen in Figure 4.35.

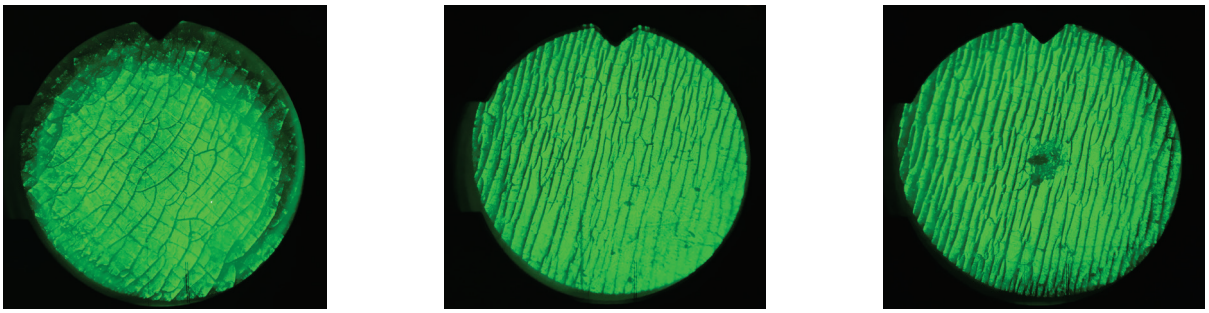

Figure 4.35. Photographs indicating severe crazing (embrittled surfaces) visible via microscope for BPP samples.

4.3.3.1 Effect of temperature (and UV history)

Plastic samples with different UV histories were immersed in seawater and exposed to different temperatures for six weeks. Microhardness values were determined after completion of the experiments. Triplicate samples were analysed on both sides. The mean values and standard errors are reported. Figure 4.36 indicates the final week six microhardness values of BPP as well as the percentage increase relative to the beginning of the tests.

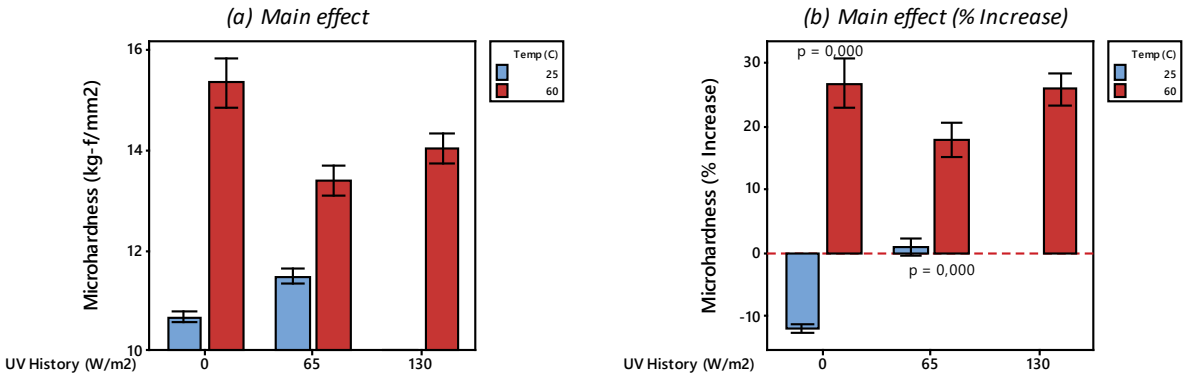

Figure 4.36. Microhardness (kg-f/mm^2) over UV history (W/m^2) for BPP samples exposed to different temperatures (°C) while immersed in seawater; (b) Percentage microhardness increase (from week 0) of samples shown in (a) with Figure 4.7 as baseline.

In view of Figure 4.36 (a) it was found that an increase in temperature from 25°C to 60°C resulted in significant increases in microhardness for both untreated material and samples with a previous UV history of 65 W/m^2. During the dry pre-treatment experiments, BPP samples showed a decrease in microhardness as UV irradiance was increased. For the UV beaker tests as in Figure 4.21 (b), both irradiances resulted in increased microhardness for BPP. The temperature beaker tests showed an increase in microhardness for the 60°C experiment. This is contrary to the results described previously for crystallinity changes during the temperature beaker tests in Figure 4.31. Possible reasons for these deviations remain unclear at this stage.

The effect of UV history was inconsistent. For the 60°C temperature, increasing the UV history from 0 W/m^2 to 65 W/m^2 resulted in a reduction in microhardness increase. Increasing the UV history further to 130 W/m^2 resulted in a sharp increase in microhardness. For the 25°C run, material with no prior UV history reflected a decrease in crystallinity, but as UV history was increased microhardness increased as well. Figure 4.37 indicates the microhardness results for PET samples.

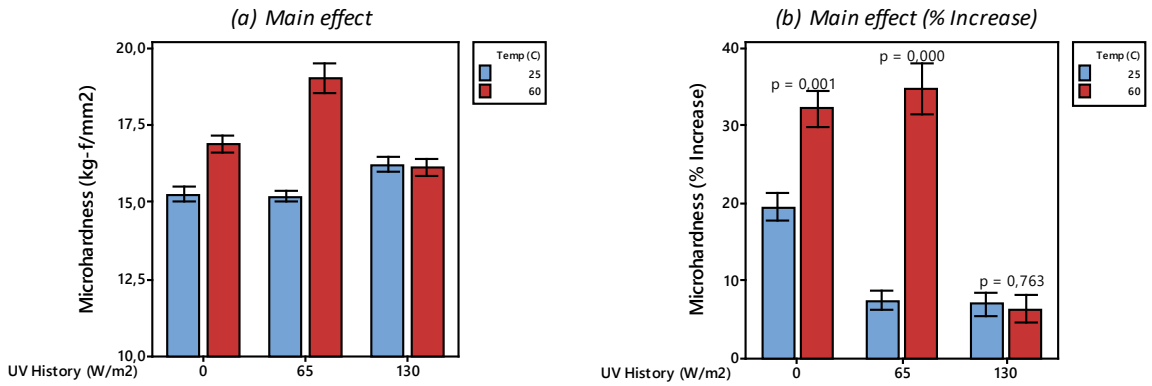

Figure 4.37. Microhardness (kg-f/mm^2) results over UV history (W/m^2) for PET samples exposed to different temperatures (°C) while immersed in seawater; (b) Percentage microhardness increase (from week 0) of samples shown in (a) with Figure 4.7 as baseline.

From Figure 4.37 (a) it is shown that for untreated PET samples, as well as those with a prior UV history of 65 W/m^2, an increase in temperatures resulted in an increase in microhardness. This corresponds well to the findings for crystallinity as in Figure 4.33. PET samples with the highest previous UV history (130 W/m^2) showed an insignificant change in crystallinity as a result of different temperatures. Recalling from the pre-treatment in Figure 4.7 (a), the highest UV irradiance resulted in the highest microhardness for PET. Again, it is implied that the sensitivity to microhardness change decreased with increased UV history. This is clearly observed for the 25°C experiment in Figure 4.37 (b) where an increase in UV history resulted in lower microhardness percentage increases.

At the higher temperature of 60°C, increasing the UV history from 0 W/m^2 to 65 W/m^2, resulted in a slight increase in microhardness, this increase was probably insignificant as error bars overlapped. By further increasing the UV history from 65 W/m^2 to 130 W/m^2, a major decrease in microhardness increase was observed. This finding also points out that most of the crystallisation (increasing microhardness) has likely already taken place during earlier experiments.

4.3.3.2 Effect of solution medium

To investigate the effect of solution medium, untreated samples with no previous UV history were immersed in different aqueous solutions and exposed to two different temperatures. Microhardness values were determined after completion of each experimental run. Triplicate samples were analysed on both sides, with results showing the means and standard errors. Figure 4.38 indicates the effect of solution medium on the microhardness of BPP and PET.

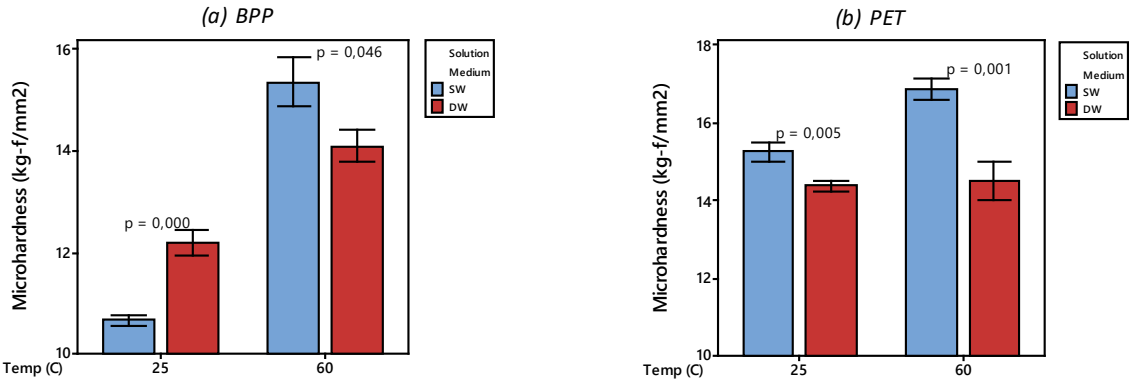

Figure 4.38. Microhardness (kg-f/mm^2) over temperature (°C) for untreated BPP and PET plastic samples (0 W/m^2 UV history) immersed in different aqueous solutions.

Starting with BPP in Figure 4.38 (a) it was found that solution medium influenced microhardness differently at both temperatures. At 25°C, BPP immersed in demineralised water showed significantly higher microhardness values than BPP immersed in seawater. This trend changed at 60°C, where in this case, seawater resulted in the highest microhardness. Currently, reasons for this reversing trend is unclear, but results suggest that there might be some higher-order interaction between temperature and solution medium on the microhardness of BPP samples.

Moving over to PET in Figure 4.38 (b), a discernible trend is apparent. At both temperatures, 25°C and 60°C, samples from seawater resulted in significantly higher microhardness values than those from demineralised water. Although previous results for the UV beaker tests in Section 4.2.3.2 showed different changes on microhardness due to solution medium, when exposed to constant temperatures, the type of solution medium significantly affected the microhardness of PET. This finding corresponds to results for the effect of solution medium on crystallinity at 60°C as shown in Figure 4.34 (c).

4.3.4 FTIR Indices

Indices were determined precisely as during the UV beaker tests. Both band areas and peak heights were used in Equations [3] and [4] to determine the final index values. Outliers were statistically identified and removed. Samples means and standard errors are reported throughout. Since they were directly comparable, results for BPP and CPP will be discussed together, with results for PET presented in a separate section.

4.3.4.1 Effect of temperature (and UV history) for PPs

To describe the effect of temperature and UV history on chemical changes of the PPs during the temperature beaker tests, samples with different UV histories were immersed in seawater and exposed to two different temperatures for six weeks. Samples were drawn and analysed on a fortnightly basis. Carbonyl- and hydroxyl-indices were determined as described in Section 3.5.3. Results obtained for BPP and CPP are shown below in Figure 4.39.

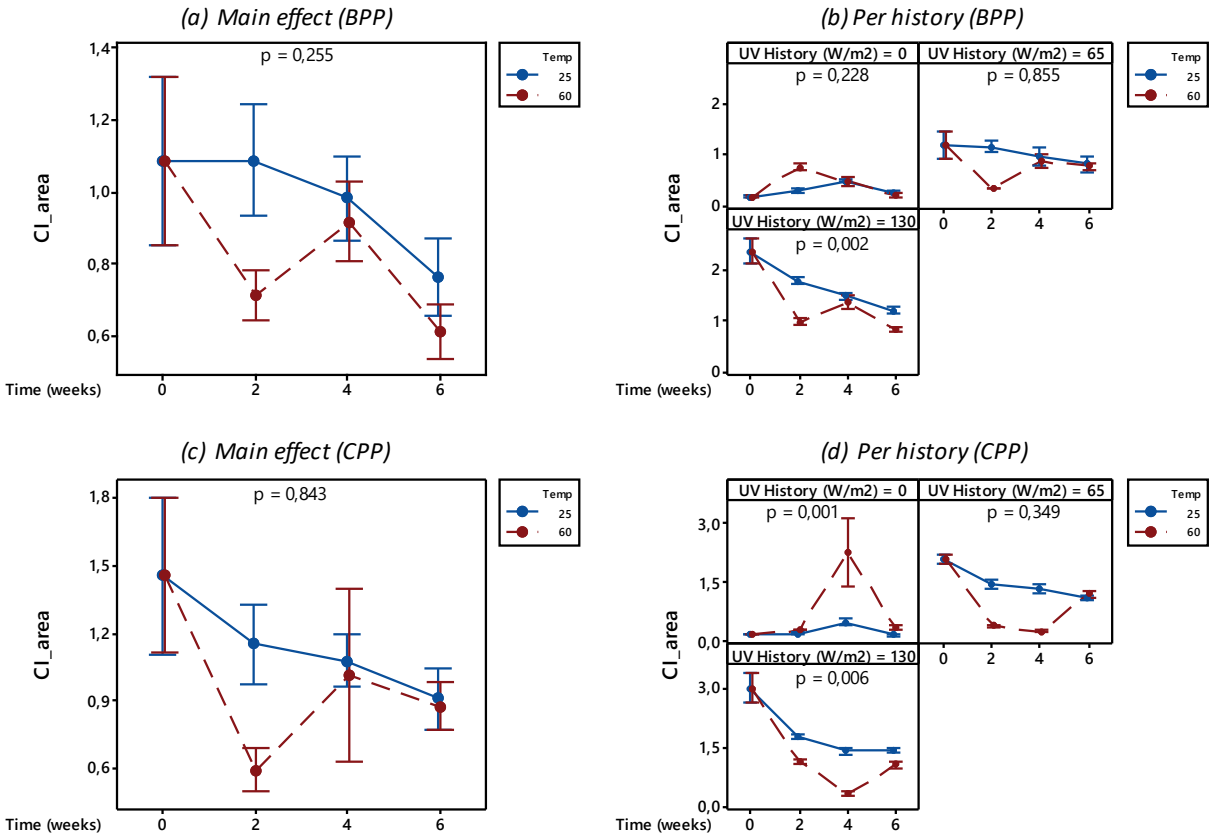

Figure 4.39. (a) Main effect of temperature on CI over time (weeks) for BPP; (b) CI over time (weeks) for BPP with different UV histories; (c) Main effect of temperature on CI over time (weeks) for CPP; (d) CI over time (weeks) for CPP with different UV histories.

The carbonyl indices for BPP during the temperature beaker tests are shown in Figure 4.39 (a) and (b). From (a) the overall trend indicates a decline in carbonyl indices for both temperatures as exposure time progressed. The 60°C experiment reflected a steeper decline and lower ultimate extent than the 25°C experiment. Recalling from the pre-treatment of BPP in Figure 4.12 (a), carbonyl indices increased significantly. The UV beaker tests in Figure 4.24 (a) showed that the higher irradiance resulted in increased carbonyl content, while a decrease was observed for the lower irradiance. Results from Figure 4.39 (b) indicate that carbonyl indices of fresh untreated BPP samples (0 W/m^2 UV history) increased slightly, but as the degree of UV history increased,

the carbonyl indices decreased accordingly. This was particularly the case for samples with the highest previous UV history of 130 W/m^2. These results suggest that carbonyl-containing degradation products are susceptible to oxidation and able to dissolve into the surrounding solution once exposed to water, especially at higher temperatures. For BPP samples with UV histories of 0 W/m^2 and 65 W/m^2, no significant difference between indices could be attributed to differences in temperature.

Moving over to CPP in Figure 4.39 (c) and (d) the same trend was apparent. As degradation time progressed, the carbonyl indices decreased. This was especially so for CPP material with previous UV histories of 65 W/m^2 and 130 W/m^2. For both of these samples, the higher temperature resulted in indices declining faster, specifically within the first four weeks of degradation. This can be attributed to increased dissolution kinetics associated with higher temperatures. The same argument as previously described for BPP holds, degradation products in the surface layer of the material were believed to dissolve into the surrounding medium, or small plastic fragments were breaking away from larger segments, possibly forming micro- and nano-scale plastics. The latter argument is confirmed by the mass loss for CPP observed in Figure 4.30 (b). The erosion (or dispersion) of the degraded surface layer left a fresher (undegraded) layer exposed to the solution which in turn reflected lower intensities of oxidation products when analysed with FTIR spectroscopy. For this reason, tracking changes in the carbonyl index is recommended only to be suitable for the early stages of degradation, as mentioned in Fernando et al. (2007).

Another possible reason for the reduction in carbonyl groups might be due to polymer chains rearranging. Since initial carbonyl products were formed on the polymer surface, subsequent exposure might have resulted in changed surface energy that allowed chain rearrangements and concealment of carbonyl products below the observed surface. This process would have complicated the identification of previously formed carbonyl groups, making them increasingly difficult to detect.

4.3.4.2 Effect of solution medium for PPs

To evaluate the effect of solution medium on carbonyl group changes during temperature exposure, fresh plastic material with no previous UV history were immersed in different aqueous solutions. Beakers containing the solutions and material were exposed to different temperatures. Indices were determined for material from both solutions and are compared in Figure 4.40. The means and standard errors of the determined indices are reported.

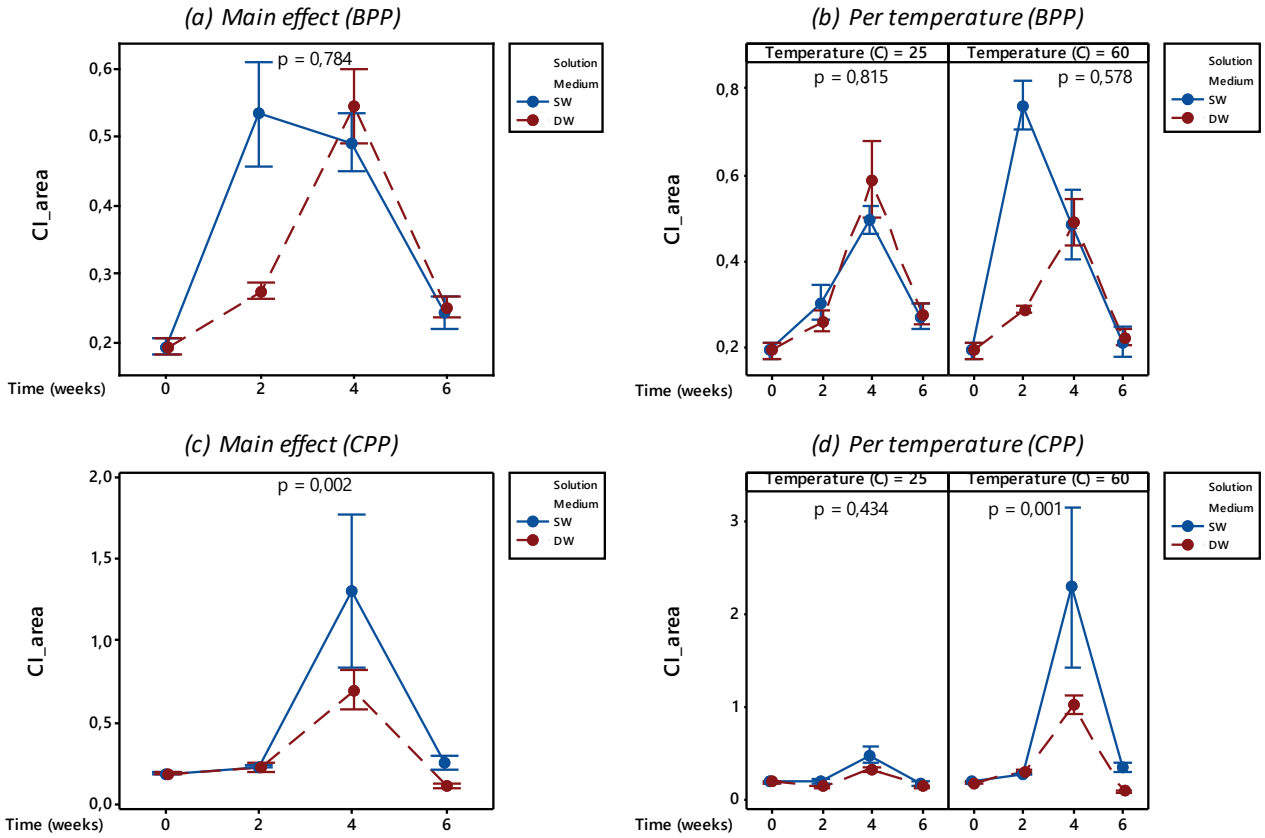

Figure 4.40. (a) Main effect of solution medium on CI over time (weeks) for BPP; (b) Effect of solution medium on CI over time (weeks) for BPP per temperature; (c) Main effect of solution medium on CI over time (weeks) for CPP; (d) Effect of solution medium on CI over time (weeks) for CPP per temperature.

When considering Figure 4.40 (a) and (b) it is evident that for BPP, solution medium did not result in significant differences in the final carbonyl indices. This was especially the case for the 25°C experiment. Although demineralised water resulted in slightly higher indices, the overlapping error bars and p-values indicated that these differences were not statistically significant. Ultimately, untreated material from both solutions resulted in slight increases in carbonyl index. The magnitudes of these increases were significantly lower than for the pre-treatment in Figure 4.8 (b) and UV beaker tests in Figure 4.26. This indicates the undeniable effect of UV radiation and its contribution to oxidative degradation. The oxidation due to temperatures (even at 60°C) was much lower and increases in carbonyl index were almost negligibly small. From this finding it can be concluded that, at the considered conditions, the effect of UV radiation was more significant than that of temperature.

Results for CPP in Figure 4.40 (c) and (d) showed a slight increase in carbonyl index for samples immersed in seawater and a slight decrease for samples immersed in demineralised water. These differences were very subtle. Again, when considering Figure 4.40 (d), it is evident that no

significant change was present for the 25°C experiment between week 0 and week 6. Moreover, the final week six indices also did not indicate a significant difference between the two solutions. Although very moderate, at 60°C, a statistically significant difference was observed with seawater resulting in a higher final index value for CPP. However, overall, the low temperatures and relatively short exposure time did not result in any major chemical changes of untreated PP samples during these experiments.

4.3.4.3 Effect of temperature (and UV history) for PET

Chemical changes were also investigated for PET. However, different frequency ranges and reference peaks were used and therefore results are presented separately. During the spectral analyses, the formation of a broad peak was observed in the hydroxyl region and therefore hydroxyl indices were also included as part of these results. Figure 4.41 provides a summary of the results obtained for PET during the temperature beaker tests.

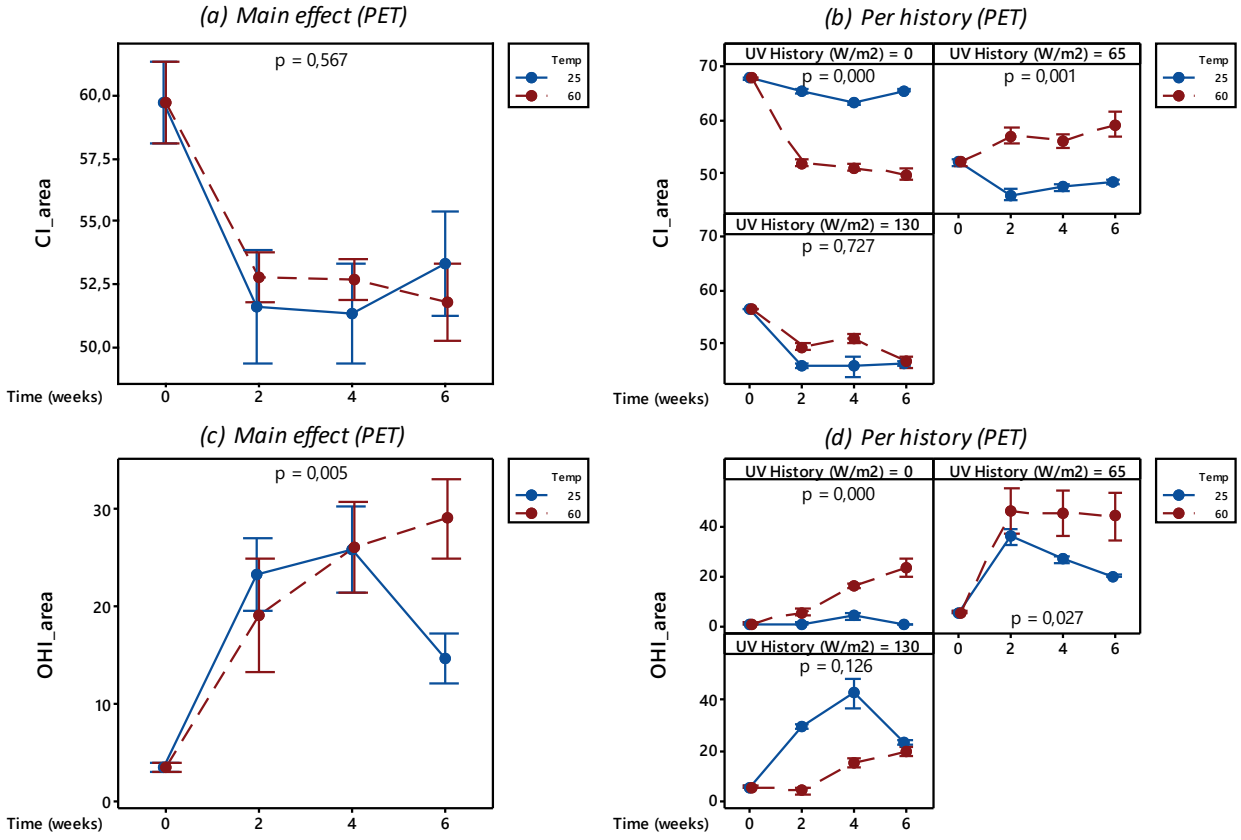

Figure 4.41. (a) Main effect of temperature on CI over time (weeks) for PET; (b) CI over time (weeks) for PET with different UV histories; (c) Main effect of temperature on OHI over time (weeks) for PET; (d) OHI over time (weeks) for PET with different UV histories.

Figure 4.41 (a) and (b) show changes in carbonyl indices for PET exposed to different temperatures. From Figure 4.41 (a) the first observation is the general decreasing tendency in carbonyl indices at both temperatures. For the first four weeks of exposure, samples from the 25°C experiment resulted in lower indices than those from the 60°C experiment. This changed in the last two weeks with the higher temperature ultimately resulting in a lower index than the lower temperature. The determined p-value indicates that the difference in these final values was not statistically significant. When considering Figure 4.41 (b), it is evident that fresh PET (0 W/m^2 history) showed a much steeper decrease for the 60°C experiment than the 25°C experiment. This trend changed for samples with previous UV histories.

In terms of hydroxyl products, Figure 4.41 (c) and (d) show an increase in hydroxyl indices for both temperatures, with the higher temperature (60°C) ultimately resulting in the highest values. This was particularly the case for untreated PET and samples with a UV history of 65 W/m^2. This finding confirms that hydrolysis occurred faster at the higher investigated temperature. As described in Section 2.5.3, hydrolysis can result in carboxylic acid and hydroxyl-ester end groups. These products might have contributed to the increased hydroxyl index as seen from the FTIR results.

4.3.4.4 Effect of solution medium for PET

To evaluate the effect of solution medium, PET samples with no previous UV history were immersed in glass beakers containing different aqueous solutions. Beakers were exposed to different temperatures for six weeks. Indices were determined for material from both solutions and results are summarised in Figure 4.42 below. The means and standard errors are reported.

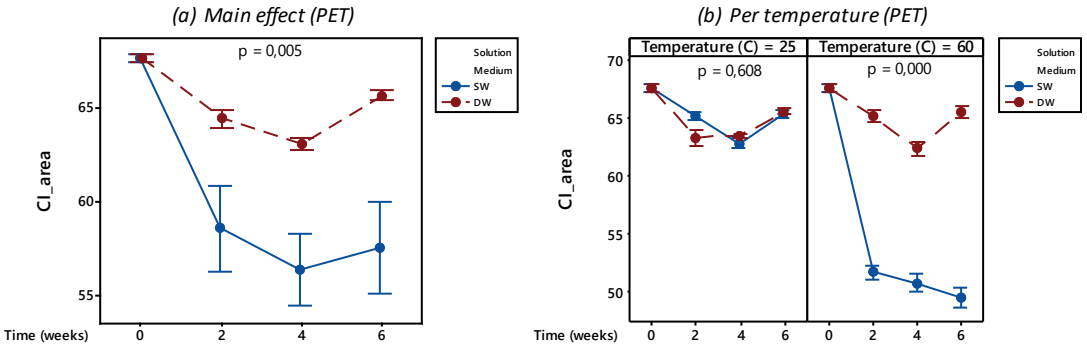

Figure 4.42. (a) Main effect of solution medium on CI over time (weeks) for PET; (b) Effect of solution medium on CI over time (weeks) for PET at different temperatures.

In Figure 4.42 (a), the effect of solution medium on carbonyl group changes for untreated PET is shown. There is a clear indication that seawater resulted in faster and higher decreases in carbonyl index than demineralised water. This trend corresponds well to Figure 4.28 for the UV beaker tests. From Figure 4.42 (b), it is evident that at the lower temperature of 25°C, no significant difference in carbonyl index could be attributed to a difference in solution medium. This was, however, not the case at 60°C where samples immersed in seawater resulted in significantly lower carbonyl index values than those immersed in demineralised water. Again, this might indicate that carbonyl degradation products were better preserved in demineralised water than in seawater.

Furthermore, the significant reduction in carbonyl index at 60°C, might indicate that degradation of PET was more pronounced in seawater than in demineralised water. It is possible that the crystallisation of PET, as described and shown earlier, might have resulted in crystallites acting as barriers that reduced the permeability of oxygen and water to the polymer interior as described in Section 2.5.3. Ultimately, these results showed that at the low temperature (25°C), the type of solution medium did not result in a significant carbonyl difference, whereas at the higher temperature, seawater resulted in a significantly lower carbonyl index value.

5. Conclusions and recommendations

The overarching aim of this study was to evaluate and compare the physicochemical degradation behaviour of PP and PET packaging exposed to UV radiation and different aqueous environments. Conclusions from the sequential degradation stages will be discussed in the following sections.

5.1 UV pre-treatment

The pre-treatment stage involved exposing samples to different UV irradiances in air.

The degree of UV irradiation proportionally instigated changes in plastic properties leading to overall higher mass loss, carbonyl indices, crystallinities, and microhardness. It was found that shape did not significantly influence degradation. Between the three investigated plastic types, CPP showed the most rapid deterioration, and factors including chemical compositions, specific wavelength sensitivities, and presence or absence of a stabilising additive (carbon black) contributed to these results.

In terms of physical observations, crazing and severe embrittlement were evident for CPP samples that also showed a colour shift from translucent to chalk-white. The colour of BPP samples changed from glossy black to matte black and PET indicated marginal yellowing.

Following UV exposure, crystallinity values increased for CPP and PET but decreased for BPP. The most significant finding was the 24% increase in crystallinity of CPP following the 65 W/m^2 experiment. Lower increases were observed for the higher irradiance of 130 W/m^2 and were believed to result from crosslinking prevailing at this irradiance. This was confirmed by determining shifts in the glass transition temperature of PET. Microhardness and crystallinity results corresponded during the pre-treatment experiments.

Spectral results showed significant increases in carbonyl content for both PPs with the higher irradiance producing higher rates and extents. By considering band areas and peak heights, the formation of carboxylic acids evolving as an energetic shoulder from the existing carbonyl peak was found for PET.

5.2 UV beaker tests

The UV beaker tests evaluated the effect of UV radiation on samples with different degradation histories immersed in either seawater or demineralised water. The same analyses as for the pre-treatment were conducted and the main conclusions are outlined below.

Results from the UV beaker tests indicated that degradation occurred slower relative to the dry pre-treatment, but faster than during the temperature beaker tests. The proportional effect of UV irradiance continued throughout these experiments and led to the most considerable property changes in fresh samples with no prior UV exposure.

Samples with previous histories reflected higher mass loss, but also reductions in crystallinity, microhardness, and carbonyl content. It was postulated that previous exposure introduced structural defects, crosslinking, and chemical irregularities that inhibited chain realignment into a compact crystalline structure.

Reductions in carbonyl index were ascribed to products degrading further resulting in peaks fading away. The liberation of small fragments containing carbonyl products might have also resulted in unaltered surfaces being analysed by FTIR. This was corroborated by findings for mass loss.

PET showed higher mass loss than during pre-treatment, as well as increased hydroxyl content. Hydrolytic degradation was believed to have contributed to this observation. PET samples became opaque following exposure to seawater indicating crystallisation to have occurred. The severity of degradation was again apparent for particularly CPP, which confirmed its high susceptibility to UV induced degradation.

At these experimental conditions, no conclusive evidence of a consistent significant effect of solution medium was found. There were some instances that suggested the possibility of higher-order interactions between solution medium and UV irradiance, as seen for PET.

5.3 Temperature beaker tests

To describe the effect of temperature, samples with different UV histories were immersed in seawater or demineralised water while being maintained at constant temperatures. The following conclusions were made from these experiments.

Results from the temperature beaker tests reflected the lowest and least significant property changes. From this, it was concluded that at the conditions considered, the effect of UV radiation was more significant than that of temperature. No significant differences in mass loss or chemical functionalities could be attributed to a temperature increase.

In terms of plastic-type, CPP again resulted in the highest mass loss but did not indicate the same signature crystallinity spike as observed for untreated samples in the pre-treatment and UV beaker

tests. In fact, increasing the temperature decreased the crystallinities of both PPs but led to an increase for PET. The rate of hydrolysis was accelerated at higher temperatures as reflected by mass loss and hydroxyl index for PET.

Some contradicting observations were present between microhardness and crystallinity where for BPP, the crystallinity decreased but microhardness increased. This was not the case for PET that indicated corresponding increases in crystallinity and microhardness as temperature was raised from 25°C to 60°C. The glass transition temperature of PET is approximately 69°C and therefore, by increasing the temperature, chain mobility increased promoting realignment into a crystalline structure.

Reductions in carbonyl content as UV histories were increased were attributed to (i) hydrophilic products dissolving into the solution medium with faster kinetics at higher temperatures, (ii) fragments breaking away from larger segments revealing an unoxidised layer being analysed or (iii) changes in surface energy allowing chain rearrangement concealing carbonyl products below the observed surface.

Structural defects and increased chemical irregularities stemming from the pre-treatment were ascribed to have resulted in reduced crystallinities as UV histories were increased. From this, the potential for a crystallinity threshold was discussed where values for untreated samples changed fairly easily, whilst samples with previous exposure did not undergo an equivalent change.

5.4 Recommendations

This section contains recommendations for future research that surfaced from this study.

CPP samples were unequivocally the most prone to degrade and form microplastic fragments. Examining the solution mediums in which these samples were immersed would be beneficial and allow MPs to be quantified and toxicity levels brought about to be determined. Liquid chromatography-mass spectroscopy (LC-MS) would be a suitable analytical technique.

The experimental durations, specifically for BPP and PET, should be increased as these plastic types did not result in the same extent of degradation as observed for CPP.

Reduced irradiation levels that would more accurately represent environmental conditions should also be considered. Different factors influencing degradation should be explored, such as relative humidity, microorganisms, and additive concentrations.

Conducting in-field experiments alongside accelerated experiments would be useful and enable direct comparison between the property changes associated with each exposure. By doing this, models produced from accelerated experiments could be extrapolated to environmentally relevant conditions.

ATR-FTIR was proven to be an insightful technique, especially for the early stages of degradation. However, spectral interpretations become complicated after prolonged exposures as products themselves degrade and peaks disappear. It is recommended to only employ this technique to earlier stages of degradation.

The developed macro program significantly reduced the tedious nature of interpreting spectral results and could be employed to evaluate other peaks of interest. Using generated spectra as fingerprints and expand on existing libraries could be advantageous to identify degradation and compare previous degradation histories of washed-up plastic pieces.

Analytical techniques used in this investigation could be supplemented by additional value-adding techniques such as nuclear magnetic resonance (NMR), scanning electron microscopy (SEM), and gel permeation chromatography (GPC). To confirm whether carbonyl products were in fact concealed below the polymer surface, it is recommended to microtome samples and develop degradation profiles as functions of sample depth. De Goede (2006) performed such a procedure.

Although it was a fair decision to investigate end-use plastic packaging, there is a need to more accurately characterise the polymers' initial properties and additives which might have considerably influenced its degradation. For future research, it is recommended to work with well-characterised resin and to customise its additive contents according to the needs of the study. Investigating the role of different additives and their concentrations would be useful.

This work could assist manufacturing companies to increase the stability of their products. For instance, incorporating UV stabilisers into CPP would have resulted in less degradation. In addition to that, data from this study should be used to improve parameter definition of existing degradation models.

6. References

Allen, N.S., Edge, M. & Mohammadian, M., 1991. Hydrolytic degradation of Poly(ethylene terephthalate): Importance of chain scission versus crystallinity. *European Polymer Journal*, 27(12):1373–1378.

Allen, N.S., Edge, M., Mohammadian, M. & Jones, K., 1994. Physicochemical aspects of the environmental degradation of poly(ethylene terephthalate). *Polymer Degradation and Stability*, 43(2):229–237.

Andrady, A.L., 2011. Microplastics in the marine environment. *Marine Pollution Bulletin*, 62(8):1596–1605.

Andrady, A.L., 2015a. Persistence of Plastic Litter in the Oceans. In: M. Bergmann, L. Gutow, & M. Klages (eds.). *Marine Anthropogenic Litter*. Switzerland: Springer International Publishing, :57–72.

Andrady, A.L., 2015b. *Plastics and Environmental Sustainability*. 1st Ed. Hoboken, New Jersey: John Wiley & Sons, Inc.

Andrady, A.L., 2017. The plastic in microplastic: A review. *Marine Pollution Bulletin*, 119:12–22.

Andrady, A.L., 2006. Wavelength Sensitivity in Polymer Photodegradation. In: *Advances in Polymer Science*. Durham, USA: Springer International Publishing, :47–94.

Andrady, A.L., Hamid, S.H., Hu, X. & Torikai, A., 1998. Effects of increased solar ultraviolet radiation on materials. *Journal of Photochemistry and Photobiology B: Biology*, 46(1998):96–103.

Auta, H.S., Emenike, C.U. & Fauziah, S.H., 2017. Distribution and importance of microplastics in the marine environment: A review of the sources, fate, effects, and potential solutions. *Environment International*, 102(2017):165–176.

Baur, E., Ruhrberg, K. & Woishnis, W., 2016. *Chemical Resistance of Commodity Thermoplastics*. 1st Ed. Oxford, United Kingdom: Elsevier.

Bocchini, S., Morlat-Therias, S., Gardette, J.L. & Camino, G., 2008. Influence of nanodispersed hydrotalcite on polypropylene photooxidation. *European Polymer Journal*, 44(11):3473–3481.

Bocchini, S., Morlat-Thérias, S., Gardette, J.L. & Camino, G., 2007. Influence of nanodispersed boehmite on polypropylene photooxidation. *Polymer Degradation and Stability*, 92(10):1847–1856.

de Bomfim, A.S.C., Maciel, M.M.Á.D., Voorwald, H.J.C., Benini, K.C.C. de C., de Oliveira, D.M. & Cioffi, M.O.H., 2019. Effect of different degradation types on properties of plastic

waste obtained from espresso coffee capsules. *Waste Management*, 83(2019):123–130.

Booth, A.M., Kubowicz, S., Beegle-Krause, C., Skancke, J., Nordam, T., Landsem, E., Thorne-Holst, M. & Jahren, S., 2017. *Microplastic in global and Norwegian marine environments: Distributions, degradation mechanisms and transport*. Trondheim, Norway.

Brandon, J., Goldstein, M. & Ohman, M.D., 2016. Long-term aging and degradation of microplastic particles: Comparing in situ oceanic and experimental weathering patterns. *Marine Pollution Bulletin*, 110(1):299–308.

Brown, E., Colling, A., Park, D., Phillips, J., Rothery, D. & Wright, J., 1989. *Seawater: Its composition, properties and behaviour*. 2nd Ed. G. Bearman (ed.). Oxford, United Kingdom: Elsevier.

Callister, W.D. & Rethwisch, D.G., 2015. *Materials Science and Engineering*. 9th Ed. Hoboken, New Jersey: John Wiley & Sons, Inc.

Canopoli, L., Coulon, F. & Wagland, S.T., 2020. Degradation of excavated polyethylene and polypropylene waste from landfill. *Science of the Total Environment*, 698(2020).

Carpenter, E.J. & Smith, K.L., 1972. Plastics on the Sargasso Sea Surface. *Science, New Series*, 175(4027):1240–1241.

Celina, M., Gillen, K.T. & Assink, R.A., 2005. Accelerated aging and lifetime prediction: Review of non-Arrhenius behaviour due to two competing processes. *Polymer Degradation and Stability*, 90(3):395–404.

Chamas, A., Moon, H., Zheng, J., Qiu, Y., Tabassum, T., Jang, J.H., Abu-Omar, M., Scott, S.L. & Suh, S., 2020. Degradation Rates of Plastics in the Environment. *ACS Sustainable Chemistry and Engineering*, 8(9):3494–3511.

Crawford, C.B. & Quinn, B., 2016. *Microplastic Pollutants*. 1st Ed. London: Elsevier Inc.

Daglen, B.C. & Tyler, D.R., 2010. Photodegradable plastics: end-of-life design principles. *Green Chemistry Letters and Reviews*, 3(2):69–82.

Davis, P., Tiganis, B.E. & Burn, L.S., 2004. The effect of photo-oxidative degradation on fracture in ABS pipe resins. *Polymer Degradation and Stability*, 84(2):233–242.

Department of Renewable Energy, 2020. *Renewable energy - solar power*. [Online]. 2020. Available from: http://www.energy.gov.za/files/esources/renewables/r_solar.html. [Accessed: 21 May 2020].

Duis, K. & Coors, A., 2016. Microplastics in the aquatic and terrestrial environment: sources (with a specific focus on personal care products), fate and effects. *Environmental Sciences Europe*, 28(2):1–25.

Edge, M., Hayes, M., Mohammadian, M., Allen, N.S., Jewitt, T.S., Brems, K. & Jones, K., 1991. Aspects of poly(ethylene terephthalate) degradation for archival life and environmental

degradation. *Polymer Degradation and Stability*, 32(2):131–153.

Encyclopedia Britannica, 2017. *Polypropylene*. [Online]. 2017. Available from: https://www.britannica.com/science/polypropylene. [Accessed: 4 June 2020].

Fagerburg, D.R. & Clauberg, H., 2003. Photodegradation of Poly(Ethylene Terephthalate) and Poly (Ethylene/1,4-Cyclohexylenedimethylene Terephthalate). In: J. Scheirs & T. E. Long (eds.). *Modern Polyesters: Chemistry and Technology of Polyesters and Copolyesters*. West Sussex, England: John Wiley & Sons, Inc., :609–638.

Fernando, S.S., Christensen, P.A., Egerton, T.A. & White, J.R., 2007. Carbon dioxide evolution and carbonyl group development during photo-degradation of polyethylene and polypropylene. *Polymer Degradation and Stability*, 92(2007):2163–2172.

Flores, A., Pieruccini, M., Stribeck, N., Funari, S.S., Bosch, E. & Baltá-Calleja, F.J., 2005. Structure formation in poly(ethylene terephthalate) upon annealing as revealed by microindentation hardness and X-ray scattering. *Polymer*, 46(22):9404–9410.

Francois-Heude, A., Richaud, E., Desnoux, E. & Colin, X., 2015. A general kinetic model for the photothermal oxidation of polypropylene. *Journal of Photochemistry and Photobiology A: Chemistry*, 296:48–65.

Fujimoto, E. & Fujimaki, T., 1995. Analysis of Photodegradation Mechanism of Aliphatic and Aromatic Polyesters Using FTIR-ATR, GPC, and DMA. *Kobunshi Ronbunshu*, 52(6):378–387.

Gardette, J.L., Colin, A., Trivis, S., German, S. & Therias, S., 2014. Impact of photooxidative degradation on the oxygen permeability of poly(ethyleneterephthalate). *Polymer Degradation and Stability*, 103(1):35–41.

GESAMP, 2015. *Sources, fate and effects of microplastic in the marine environment: Part 2 of a Global Assessment*. London.

Gewert, B., 2018. *Chemical Pollutants Released To the Marine Environment By Degradation of Plastic Debris*. PhD Diss. Stockholm University, Sweden.

Gewert, B., Plassmann, M.M. & Macleod, M., 2015. Pathways for degradation of plastic polymers floating in the marine environment. *Environmental Sciences: Processes and Impacts*, 17(9):1513–1521.

de Goede, S., 2006. *Novel analytical approaches for studying degradation in polypropylene and propylene-1-1pentene copolymers*. PhD Diss. Stellenbosch University, South Africa.

Gok, A., 2016. *Degradation pathway models of Poly(ethylene-terephthalate) under accelerated weathering exposures*. PhD Diss. Case Western Reserve University, Cleveland, USA.

Ter Halle, A., Ladirat, L., Gendre, X., Goudouneche, D., Pusineri, C., Routaboul, C., Tenailleau, C., Duployer, B. & Perez, E., 2016. Understanding the Fragmentation Pattern of Marine Plastic Debris. *Environmental Science and Technology*, 50(11):5668–5675.

Ter Halle, A., Ladirat, L., Martignac, M., Mingotaud, A.F., Boyron, O. & Perez, E., 2017. To what extent are microplastics from the open ocean weathered? *Environmental Pollution*, 227:167–174.

Hatanaka, T., Mori, H. & Terano, M., 1999. Study of thermo-oxidative degradation of molten state polypropylenes with a variety of tacticities. *Polymer Degradation and Stability*, 64(2):313–319.

Henderson, S.T., 1970. Daylight and Its Spectrum. *Science*, 170(3959):278.

Heo, N.W., Hong, S.H., Han, G.M., Hong, S., Lee, J., Song, Y.K., Jang, M. & Shim, W.J., 2013. Distribution of small plastic debris in cross-section and high strandline on Heungnam beach, South Korea. *Ocean Science Journal*, 48(2013):225–233.

Hosseini, S.S., Taheri, S., Zadhoush, A. & Mehrabani-Zeinabad, A., 2007. Hydrolytic degradation of poly(ethylene terephthalate). *Journal of Applied Polymer Science*, 103(4):2304–2309.

Hurley, C.R. & Leggett, G.J., 2009. Quantitative Investigation of the Photodegradation of Polyethylene Terephthalate Film by Friction Force Microscopy, Contact-Angle Goniometry, and X-ray Photoelectron Spectroscopy. *ACS Applied Materials and Interfaces*, 1(8):1688–1697.

Iñiguez, M.E., Conesa, J.A. & Fullana, A., 2018. Recyclability of four types of plastics exposed to UV irradiation in a marine environment. *Waste Management*, 79(2018):339–345.

ISO, 2019. *Degradation*. ISO 1629:2019(en). Geneva: International Organization of Standardization.

Jahnke, A., Arp, H.P.H., Escher, B.I., Gewert, B., Gorokhova, E., Kühnel, D., Ogonowski, M., Potthoff, A., Rummel, C., Schmitt-Jansen, M., Toorman, E. & MacLeod, M., 2017. Reducing Uncertainty and Confronting Ignorance about the Possible Impacts of Weathering Plastic in the Marine Environment. *Environmental Science and Technology Letters*, 4(3):85–90.

Jambeck, J.R., Geyer, R., Wilcox, C., Siegler, T.R., Perryman, M., Andrady, A.L., Narayan, R. & Law, K.L., 2015. Plastic waste inputs from land into the ocean. *Science*, 347(6223):768–771.

Jellinek, H.H.G., 1978. *Aspects of Degradation and Stabilization of Polymers*. 1st Ed. New York: Elsevier Science Ltd.

Karger-Kocsis, J., 1995. Structure and morphology. In: *Polypropylene: Structure, blends and composites.* London: Chapman & Hall.

Khoironi, A., Hadiyanto, H., Anggoro, S. & Sudarno, S., 2020. Evaluation of polypropylene plastic degradation and microplastic identification in sediments at Tambak Lorok coastal area, Semarang, Indonesia. *Marine Pollution Bulletin*, 151.

Koltzenburg, S., Maskos, M. & Nuyken, O., 2014. *Polymere: Sythese, Eigenschaften und Anwendungen*. 1st Ed. Berlin: Springer Spektrum.

Kyrikou, I. & Briassoulis, D., 2007. Biodegradation of Agricultural Plastic Films: A Critical Review. *Journal of Polymers and the Environment*, 15(2007):125–150.

Lacoste, J., Vaillant, D. & Carlsson, D.J., 1993. Gamma-, photo-, and thermally-initiated oxidation of isotactic polypropylene. *Journal of Polymer Science Part A: Polymer Chemistry*, 31(3):715–722.

Laird, M., Write, A., Massie, V. & Clark, B., 2017. *Marine Environmental Impact Assessment for the Proposed Desalination Plants around the Cape Peninsula, South Africa.* Cape Town, South Africa.

Lebreton, L.C.M., Van Der Zwet, J., Damsteeg, J.W., Slat, B., Andrady, A. & Reisser, J., 2017. River plastic emissions to the world's oceans. *Nature Communications*, (8):15611.

Lee, C.O., Chae, B., Kim, S. Bin, Jung, Y.M. & Lee, S.W., 2012. Two-dimensional correlation analysis study of the photo-degradation of poly(ethylene terephthalate) film. *Vibrational Spectroscopy*, 60:142–145.

Longo, C., Savaris, M., Zeni, M., Brandalise, R. & Coulon, A., 2011. Degradation study of polypropylene (PP) and bioriented polypropylene (BOPP) in the environment. *Materials Research*, 14(4):422–448.

McIntrye, J., 1985. *Handbook of Fibre Chemistry*. 1st Ed. M. Lewin & M. Pearce (eds.). New York: Marcel Dekker.

McKeen, L.W., 2013. *The Effect of UV Light and Weather on Plastics and Elastomers*. 3rd Ed. Waltham, USA: Elsevier.

Meyer, T.J. & Caspar, J. V., 1985. Photochemistry of metal-metal bonds. *Chemical Reviews*, 85(3):187–218.

Mierzwa-Hersztek, M., Gondek, K. & Kopeć, M., 2019. Degradation of Polyethylene and Biocomponent-Derived Polymer Materials: An Overview. *Journal of Polymers and the Environment*, 27(3):600–611.

Moore, C.J., 2008. Synthetic polymers in the marine environment: A rapidly increasing, long-term threat. *Environmental Research*, 108(2):131–139.

Moore, G.F. & Saunders, S.M., 1998. *Advances in Biodegradable Polymers*. 1st Ed. Boca Raton, United States: CRC Press.

Mueller, M., 2000. PET bottle grade resin advancements in SSP technology. In: *Presentation given at the Polyester 2000 5th World Congress, Maack Business Services, 8804*. 2000, Zurich, Switzerland.

Muthukumar, T. & Doble, M., 2014. Biodegradation of Polymers in Marine Environment. In: M. Doble, R. Venkatesan, N. V. Kumar, & R. Kumar (eds.). *Polymers in a Marine Environment.* Shrewsbury, United Kingdom: iSmithers Rapra Publishing, :73–97.

Nagai, Y., Ogawa, T., Zhen, L.Y., Nishimoto, Y. & Ohishi, F., 1997. Analysis of weathering of thermoplastic polyester elastomers - I. Polyether-polyester elastomers. *Polymer Degradation and Stability*, 56(1):115–121.

Niemczyk, A., Dziubek, K., Grzymek, M. & Czaja, K., 2019. Accelerated laboratory weathering of polypropylene composites filled with synthetic silicon-based compounds. *Polymer Degradation and Stability*, 161(2019):30–38.

Ojeda, T., Freitas, A., Birck, K., Dalmolin, E., Jacques, R., Bento, F. & Camargo, F., 2011. Degradability of linear polyolefins under natural weathering. *Polymer Degradation and Stability*, 96(4):703–707.

Osram GmbH, 2013. *More than just light - Solutions in ultraviolet light*. [Online]. Munich, Germany. Available from: https://docs-emea.rs-online.com/webdocs/1506/0900766b81506d14.pdf.

Pecheva, E., 2017. *Study of Biocompatible and Biological Materials*. 11th Ed. Millersville, United States: Materials Research Forum LLC.

Pegram, J.E. & Andrady, A.L., 1989. Outdoor weathering of selected polymeric materials under marine exposure conditions. *Polymer Degradation and Stability*, 26(4):333–345.

Philippart, J.L. & Gardette, J.L., 2001. Thermo-oxidation of isotactic polypropylene in 32O2-36O2: Comparison of the mechanisms of thermo- and photo-oxidation. *Polymer Degradation and Stability*, 73(1):185–187.

Pilař, J., Michálková, D., Šlouf, M. & Vacková, T., 2015. Long-term accelerated weathering of HAS stabilized PE and PP plaques: Compliance of ESRI, IR, and microhardness data characterizing heterogeneity of photooxidation. *Polymer Degradation and Stability*, 120(2015):114–121.

Pitt, C.., Gratzl, M.., Kimmel, G.., Surles, J. & Schindler, A., 1981. Aliphatic polyesters II. The degradation of poly (DL-lactide), poly (epsilon-caprolactone), and their copolymers in vivo. *Biomaterials*, 2(4):215–220.

PlasticsEurope, 2020. *How plastics are made*. [Online]. 2020. Available from: https://www.plasticseurope.org/en/about-plastics/what-are-plastics/how-plastics-are-made. [Accessed: 4 June 2020].

PlasticsEurope, 2019. *Plastics - The Facts 2019: An analysis of European plastics production, demand and waste data*. [Online]. Available from: https://www.plasticseurope.org/en/resources/market-data.

Pospíšil, J., Pilař, J., Billingham, N.C., Marek, A., Horák, Z. & Nešpůrek, S., 2006. Factors affecting accelerated testing of polymer photostability. *Polymer Degradation and Stability*, 91(3):417–422.

Puoci, F., 2014. *Advanced Polymers in Medicine*. 1st Ed. Germany: Springer International Publishing.

Quan, Z. & Frey, E.S., 1995. Empirical equation for the index of refraction of seawater. *Applied Optics*, 34(18):3477–3480.

Rabek, J.F., 1995. *Polymer Photodegradation. Mechanisms and experimental methods*. 1st Ed. London: Chapman & Hall.

Rabello, M.S. & White, J.R., 1966. Photodegradation of polypropylene containing a nucleating agent. *Applied Polymer Science*, 64(13):2505–2517.

Raka, L. & Bogoeva-Gaceva, G., 2008. Crystallization of polypropylene: Application of Differential Scanning Calorimetry. *Contributions, Section of Mathematical Sciences*, 29(1):49–67.

Rieckmann, T. & Volker, S., 2003. Poly(ethylene Terephthalate) Polymerization - Mechanism, Catalysis, Kinetics, Mass Transfer and Reactor Design. In: J. Scheirs & T. E. Long (eds.). *Modern Polyesters: Chemistry and Technology of Polyesters and Copolyesters*. Oxford: John Wiley & Sons, Inc., :41–48.

Riley, J. & Skirrow, G., 1975. *Chemical Oceanography. Volume 2*. 2nd Ed. London: Academic Press.

Rocha-Santos, T. & Duarte, A.C., 2015. A critical overview of the analytical approaches to the occurrence, the fate and the behavior of microplastics in the environment. *TrAC - Trends in Analytical Chemistry*, 65(2015):47–53.

Savchuk, T.M. & Neverov, A.N., 1982. The effects of orientation and crystallinity on the resistance of polyethylene terephthalate to photooxidation. *Polymer Science U.S.S.R.*, 24(5):1138–1143.

Scheirs, J. & Gardette, J.L., 1997. Photo-oxidation and photolysis of poly(ethylene naphthalate). *Polymer Degradation and Stability*, 56(3):339–350.

Severini, F., Gallo, R. & Ipsale, S., 1988. Environmental degradation of polypropylene. *Polymer Degradation and Stability*, 22(2):185–194.

Shaw, D.G. & Day, R.H., 1994. Colour- and form-dependent loss of plastic micro-debris from the North Pacific Ocean. *Marine Pollution Bulletin*, 28(1):39–43.

Singh, B. & Sharma, N., 2008. Mechanistic implications of plastic degradation. *Polymer Degradation and Stability*, 93(3):561–584.

Sowmya, H. V, Ramalingappa, Krishnappa, M. & Thippeswamy, B., 2014. Degradation of polyethylene by Trichoderma harzianum-SEM, FTIR and NMR analyses. *Environmental Monitoring and Assessment*, 186(10):6577–6486.

Stutz, H., Illers, K.H. & Mertes, J., 1990. A Generalized Theory for the Glass Transition Temperature of Crosslinked and Uncrosslinked Polymers. *Journal of Polymer Science: Part B: Polymer Physics*, 28(1990):1483–1498.

Tang, L., Wu, Q. & Qu, B., 2005. The effects of chemical structure and synthesis method on photodegradation of polypropylene. *Journal of Applied Polymer Science*, 95(2):270–279.

Wang, W. & Wang, J., 2018. Investigation of microplastics in aquatic environments: An overview of the methods used, from field sampling to laboratory analysis. *TrAC - Trends in Analytical Chemistry*, 108(2018):195–202.

Weiss, R.F., 1970. The solubility of nitrogen, oxygen and argon in water and seawater. *Deep-Sea Research and Oceanographic Abstracts*, 17(4):721–735.

Winslow, F.H., Hellman, M.Y., Matreyek, W. & Salovey, R., 1966. Etching of solution-crystallized polyethylene with fuming nitric acid. *Polymer Engineering & Science*, 5(1):89–93.

World Bank, 2020. *Global Solar Atlas*. [Online]. 2020. Available from: https://globalsolaratlas.info/map. [Accessed: 21 May 2020].

World Economic Forum, 2016. *The New Plastics Economy: Rethinking the future of plastics.* [Online]. Geneva. Available from: http://www3.weforum.org/docs/WEF_The_New_Plastics_Economy.pdf.

Wu, Z., Peng, J., Tan, X., Wang, J. & Cai, L., 2018. Observation of the degradation of three types of plastic pellets exposed to UV irradiation in three different environments. *Science of The Total Environment*, 628–629(2018):740–747.

Wunderlich, B., 1973. *Macromolecular Physics V1*. 1st Ed. New York: Elsevier Inc.

Yadav, P., Verma, U., Shrivastava, A.K., Semwal, R.P., Yadav, B.S. & Chauhan, R.S., 2011. Tensile properties of photoexposed poly(ethylene-terephthalate) films. *Journal of Polymer Materials*, 28(4):587–598.

Yamada-Onodera, K., Mukumoto, H., Katsuyaya, Y., Saiganji, A. & Tani, Y., 2001. Degradation of polyethylene by a fungus, Penicillium simplicissimum YK. *Polymer Degradation and Stability*, 72(2):323–327.

Zimmerman, H., 1984. Degradation and stabilisation of polyesters. In: N. Grassie (ed.). *Developments in Polymer Degradation Vol 5*. London: Applied Science Publishers, :79–119.

Zimmerman, H. & Becker, D., 1976. Polymeranalytische Untersuchungen zum Abbau von Polyathylenterephthalat in fester Phase. *Faserforschung Textiltechnik*, 27:229–235.

Appendix A: Supplementary material

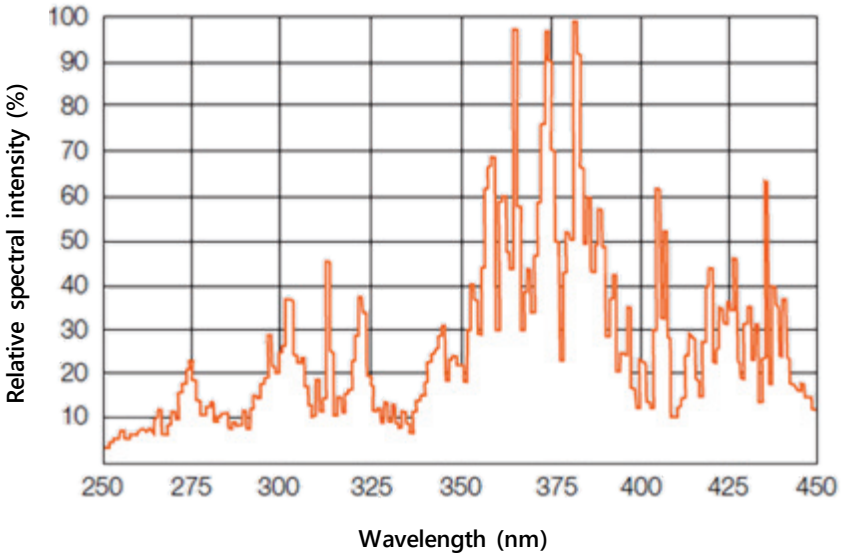

Figure A.1. Relative spectral intensity (%) versus wavelength (nm) for the OSRAM Supratech HTC (400-221) lamps used in this investigation [Adapted from Osram GmbH (2013)].

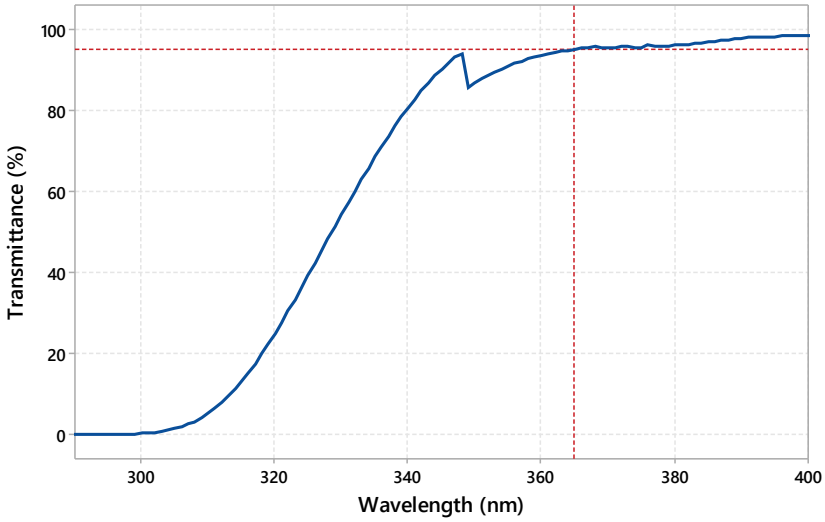

Figure A.2. Ultraviolet-visible (UV-Vis) spectroscopy plot indicating transmittance (%) versus wavelength (nm) for glass beakers used in the beaker tests. It is evident that at the peak wavelength intensity of the UV lamps (365 nm), more than 95% of light was transmitted.

Appendix B: Experimental data

Note: The experimental and processed data for this work is provided separately, please refer to the attached .xlsm file where necessary.

Appendix C: ANOVA results

C.1 UV pre-treatment

Table C.1. ANOVA results for the effect of UV irradiance on week six mass loss (%).

Factor Information					
Factor	Levels	Values			
UV Irradiance (W/m2)	2	65. 130			
Analysis of Variance					
Source	DF	Adj SS	Adj MS	F-Value	P-Value
UV Irradiance (W/m2)	1	568,4	568,42	33,51	0,000
Error	232	3935,3	16,96		
Total	233	4503,7			
Model Summary					
S	R-sq	R-sq(adj)	R-sq(pred)		
4,11854	12,62%	12,24%	11,11%		
Means					
UV Irradiance (W/m2)	N	Mean	StDev	95% CI	
65	116	1,383	3,048	(0,629. 2,136)	
130	118	4,500	4,950	(3,753. 5,247)	

Table C.2. ANOVA results for the effect of shape on week six mass loss (%).

Factor Information					
Factor	Levels	Values			
Shape	4	LC. LR. SC. SR			
Analysis of Variance					
Source	DF	Adj SS	Adj MS	F-Value	P-Value
Shape	3	22,05	7,351	0,38	0,769
Error	230	4481,64	19,485		
Total	233	4503,7			
Model Summary					
S	R-sq	R-sq(adj)	R-sq(pred)		
4,41423	0,49%	0,00%	0,00%		
Means					
Shape	N	Mean	StDev	95% CI	
LC	60	3,046	4,238	(1,923. 4,168)	
LR	59	2,871	5,819	(1,738. 4,003)	
SC	58	2,525	3,515	(1,383. 3,667)	
SR	57	3,383	3,670	(2,231. 4,535)	

Table C.3. ANOVA results for the effect of plastic-type on week six mass loss (%).

Factor Information					
Factor	Levels	Values			
Plastic	3	BPP. CPP. PET			
Analysis of Variance					
Source	DF	Adj SS	Adj MS	F-Value	P-Value
Plastic	2	601,2	300,62	17,80	0,000
Error	231	3902,4	16,89		
Total	233	4503,7			
Model Summary					
S	R-sq	R-sq(adj)	R-sq(pred)		
4,11020	13,35%	12,60%	11,10%		
Means					
Plastic	N	Mean	StDev	95% CI	
BPP	77	2,272	3,911	(1,349. 3,194)	
CPP	80	5,122	4,815	(4,217. 6,027)	
PET	77	1,386	3,457	(0,463. 2,309)	

Table C.4. ANOVA results for week six crystallinity increase (%) for BPP.

Factor Information					
Factor	Levels	Values			
UV Irradiance (W/m2)	2	65. 130			
Analysis of Variance					
Source	DF	Adj SS	Adj MS	F-Value	P-Value
UV Irradiance (W/m2)	1	4,201	4,2008	8,23	0,024
Error	7	3,571	0,5102		
Total	8	7,772			
Model Summary					
S	R-sq	R-sq(adj)	R-sq(pred)		
0,714272	54,05%	47,49%	28,65%		
Means					
UV Irradiance (W/m2)	N	Mean	StDev	95% CI	
65	3	-2,329	0,498	(-3,304. -1,354)	
130	6	-3,778	0,784	(-4,468. -3,089)	

Table C.5. ANOVA results for week six crystallinity increase (%) for CPP.

Factor Information					
Factor	Levels	Values			
UV Irradiance (W/m2)	2	65. 130			
Analysis of Variance					
Source	DF	Adj SS	Adj MS	F-Value	P-Value
UV Irradiance (W/m2)	1	240,59	240,591	24,07	0,002
Error	7	69,98	9,997		
Total	8	310,57			
Model Summary					
S	R-sq	R-sq(adj)	R-sq(pred)		
3,16178	77,47%	74,25%	67,52%		
Means					
UV Irradiance (W/m2)	N	Mean	StDev	95% CI	
65	3	24,025	0,236	(19,708. 28,341)	
130	6	13,06	3,74	(10,00. 16,11)	

Table C.6. ANOVA results for week six crystallinity increase (%) for PET.

Factor Information					
Factor	Levels	Values			
UV Irradiance (W/m2)	2	65. 130			
Analysis of Variance					
Source	DF	Adj SS	Adj MS	F-Value	P-Value
UV Irradiance (W/m2)	1	18,87	18,87	1,07	0,335
Error	7	123,28	17,61		
Total	8	142,15			
Model Summary					
S	R-sq	R-sq(adj)	R-sq(pred)		
4,19658	13,27%	0,89%	0,00%		
Means					
UV Irradiance (W/m2)	N	Mean	StDev	95% CI	
65	3	6,401	1,627	(0,671. 12,130)	
130	6	3,33	4,86	(-0,72. 7,38)	

Table C.7. ANOVA results for week six microhardness increase (%) for BPP.

Factor Information					
Factor	Levels	Values			
UV Irradiance (W/m2)	2	65. 130			
Analysis of Variance					
Source	DF	Adj SS	Adj MS	F-Value	P-Value
UV Irradiance (W/m2)	1	19,86	19,861	2,20	0,149
Error	28	252,36	9,013		
Total	29	272,22			
Model Summary					
S	R-sq	R-sq(adj)	R-sq(pred)		
0,714272	7,30%	3,99%	0,00%		
Means					
UV Irradiance (W/m2)	N	Mean	StDev	95% CI	
65	15	-5,948	3,541	(-7,536. -4,360)	
130	15	-7,575	2,343	(-9,163. -5,987)	

Table C. 8. ANOVA results for week six microhardness increase (%) for PET.

Factor Information					
Factor	Levels	Values			
UV Irradiance (W/m2)	2	65. 130			
Analysis of Variance					
Source	DF	Adj SS	Adj MS	F-Value	P-Value
UV Irradiance (W/m2)	1	467,0	467,00	28,38	0,000
Error	28	460,7	16,45		
Total	29	927,7			
Model Summary					
S	R-sq	R-sq(adj)	R-sq(pred)		
4,05633	50,34%	48,57%	42,99%		
Means					
UV Irradiance (W/m2)	N	Mean	StDev	95% CI	
65	15	10,780	2,890	(8,635. 12,926)	
130	15	18,67	4,96	(16,53. 20,82)	

Table C.9. ANOVA results for the effect of UV irradiance on week six $CI_{(Areas)}$ for PPs.

Factor Information					
Factor	Levels	Values			
UV Irradiance (W/m2)	2	65. 130			
Analysis of Variance					
Source	DF	Adj SS	Adj MS	F-Value	P-Value
UV Irradiance (W/m2)	1	56,51	56,5141	60,58	0,000
Error	171	159,53	0,9329		
Total	172	216,05			
Model Summary					
S	R-sq	R-sq(adj)	R-sq(pred)		
0,965890	26,16%	25,73%	24,30%		
Means					
UV Irradiance (W/m2)	N	Mean	StDev	95% CI	
65	97	1,5461	0,6758	(1,3525. 1,7397)	
130	76	2,698	1,242	(2,479. 2,916)	

Table C.10. ANOVA results for the effect of shape on week six $CI_{(Areas)}$ for PPs.

Factor Information					
Factor	Levels	Values			
Shape	4	LC. LR. SC. SR			
Analysis of Variance					
Source	DF	Adj SS	Adj MS	F-Value	P-Value
Shape	3	3,880	1,293	1,03	0,381
Error	169	212,168	1,255		
Total	172	216,04			
Model Summary					
S	R-sq	R-sq(adj)	R-sq(pred)		
1,12046	1,80%	0,05%	0,00%		
Means					
Shape	N	Mean	StDev	95% CI	
LC	57	2,203	1,437	(1,911. 2,496)	
LR	71	1,877	0,950	(1,614. 2,140)	
SC	19	2,088	0,901	(1,580. 2,595)	
SR	26	2,172	0,866	(1,738. 2,606)	

Table C.11. ANOVA results for the effect of plastic-type on week six $CI_{(Areas)}$ for PPs.

Factor Information					
Factor	Levels	Values			
Plastic	2	BPP. CPP			
Analysis of Variance					
Source	DF	Adj SS	Adj MS	F-Value	P-Value
Plastic	1	49,31	49,3056	50,56	0,000
Error	171	166,74	0,9751		
Total	172	216,05			
Model Summary					
S	R-sq	R-sq(adj)	R-sq(pred)		
0,987471	22,82%	22,37%	21,02%		
Means					
Plastic	N	Mean	StDev	95% CI	
BPP	88	1,527	1,147	(1,320. 1,735)	
CPP	85	2,5952	0,7883	(2,3838. 2,8066)	

Table C.12. ANOVA results for the effect of UV irradiance on week six $CI_{(Areas)}$ for PET.

Factor Information					
Factor	Levels	Values			
UV Irradiance (W/m2)	2	65. 130			
Analysis of Variance					
Source	DF	Adj SS	Adj MS	F-Value	P-Value
UV Irradiance (W/m2)	1	1797	1796,81	139,62	0,000
Error	84	1081	12,87		
Total	85	2878			
Model Summary					
S	R-sq	R-sq(adj)	R-sq(pred)		
3,58735	62,44%	61,99%	60,59%		
Means					
UV Irradiance (W/m2)	N	Mean	StDev	95% CI	
65	44	57,391	1,827	(56,316. 58,467)	
130	42	66,535	4,782	(65,435. 67,636)	

Table C.13. ANOVA results for the effect of shape on week six $CI_{(Areas)}$ for PET.

Factor Information					
Factor	Levels	Values			
Shape	4	LC. LR. SC. SR			
Analysis of Variance					
Source	DF	Adj SS	Adj MS	F-Value	P-Value
Shape	3	234,2	78,08	2,42	0,072
Error	82	2643,6	32,24		
Total	85	2877,8			
Model Summary					
S	R-sq	R-sq(adj)	R-sq(pred)		
5,67792	8,14%	4,78%	0,00%		
Means					
Shape	N	Mean	StDev	95% CI	
LC	25	59,286	2,934	(57,027. 61,545)	
LR	36	62,848	5,639	(60,965. 64,731)	
SC	12	62,80	8,47	(59,54. 66,06)	
SR	13	63,18	6,68	(60,05. 66,32)	

C.2 UV beaker tests

Table C.14. ANOVA results for the effect of UV irradiance on week six mass loss (%).

Factor Information					
Factor	Levels	Values			
UV Irradiance (W/m2)	2	65. 130			
Analysis of Variance					
Source	DF	Adj SS	Adj MS	F-Value	P-Value
UV Irradiance (W/m2)	1	176,2	176,18	5,49	0,020
Error	164	5265,9	32,11		
Total	165	5442,0			
Model Summary					
S	R-sq	R-sq(adj)	R-sq(pred)		
5,66647	3,24%	2,65%	0,80%		
Means					
UV Irradiance					
(W/m2)	N	Mean	StDev	95% CI	
65	92	2,149	5,077	(0,982. 3,315)	
130	74	4,222	6,325	(2,921. 5,522)	

Table C.15. ANOVA results for the effect of plastic-type on week six mass loss (%).

Factor Information					
Factor	Levels	Values			
Plastic	3	BPP. CPP. PET			
Analysis of Variance					
Source	DF	Adj SS	Adj MS	F-Value	P-Value
Plastic	2	1598	798,82	33,87	0,000
Error	163	3844	23,59		
Total	165	5442			
Model Summary					
S	R-sq	R-sq(adj)	R-sq(pred)		
4,85647	29,36%	28,49%	26,63%		
Means					
Plastic	N	Mean	StDev	95% CI	
BPP	57	1,231	3,456	(-0,039. 2,501)	
CPP	52	7,66	7,46	(6,33. 8,99)	
PET	57	0,733	2,446	(-0,537. 2,003)	

Table C.16. ANOVA results for the effect of UV history on week six mass loss (%).

Factor Information					
Factor	Levels	Values			
UV History (W/m2)	3	0. 65. 130			
Analysis of Variance					
Source	DF	Adj SS	Adj MS	F-Value	P-Value
UV History (W/m2)	2	707,1	353,53	12,17	0,000
Error	163	4735,0	29,05		
Total	165	5442,0			
Model Summary					
S	R-sq	R-sq(adj)	R-sq(pred)		
5,38971	12,99%	11,92%	9,94%		
Means					
UV History					
(W/m2)	N	Mean	StDev	95% CI	
0	49	0,848	2,751	(-0,672. 2,368)	
65	57	2,198	3,859	(0,788. 3,607)	
130	60	5,72	7,74	(4,35. 7,10)	

Table C.17. ANOVA results for the effect of solution medium on week six mass loss (%).

Factor Information					
Factor	Levels	Values			
Solution medium	2	SW. DW			
Analysis of Variance					
Source	DF	Adj SS	Adj MS	F-Value	P-Value
Solution medium	1	43,68	43,68	3,87	0,052
Error	108	1219,98	11,30		
Total	109	1263,67			
Model Summary					
S	R-sq	R-sq(adj)	R-sq(pred)		
3,36097	3,46%	2,56%	0,00%		
Means					
Solution medium	N	Mean	StDev	95% CI	
SW	49	0,848	2,751	(-0,104. 1,800)	
DW	61	2,116	3,779	(1,263. 2,969	

Table C.18. ANOVA results for the effect of UV irradiance on week six crystallinity increase (%) for BPP.

Factor Information					
Factor	Levels	Values			
UV Irradiance (W/m2)	2	65. 130			
Analysis of Variance					
Source	DF	Adj SS	Adj MS	F-Value	P-Value
UV Irradiance (W/m2)	1	2,148	2,1476	2,40	0,141
Error	16	14,324	0,8952		
Total	17	16,471			
Model Summary					
S	R-sq	R-sq(adj)	R-sq(pred)		
0,946174	13,04%	7,60%	0,00%		
Means					
UV Irradiance					
(W/m2)	N	Mean	StDev	95% CI	
65	9	38,440	0,878	(37,772. 39,109)	
130	9	37,749	1,010	(37,081. 38,418)	

Table C.19. ANOVA results for the effect of UV irradiance on week six crystallinity increase (%) for CPP.

Factor Information					
Factor	Levels	Values			
UV Irradiance (W/m2)	2	65. 130			
Analysis of Variance					
Source	DF	Adj SS	Adj MS	F-Value	P-Value
UV Irradiance (W/m2)	1	160,8	160,78	1,65	0,217
Error	16	1557,9	97,37		
Total	17	1718,6			
Model Summary					
S	R-sq	R-sq(adj)	R-sq(pred)		
9,86747	9,35%	3,69%	0,00%		
Means					
UV Irradiance					
(W/m2)	N	Mean	StDev	95% CI	
65	9	1,09	4,40	(-5,88. 8,07)	
130	9	7,07	13,24	(0,10. 14,04)	

Table C.20. ANOVA results for the effect of UV irradiance on week six crystallinity increase (%) for PET.

Factor Information					
Factor	Levels	Values			
UV Irradiance (W/m2)	2	65. 130			
Analysis of Variance					
Source	DF	Adj SS	Adj MS	F-Value	P-Value
UV Irradiance (W/m2)	1	130,3	130,26	12,80	0,003
Error	16	162,8	10,18		
Total	17	293,1			
Model Summary					
S	R-sq	R-sq(adj)	R-sq(pred)		
3,19018	44,44%	40,97%	29,69%		
Means					
UV Irradiance (W/m2)	N	Mean	StDev	95% CI	
65	9	-0,855	2,050	(-3,110. 1,399)	
130	9	4,53	4,02	(2,27. 6,78)	

Table C.21. ANOVA results for the effect of solution medium on week six crystallinity increase (%) for BPP.

Factor Information					
Factor	Levels	Values			
Solution Medium	2	SW. DW			
Analysis of Variance					
Source	DF	Adj SS	Adj MS	F-Value	P-Value
Solution Medium	1	0,2958	0,2958	0,61	0,454
Error	10	4,8684	0,4868		
Total	11	5,1643			
Model Summary					
S	R-sq	R-sq(adj)	R-sq(pred)		
0,697742	5,73%	0,00%	0,00%		
Means					
Solution Medium	N	Mean	StDev	95% CI	
SW	6	38,865	0,719	(38,230. 39,499)	
DW	6	38,551	0,676	(37,916. 39,185)	

Table C.22. ANOVA results for the effect of solution medium on week six crystallinity increase (%) for CPP.

Factor Information					
Factor	Levels	Values			
Solution Medium	2	SW. DW			
Analysis of Variance					
Source	DF	Adj SS	Adj MS	F-Value	P-Value
Solution Medium	1	0,401	0,4009	0,01	0,921
Error	10	388,059	38,8059		
Total	11	388,459			
Model Summary					
S	R-sq	R-sq(adj)	R-sq(pred)		
6,22944	0,10%	0,00%	0,00%		
Means					
Solution Medium	N	Mean	StDev	95% CI	
SW	6	45,43	5,95	(39,76. 51,10)	
DW	6	45,80	6,50	(40,13. 51,46)	

Table C.23. ANOVA results for the effect of solution medium on week six crystallinity increase (%) for PET.

Factor Information					
Factor	Levels	Values			
Solution Medium	2	SW. DW			
Analysis of Variance					
Source	DF	Adj SS	Adj MS	F-Value	P-Value
Solution Medium	1	0,1172	0,1172	0,08	0,784
Error	10	14,7278	1,4728		
Total	11	14,8450			
Model Summary					
S	R-sq	R-sq(adj)	R-sq(pred)		
1,21358	0,79%	0,00%	0,00%		
Means					
Solution Medium	N	Mean	StDev	95% CI	
SW	6	32,088	1,410	(30,984. 33,192)	
DW	6	32,286	0,978	(31,182. 33,390)	

Table C.24. ANOVA results for the effect of UV history on week six crystallinity increase (%) for BPP.

Factor Information					
Factor	Levels	Values			
UV History (W/m2)	3	0. 65. 130			
Analysis of Variance					
Source	DF	Adj SS	Adj MS	F-Value	P-Value
UV History (W/m2)	2	1,636	0,8181	0,21	0,810
Error	15	57,563	3,8375		
Total	17	59,199			
Model Summary					
S	R-sq	R-sq(adj)	R-sq(pred)		
1,95896	2,76%	0,00%	0,00%		
Means					
UV History (W/m2)	N	Mean	StDev	95% CI	
0	6	-3,906	1,778	(-5,610. -2,201)	
65	6	-3,461	1,519	(-5,166. -1,756)	
130	6	-4,19	2,46	(-5,90. -2,49)	

Table C.25. ANOVA results for the effect of UV history on week six crystallinity increase (%) for CPP.

Factor Information					
Factor	Levels	Values			
UV History (W/m2)	3	0. 65. 130			
Analysis of Variance					
Source	DF	Adj SS	Adj MS	F-Value	P-Value
UV History (W/m2)	2	575,7	287,84	3,78	0,047
Error	15	1143,0	76,20		
Total	17	1718,6			
Model Summary					
S	R-sq	R-sq(adj)	R-sq(pred)		
8,72916	33,50%	24,63%	4,23%		
Means					
UV History (W/m2)	N	Mean	StDev	95% CI	
0	6	11,18	14,55	(3,59. 18,78)	
65	6	-2,653	1,867	(-10,249. 4,943)	
130	6	3,72	3,66	(-3,88. 11,31)	

Table C.26. ANOVA results for the effect of UV history on week six crystallinity increase (%) for PET.

Factor Information					
Factor	Levels	Values			
UV History (W/m2)	3	0. 65. 130			
Analysis of Variance					
Source	DF	Adj SS	Adj MS	F-Value	P-Value
UV History (W/m2)	2	111,6	55,82	4,61	0,027
Error	15	181,5	12,10		
Total	17	293,1			
Model Summary					
S	R-sq	R-sq(adj)	R-sq(pred)		
3,47804	38,09%	29,84%	10,85%		
Means					
UV History (W/m2)	N	Mean	StDev	95% CI	
0	6	5,07	4,62	(2,04. 8,09)	
65	6	-0,993	2,437	(-4,019. 2,034)	
130	6	1,43	3,00	(-1,60. 4,46)	

Table C.27. ANOVA results for the effect of UV irradiance on week six microhardness increase (%) for BPP.

Factor Information					
Factor	Levels	Values			
UV Irradiance (W/m2)	2	65. 130			
Analysis of Variance					
Source	DF	Adj SS	Adj MS	F-Value	P-Value
UV Irradiance (W/m2)	1	3736	3735,61	52,37	0,000
Error	51	3638	71,33		
Total	52	7373			
Model Summary					
S	R-sq	R-sq(adj)	R-sq(pred)		
8,44551	50,66%	49,70%	46,72%		
Means					
UV Irradiance (W/m2)	N	Mean	StDev	95% CI	
65	26	6,20	8,32	(2,87. 9,52)	
130	27	22,99	8,56	(19,73. 26,25	

Table C.28. ANOVA results for the effect of UV irradiance on week six microhardness increase (%) for PET.

Factor Information					
Factor	Levels	Values			
UV Irradiance (W/m2)	2	65. 130			
Analysis of Variance					
Source	DF	Adj SS	Adj MS	F-Value	P-Value
UV Irradiance (W/m2)	1	15,91	15,91	0,12	0,728
Error	52	6764,84	130,09		
Total	53	6780,75			
Model Summary					
S	R-sq	R-sq(adj)	R-sq(pred)		
11,4058	0,23%	0,00%	0,00%		
Means					
UV Irradiance (W/m2)	N	Mean	StDev	95% CI	
65	27	18,04	6,51	(13,63. 22,44)	
130	27	19,12	14,76	(14,72. 23,53)	

Table C.29. ANOVA results for the effect of solution medium on week six microhardness increase (%) for BPP.

Factor Information					
Factor	Levels	Values			
Solution Medium	2	SW. DW			
Analysis of Variance					
Source	DF	Adj SS	Adj MS	F-Value	P-Value
Solution Medium	1	13,92	13,92	0,07	0,796
Error	33	6737,11	204,15		
Total	34	6751,03			
Model Summary					
S	R-sq	R-sq(adj)	R-sq(pred)		
14,2883	0,21%	0,00%	0,00%		
Means					
Solution Medium	N	Mean	StDev	95% CI	
SW	17	16,16	10,89	(9,10. 23,21)	
DW	18	17,42	16,87	(10,56. 24,27)	

Table C.30. ANOVA results for the effect of solution medium on week six microhardness increase (%) for PET.

Factor Information					
Factor	Levels	Values			
Solution Medium	2	SW. DW			
Analysis of Variance					
Source	DF	Adj SS	Adj MS	F-Value	P-Value
Solution Medium	1	6,29	6,285	0,13	0,716
Error	34	1589,16	46,740		
Total	35	1595,45			
Model Summary					
S	R-sq	R-sq(adj)	R-sq(pred)		
6,83667	0,39%	0,00%	0,00%		
Means					
Solution Medium	N	Mean	StDev	95% CI	
SW	18	28,93	6,91	(25,66. 32,21)	
DW	18	28,10	6,76	(24,82. 31,37)	

Table C.31. ANOVA results for the effect of UV history on week six microhardness increase (%) for BPP.

Factor Information					
Factor	Levels	Values			
UV History (W/m2)	3	0. 65. 130			
Analysis of Variance					
Source	DF	Adj SS	Adj MS	F-Value	P-Value
UV History (W/m2)	2	125,9	62,97	0,43	0,650
Error	50	7247,3	144,95		
Total	52	7373,3			
Model Summary					
S	R-sq	R-sq(adj)	R-sq(pred)		
12,0394	1,71%	0,00%	0,00%		
Means					
UV History (W/m2)	N	Mean	StDev	95% CI	
0	17	16,16	10,89	(10,29. 22,02)	
65	18	12,63	8,38	(6,93. 18,33)	
130	18	15,55	15,64	(9,85. 21,25)	

Table C.32. ANOVA results for the effect of UV history on week six microhardness increase (%) for PET.

Factor Information					
Factor	Levels	Values			
UV History (W/m2)	3	0. 65. 130			
Analysis of Variance					
Source	DF	Adj SS	Adj MS	F-Value	P-Value
UV History (W/m2)	2	3658	1829,12	29,88	0,000
Error	51	3123	61,23		
Total	53	6781			
Model Summary					
S	R-sq	R-sq(adj)	R-sq(pred)		
7,82468	53,95%	52,14%	48,37%		
Means					
UV History (W/m2)	N	Mean	StDev	95% CI	
0	18	28,93	6,91	(25,23. 32,63)	
65	18	18,01	5,58	(14,31. 21,71)	
130	18	8,79	10,24	(5,09. 12,50)	

Table C.33. ANOVA results for the effect of UV irradiance on week six $CI_{(Areas)}$ for BPP.

Factor Information					
Factor	Levels	Values			
UV Irradiance (W/m2)	2	65. 130			
Analysis of Variance					
Source	DF	Adj SS	Adj MS	F-Value	P-Value
UV Irradiance (W/m2)	1	3,083	3,0834	6,07	0,019
Error	35	17,773	0,5078		
Total	36	20,85			
Model Summary					
S	R-sq	R-sq(adj)	R-sq(pred)		
0,712592	14,78%	12,35%	4,58%		
Means					
UV Irradiance (W/m2)	N	Mean	StDev	95% CI	
65	19	0,787	0,441	(0,456. 1,119)	
130	18	1,365	0,916	(1,024. 1,706)	

Table C.34. ANOVA results for the effect of UV irradiance on week six $CI_{(Areas)}$ for CPP.

Factor Information					
Factor	Levels	Values			
UV Irradiance (W/m2)	2	65. 130			
Analysis of Variance					
Source	DF	Adj SS	Adj MS	F-Value	P-Value
UV Irradiance (W/m2)	1	2,304	2,3039	11,09	0,002
Error	32	6,646	0,2077		
Total	33	8,950			
Model Summary					
S	R-sq	R-sq(adj)	R-sq(pred)		
0,455740	25,74%	23,42%	16,22%		
Means					
UV Irradiance (W/m2)	N	Mean	StDev	95% CI	
65	18	0,825	0,472	(0,607. 1,044)	
130	16	1,347	0,437	(1,115. 1,579)	

Table C.35. ANOVA results for the effect of UV irradiance on week 6 $CI_{(Areas)}$ for PET.

Factor Information					
Factor	Levels	Values			
UV Irradiance (W/m2)	2	65. 130			
Analysis of Variance					
Source	DF	Adj SS	Adj MS	F-Value	P-Value
UV Irradiance (W/m2)	1	320,1	320,14	10,81	0,002
Error	34	1007,1	29,62		
Total	35	1327,2			
Model Summary					
S	R-sq	R-sq(adj)	R-sq(pred)		
5,44245	24,12%	21,89%	14,93%		
Means					
UV Irradiance (W/m2)	N	Mean	StDev	95% CI	
65	18	54,32	7,36	(51,72. 56,93)	
130	18	48,359	2,263	(45,752. 50,966)	

Table C.36. ANOVA results for the effect of UV history on week six $CI_{(Areas)}$ for BPP.

Factor Information					
Factor	Levels	Values			
UV History (W/m2)	3	0. 65. 130			
Analysis of Variance					
Source	DF	Adj SS	Adj MS	F-Value	P-Value
UV History (W/m2)	2	8,727	4,3633	12,23	0,000
Error	34	12,129	0,3567		
Total	36	20,856			
Model Summary					
S	R-sq	R-sq(adj)	R-sq(pred)		
0,597281	41,84%	38,42%	30,80%		
Means					
UV History (W/m2)	N	Mean	StDev	95% CI	
0	13	0,4602	0,1219	(0,1236. 0,7969)	
65	12	1,632	1,032	(1,281. 1,982)	
130	12	1,1641	0,1495	(0,8137. 1,5145)	

Table C.37. ANOVA results for the effect of UV history on week six $CI_{(Areas)}$ for CPP.

Factor Information					
Factor	Levels	Values			
UV History (W/m2)	3	0. 65. 130			
Analysis of Variance					
Source	DF	Adj SS	Adj MS	F-Value	P-Value
UV History (W/m2)	2	0,5358	0,2679	0,99	0,384
Error	31	8,4145	0,2714		
Total	33	8,9503			
Model Summary					
S	R-sq	R-sq(adj)	R-sq(pred)		
0,520993	5,99%	0,00%	0,00%		
Means					
UV History (W/m2)	N	Mean	StDev	95% CI	
0	10	0,892	0,940	(0,556. 1,228)	
65	12	1,2040	0,1803	(0,8972. 1,5107)	
130	12	1,0867	0,0981	(0,7800. 1,3935)	

Table C.38. ANOVA results for the effect of UV history on week six $CI_{(Areas)}$ for PET.

Factor Information					
Factor	Levels	Values			
UV History (W/m2)	3	0. 65. 130			
Analysis of Variance					
Source	DF	Adj SS	Adj MS	F-Value	P-Value
UV History (W/m2)	2	307,5	153,73	4,97	0,013
Error	33	1019,8	30,90		
Total	35	1327,2			
Model Summary					
S	R-sq	R-sq(adj)	R-sq(pred)		
5,55898	23,17%	18,51%	8,56%		
Means					
UV History (W/m2)	N	Mean	StDev	95% CI	
0	12	55,46	9,36	(52,20. 58,73)	
65	12	49,005	1,689	(45,740. 52,269)	
130	12	49,557	1,503	(46,292. 52,822)	

Table C.39. ANOVA results for the effect of solution medium on week six $CI_{(Areas)}$ for BPP.

Factor Information					
Factor	Levels	Values			
Solution Medium	2	SW. DW			
Analysis of Variance					
Source	DF	Adj SS	Adj MS	F-Value	P-Value
Solution Medium	1	3,542	3,5420	9,25	0,006
Error	23	8,807	0,3829		
Total	24	12,349			
Model Summary					
S	R-sq	R-sq(adj)	R-sq(pred)		
0,618805	28,68%	25,58%	15,15%		
Means					
Solution Medium	N	Mean	StDev	95% CI	
SW	13	0,4602	0,1219	(0,1052. 0,8153)	
DW	12	1,214	0,886	(0,844. 1,583)	

Table C.40. ANOVA results for the effect of solution medium on week six $CI_{(Areas)}$ for PET.

Factor Information					
Factor	Levels	Values			
Solution Medium	2	SW. DW			
Analysis of Variance					
Source	DF	Adj SS	Adj MS	F-Value	P-Value
Solution Medium	1	228,3	228,33	4,45	0,048
Error	20	1025,8	51,29		
Total	21	1254,1			
Model Summary					
S	R-sq	R-sq(adj)	R-sq(pred)		
7,16167	18,21%	14,12%	2,44%		
Means					
Solution Medium	N	Mean	StDev	95% CI	
SW	12	55,46	9,36	(51,15. 59,77)	
DW	10	61,932	2,630	(57,207. 66,656)	

Table C.41. ANOVA results for the effect of solution medium on week six $CI_{(Areas)}$ for CPP.

Factor Information					
Factor	Levels	Values			
Solution	Medium	2	SW. DW		
Analysis of Variance					
Source	DF	Adj SS	Adj MS	F-Value	P-Value
Solution Medium	1	0,1743	0,1743	0,29	0,595
Error	20	11,9177	0,5959		
Total	21	12,0920			
Model Summary					
S	R-sq	R-sq(adj)	R-sq(pred)		
0,771936	1,44%	0,00%	0,00%		
Means					
Solution Medium	N	Mean	StDev	95% CI	
SW	10	0,892	0,940	(0,383. 1,401)	
DW	12	1,071	0,601	(0,606. 1,536)	

C.3 Temperature beaker tests

Table C.42. ANOVA results for the effect of temperature on week six mass loss (%).

Factor Information					
Factor	Levels	Values			
Temp (C)	2	25. 60			
Analysis of Variance					
Source	DF	Adj SS	Adj MS	F-Value	P-Value
Temp (C)	1	9,37	9,368	0,52	0,473
Error	156	2818,85	18,070		
Total	157	2828,22			
Model Summary					
S	R-sq	R-sq(adj)	R-sq(pred)		
4,25083	0,33%	0,00%	0,00%		
Means					
Temp (C)	N	Mean	StDev	95% CI	
25	95	2,110	4,150	(1,248. 2,971)	
60	63	1,613	4,399	(0,555. 2,671)	

Table C.43. ANOVA results for the effect of plastic-type on week six mass loss (%).

Factor Information					
Factor	Levels	Values			
Plastic	3	BPP. CPP. PET			
Analysis of Variance					
Source	DF	Adj SS	Adj MS	F-Value	P-Value
Plastic	2	144,4	72,19	4,17	0,017
Error	155	2683,8	17,32		
Total	157	2828,2			
Model Summary					
S	R-sq	R-sq(adj)	R-sq(pred)		
4,16114	5,10%	3,88%	1,24%		
Means					
Plastic	N	Mean	StDev	95% CI	
BPP	57	0,693	3,019	(-0,396. 1,782)	
CPP	61	2,878	4,469	(1,826. 3,930)	
PET	40	2,175	5,001	(0,875. 3,474)	

Table C.44. ANOVA results for the effect of UV history on week six mass loss (%).

Factor Information					
Factor	Levels	Values			
UV History (W/m2)	3	0. 65. 130			
Analysis of Variance					
Source	DF	Adj SS	Adj MS	F-Value	P-Value
UV History (W/m2)	2	370,3	185,17	11,68	0,000
Error	155	2457,9	15,86		
Total	157	2828,2			
Model Summary					
S	R-sq	R-sq(adj)	R-sq(pred)		
3,98213	13,09%	11,97%	9,65%		
Means					
UV History (W/m2)	N	Mean	StDev	95% CI	
0	51	1,558	4,601	(0,457. 2,660)	
65	55	0,294	2,627	(-0,766. 1,355)	
130	52	3,969	4,487	(2,878. 5,060)	

Table C.45. ANOVA results for the effect of solution medium on week six mass loss (%).

Factor Information					
Factor	Levels	Values			
Solution medium	2	SW. DW			
Analysis of Variance					
Source	DF	Adj SS	Adj MS	F-Value	P-Value
Solution	1	72,30	72,30	1,78	0,185
Error	102	4133,01	40,52		
Total	103	4205,32			
Model Summary					
S	R-sq	R-sq(adj)	R-sq(pred)		
6,36551	1,72%	0,76%	0,00%		
Means					
Solution	N	Mean	StDev	95% CI	
SW	51	1,558	4,601	(-0,210. 3,326)	
DW	53	3,23	7,69	(1,49. 4,96)	

Table C.46. ANOVA results for the effect of temperature on week six crystallinity increase (%) for BPP.

Factor Information					
Factor	Levels	Values			
Temp (C)	2	25. 60			
Analysis of Variance					
Source	DF	Adj SS	Adj MS	F-Value	P-Value
Temp (C)	1	35,92	35,918	7,92	0,012
Error	16	72,61	4,538		
Total	17	108,52			
Model Summary					
S	R-sq	R-sq(adj)	R-sq(pred)		
2,13024	33,10%	28,92%	15,33%		
Means					
Temp (C)	N	Mean	StDev	95% CI	
25	9	-1,765	2,360	(-3,270. -0,260)	
60	9	-4,590	1,872	(-6,095. -3,085)	

Table C.47. ANOVA results for the effect of temperature on week six crystallinity increase (%) for CPP.

Factor Information					
Factor	Levels	Values			
Temp (C)	2	25. 60			
Analysis of Variance					
Source	DF	Adj SS	Adj MS	F-Value	P-Value
Temp (C)	1	0,0273	0,02733	0,01	0,933
Error	16	59,3045	3,70653		
Total	17	59,3319			
Model Summary					
S	R-sq	R-sq(adj)	R-sq(pred)		
1,92524	0,05%	0,00%	0,00%		
Means					
Temp (C)	N	Mean	StDev	95% CI	
25	9	-3,445	2,070	(-4,805. -2,084)	
60	9	-3,523	1,769	(-4,883. -2,162)	

Table C.48. ANOVA results for the effect of temperature on week six crystallinity increase (%) for PET.

Factor Information					
Factor	Levels	Values			
Temp (C)	2	25. 60			
Analysis of Variance					
Source	DF	Adj SS	Adj MS	F-Value	P-Value
Temp (C)	1	59,14	59,14	4,40	0,052
Error	16	214,84	13,43		
Total	17	273,98			
Model Summary					
S	R-sq	R-sq(adj)	R-sq(pred)		
3,66431	21,59%	16,69%	0,76%		
Means					
Temp (C)	N	Mean	StDev	95% CI	
25	9	1,316	1,876	(-1,273. 3,905)	
60	9	4,94	4,83	(2,35. 7,53)	

Table C.49. ANOVA results for the effect of solution medium on week six crystallinity (%) for BPP.

Factor Information					
Factor	Levels	Values			
Solution Medium	2	SW. DW			
Analysis of Variance					
Source	DF	Adj SS	Adj MS	F-Value	P-Value
Solution Medium	1	0,1196	0,1196	0,22	0,651
Error	10	5,5031	0,5503		
Total	11	5,6227			
Model Summary					
S	R-sq	R-sq(adj)	R-sq(pred)		
0,741826	2,13%	0,00%	0,00%		
Means					
Solution Medium	N	Mean	StDev	95% CI	
SW	6	38,673	0,922	(37,998. 39,348)	
DW	6	38,873	0,501	(38,198. 39,548)	

Table C.50. ANOVA results for the effect of solution medium on week six crystallinity (%) for CPP.

Factor Information					
Factor	Levels	Values			
Solution Medium	2	SW. DW			
Analysis of Variance					
Source	DF	Adj SS	Adj MS	F-Value	P-Value
Solution Medium	1	0,03337	0,03337	0,17	0,686
Error	10	1,92221	0,19222		
Total	11	1,95559			
Model Summary					
S	R-sq	R-sq(adj)	R-sq(pred)		
0,438430	1,71%	0,00%	0,00%		
Means					
Solution Medium	N	Mean	StDev	95% CI	
SW	6	39,734	0,498	(39,335. 40,133)	
DW	6	39,629	0,370	(39,230. 40,028)	

Table C.51. ANOVA results for the effect of solution medium on week six crystallinity (%) for PET.

Factor Information					
Factor	Levels	Values			
Solution Medium	2	SW. DW			
Analysis of Variance					
Source	DF	Adj SS	Adj MS	F-Value	P-Value
Solution Medium	1	0,9075	0,9075	1,13	0,314
Error	10	8,0651	0,8065		
Total	11	8,9726			
Model Summary					
S	R-sq	R-sq(adj)	R-sq(pred)		
0,898061	10,11%	1,13%	0,00%		
Means					
Solution Medium	N	Mean	StDev	95% CI	
SW	6	31,969	1,185	(31,152. 32,786)	
DW	6	31,419	0,457	(30,602. 32,236)	

Table C.52. ANOVA results for the effect of UV history on week six crystallinity increase (%) for BPP.

Factor Information					
Factor	Levels	Values			
UV History (W/m2)	3	0. 65. 130			
Analysis of Variance					
Source	DF	Adj SS	Adj MS	F-Value	P-Value
UV History (W/m2)	2	28,36	14,182	2,65	0,103
Error	15	80,16	5,344		
Total	17	108,52			
Model Summary					
S	R-sq	R-sq(adj)	R-sq(pred)		
2,31172	26,14%	16,29%	0,00%		
Means					
UV History (W/m2)	N	Mean	StDev	95% CI	
0	6	-4,380	2,279	(-6,391. -2,368)	
65	6	-1,45	2,56	(-3,46. 0,57)	
130	6	-3,708	2,067	(-5,719. -1,696)	

Table C.53. ANOVA results for the effect of UV history on week six crystallinity increase (%) for CPP.

Factor Information					
Factor	Levels	Values			
UV History (W/m2)	3	0. 65. 130			
Analysis of Variance					
Source	DF	Adj SS	Adj MS	F-Value	P-Value
UV History (W/m2)	2	13,33	6,663	2,17	0,148
Error	15	46,01	3,067		
Total	17	59,33			
Model Summary					
S	R-sq	R-sq(adj)	R-sq(pred)		
1,75132	22,46%	12,12%	0,00%		
Means					
UV History (W/m2)	N	Mean	StDev	95% CI	
0	6	-2,755	1,218	(-4,279. -1,231)	
65	6	-3,004	1,860	(-4,528. -1,480)	
130	6	-4,692	2,064	(-6,216. -3,168)	

Table C.54. ANOVA results for the effect of UV history on week six crystallinity increase (%) for PET.

Factor Information					
Factor	Levels	Values			
UV History (W/m2)	3	0. 65. 130			
Analysis of Variance					
Source	DF	Adj SS	Adj MS	F-Value	P-Value
UV History (W/m2)	2	138,7	69,332	7,69	0,005
Error	15	135,3	9,021		
Total	17	274,0			
Model Summary					
S	R-sq	R-sq(adj)	R-sq(pred)		
3,00348	50,61%	44,03%	28,88%		
Means					
UV History (W/m2)	N	Mean	StDev	95% CI	
0	6	4,68	3,88	(2,06. 7,29)	
65	6	-0,769	1,186	(-3,383. 1,844)	
130	6	5,48	3,26	(2,86. 8,09)	

Table C.55. ANOVA results for the effect of temperature on week six microhardness increase (%) for BPP.

Factor Information					
Factor	Levels	Values			
Temp (C)	2	25. 60			
Analysis of Variance					
Source	DF	Adj SS	Adj MS	F-Value	P-Value
Temp (C)	1	8541	8540,94	103,43	0,000
Error	42	3468	82,58		
Total	43	12009			
Model Summary					
S	R-sq	R-sq(adj)	R-sq(pred)		
9,08731	71,12%	70,43%	68,49%		
Means					
Temp (C)	N	Mean	StDev	95% CI	
25	17	-5,10	7,37	(-9,55. -0,66)	
60	27	23,51	10,00	(19,98. 27,04)	

Table C.56. ANOVA results for the effect of temperature on week six microhardness increase (%) for PET.

Factor Information					
Factor	Levels	Values			
Temp (C)	2	25. 60			
Analysis of Variance					
Source	DF	Adj SS	Adj MS	F-Value	P-Value
Temp (C)	1	2291	2291,2	16,52	0,000
Error	52	7212	138,7		
Total	53	9503			
Model Summary					
S	R-sq	R-sq(adj)	R-sq(pred)		
11,7768	24,11%	22,65%	18,16%		
Means					
Temp (C)	N	Mean	StDev	95%	CI
25	27	11,34	7,34	(6,79.	15,89)
60	27	24,37	14,95	(19,82.	28,92)

Table C.57. ANOVA results for the effect of solution medium on week six microhardness (kg-f/mm^2) for BPP.

Factor Information					
Factor	Levels	Values			
Solution Medium	2	SW. DW			
Analysis of Variance					
Source	DF	Adj SS	Adj MS	F-Value	P-Value
Solution Medium	1	0,001	0,00053	0,00	0,991
Error	33	139,568	4,22932		
Total	34	139,568			
Model Summary					
S	R-sq	R-sq(adj)	R-sq(pred)		
2,05653	0,00%	0,00%	0,00%		
Means					
Solution Medium	N	Mean	StDev	95% CI	
SW	17	13,146	2,632	(12,131. 14,161)	
DW	18	13,138	1,299	(12,152. 14,125)	

Table C.58. ANOVA results for the effect of solution medium on week six microhardness (kg-f/mm^2) for PET.

Factor Information					
Factor	Levels	Values			
Solution Medium	2	SW. DW			
Analysis of Variance					
Source	DF	Adj SS	Adj MS	F-Value	P-Value
Solution Medium	1	23,57	23,575	20,21	0,000
Error	34	39,66	1,166		
Total	35	63,23			
Model Summary					
S	R-sq	R-sq(adj)	R-sq(pred)		
1,07998	37,28%	35,44%	29,69%		
Means					
Solution Medium	N	Mean	StDev	95% CI	
SW	18	16,064	1,131	(15,546. 16,581)	
DW	18	14,445	1,026	(13,928. 14,963)	

Table C.59. ANOVA results for the effect of UV history on week six microhardness increase (%) for BPP.

Factor Information					
Factor	Levels	Values			
UV History (W/m2)	3	0. 65. 130			
Analysis of Variance					
Source	DF	Adj SS	Adj MS	F-Value	P-Value
UV History (W/m2)	2	2041	1020,7	4,20	0,022
Error	41	9968	243,1		
Total	43	12009			
Model Summary					
S	R-sq	R-sq(adj)	R-sq(pred)		
15,5922	17,00%	12,95%	5,90%		
Means					
UV History (W/m2)	N	Mean	StDev	95% CI	
0	17	8,57	21,74	(0,93. 16,20)	
65	18	9,42	10,68	(2,00. 16,84)	
130	9	25,87	7,63	(15,37. 36,36)	

Table C.60. ANOVA results for the effect of UV history on week six microhardness increase (%) for PET.

Factor Information					
Factor	Levels	Values			
UV History (W/m2)	3	0. 65. 130			
Analysis of Variance					
Source	DF	Adj SS	Adj MS	F-Value	P-Value
UV History (W/m2)	2	3564	1782,1	15,30	0,000
Error	51	5939	116,5		
Total	53	9503			
Model Summary					
S	R-sq	R-sq(adj)	R-sq(pred)		
10,7912	37,51%	35,05%	29,94%		
Means					
UV History (W/m2)	N	Mean	StDev	95% CI	
0	18	25,81	8,86	(20,71. 30,92)	
65	18	21,05	15,70	(15,95. 26,16)	
130	18	6,70	4,92	(1,59. 11,81)	

Table C.61. ANOVA results for the effect of temperature on week six $CI_{(Areas)}$ for BPP.

Factor Information					
Factor	Levels	Values			
Temp	2	25. 60			
Analysis of Variance					
Source	DF	Adj SS	Adj MS	F-Value	P-Value
Temp (C)	1	0,2088	0,2088	1,34	0,255
Error	34	5,2877	0,1555		
Total	35	5,4965			
Model Summary					
S	R-sq	R-sq(adj)	R-sq(pred)		
0,394362	3,80%	0,97%	0,00%		
Means					
Temp	N	Mean	StDev	95% CI	
25	18	0,767	0,456	(0,578. 0,956)	
60	18	0,6150	0,3206	(0,4261. 0,8039)	

Table C.62. ANOVA results for the effect of temperature on week six $CI_{(Areas)}$ for CPP.

Factor Information					
Factor	Levels	Values			
Temperature (C)	2	25. 60			
Analysis of Variance					
Source	DF	Adj SS	Adj MS	F-Value	P-Value
Temp (C)	1	0,01056	0,01056	0,04	0,843
Error	34	9,00932	0,26498		
Total	35	9,01988			
Model Summary					
S	R-sq	R-sq(adj)	R-sq(pred)		
0,514762	0,12%	0,00%	0,00%		
Means					
Temp	N	Mean	StDev	95% CI	
25	18	0,912	0,582	(0,665. 1,158)	
60	18	0,877	0,438	(0,631. 1,124)	

Table C.63. ANOVA results for the effect of temperature on week six $CI_{(Areas)}$ for PET.

Factor Information					
Factor	Levels	Values			
Temperature (C)	2	25. 60			
Analysis of Variance					
Source	DF	Adj SS	Adj MS	F-Value	P-Value
Temp (C)	1	20,45	20,45	0,33	0,567
Error	34	2084,31	61,30		
Total	35	2104,76			
Model Summary					
S	R-sq	R-sq(adj)	R-sq(pred)		
7,82965	0,97%	0,00%	0,00%		
Means					
Temp	N	Mean	StDev	95% CI	
25	18	53,26	8,90	(49,51. 57,01)	
60	18	51,75	6,58	(48,00. 55,50)	

Table C.64. ANOVA results for the effect of UV history on week six $CI_{(Areas)}$ for BPP.

Factor Information					
Factor	Levels	Values			
UV History (W/m2)	3	0. 65. 130			
Analysis of Variance					
Source	DF	Adj SS	Adj MS	F-Value	P-Value
UV History (W/m2)	2	3,949	1,97427	42,09	0,000
Error	33	1,548	0,04691		
Total	35	5,497			
Model Summary					
S	R-sq	R-sq(adj)	R-sq(pred)		
0,216585	71,84%	70,13%	66,48%		
Means					
UV History (W/m2)	N	Mean	StDev	95% CI	
0	12	0,2419	0,0839	(0,1146. 0,3691)	
65	12	0,8015	0,2734	(0,6743. 0,9287)	
130	12	1,0303	0,2427	(0,9031. 1,1575)	

Table C.65. ANOVA results for the effect of UV history on week six $CI_{(Areas)}$ for CPP.

Factor Information					
Factor	Levels	Values			
UV History (W/m2)	3	0. 25. 60			
Analysis of Variance					
Source	DF	Adj SS	Adj MS	F-Value	P-Value
UV History (W/m2)	2	7,611	3,80553	89,14	0,000
Error	33	1,409	0,04269		
Total	35	9,020			
Model Summary					
S	R-sq	R-sq(adj)	R-sq(pred)		
0,206619	84,38%	83,43%	81,41%		
Means					
UV History (W/m2)	N	Mean	StDev	95% CI	
0	12	0,2482	0,1347	(0,1268. 0,3695)	
65	12	1,1567	0,1854	(1,0353. 1,2780)	
130	12	1,2789	0,2749	(1,1576. 1,4003)	

Table C.66. ANOVA results for the effect of UV history on week six $CI_{(Areas)}$ for PET.

Factor Information					
Factor	Levels	Values			
UV History (W/m2)	3	0. 65. 130			
Analysis of Variance					
Source	DF	Adj SS	Adj MS	F-Value	P-Value
UV History (W/m2)	2	745,7	372,84	9,05	0,001
Error	33	1359,1	41,18		
Total	35	2104,8			
Model Summary					
S	R-sq	R-sq(adj)	R-sq(pred)		
6,41751	35,43%	31,51%	23,15%		
Means					
UV History (W/m2)	N	Mean	StDev	95% CI	
0	12	57,47	8,44	(53,71. 61,24)	
65	12	53,57	6,97	(49,80. 57,34)	
130	12	46,479	1,965	(42,710. 50,248)	

Table C.67. ANOVA results for the effect of solution medium on week six $CI_{(Areas)}$ for BPP.

Factor Information					
Factor	Levels	Values			
Solution	Medium	2	SW. DW		
Analysis of Variance					
Source	DF	Adj SS	Adj MS	F-Value	P-Value
Solution Medium	1	0,000393	0,000393	0,08	0,784
Error	22	0,112867	0,005130		
Total	23	0,113261			
Model Summary					
S	R-sq	R-sq(adj)	R-sq(pred)		
0,0716263	0,35%	0,00%	0,00%		
Means					
Solution Medium	N	Mean	StDev	95% CI	
SW	12	0,2419	0,0839	(0,1990. 0,2847)	
DW	12	0,2499	0,0567	(0,2071. 0,2928)	

Table C.68. ANOVA results for the effect of solution medium on week six $CI_{(Areas)}$ for PET.

Factor Information					
Factor	Levels	Values			
Solution Medium	2	SW. DW			
Analysis of Variance					
Source	DF	Adj SS	Adj MS	F-Value	P-Value
Solution Medium	1	381,1	381,13	10,10	0,005
Error	21	792,8	37,75		
Total	22	1173,9			
Model Summary					
S	R-sq	R-sq(adj)	R-sq(pred)		
6,14418	32,47%	29,25%	19,61%		
Means					
Solution Medium	N	Mean	StDev	95% CI	
SW	12	57,47	8,44	(53,79. 61,16)	
DW	11	65,624	0,993	(61,771. 69,476)	

Table C.69. ANOVA results for the effect of solution medium on week six $CI_{(Areas)}$ for CPP.

Factor Information					
Factor	Levels	Values			
Solution Medium	2	SW. DW			
Analysis of Variance					
Source	DF	Adj SS	Adj MS	F-Value	P-Value
Solution Medium	1	0,1168	0,116821	11,94	0,002
Error	22	0,2153	0,009786		
Total	23	0,3321			
Model Summary					
S	R-sq	R-sq(adj)	R-sq(pred)		
0,0989263	35,17%	32,23%	22,85%		
Means					
Solution Medium	N	Mean	StDev	95% CI	
SW	12	0,2482	0,1347	(0,1889. 0,3074)	
DW	12	0,1086	0,0378	(0,0494. 0,1679)	